UNIVERSITÀ DEGLI STUDI DI MILANO

Ph.D. course in Translational Medicine

XXXIV Cycle

Department of Biomedical Sciences for Health

Ph.D. Thesis

Deciphering the role of the serine threonine kinase LRRK2 in the central nervous system and in peripheral tissues: implication for Parkinson's disease treatment

Candidate:

Algerta Marku

Tutor: Prof. Carla Perego

Degree course coordinator: Prof. Chiarella Sforza

A.A. 2020-2021

Abstract

Leucine-rich repeat kinase 2 (LRRK2) encodes a large and complex protein which is widely expressed in brain and peripheral organs. Mutations in LRRK2 are a major cause of inherited and sporadic Parkinson's disease (PD), an age-dependent neurodegenerative disorder characterized by neuronal damage in multiple brain regions and consequent motor defects. Studies performed in the Central Nervous System (CNS) support a role of the protein in different functions, but despite extensive studies, the pathophysiological role of LRRK2 still remains enigmatic.

LRRK2 encompasses two enzymatic domains (a kinase and GTPase domain) and multiple protein-protein interaction modules that can scaffold several protein complexes. Therefore, defining the LRRK2 interactome and understanding how its composition is modulated can be useful to identify its function.

Since LRRK2 is notably involved in vesicular trafficking, the first aim for the proposed study was to investigate the role of the N-terminal domain of LRRK2 as a scaffold and its functional impact on synaptic vesicle (SV) dynamics in the N2a neuroblastoma cell line. High resolution fluorescence microscopy techniques coupled to genetically encoded sensors of SV fusion and recycling, demonstrated that the N-terminal domain is crucial for LRRK2 targeting to membrane structures and for its interaction with proteins involved in the control of SV mobilization and recycling. Our data confirm LRRK2 as a component of the presynaptic protein network, coordinating both storage and mobilization of SV through its N-terminal domain. Mutations in this domain (PD-linked E193K variant studied in this work) or modulation of its phosphorylation (in particular at serine 935) affects LRRK2 function via perturbation of its physiological network of interactors, thus resulting in impaired SV dynamics (Chapter I).

In addition to being expressed in the CNS, LRRK2 can be detected in a variety of peripheral organs, including the endocrine pancreas, thus leading to the suggestion that the protein may be implicated in other functions. Therefore, in the second part of the project we focused on the endocrine pancreas and explored the possible involvement of LRRK2 in the control of insulin release and glucose homeostasis, using both cellular and animal models. Through pharmacological, molecular, and functional approaches we demonstrated that LRRK2 and its kinase activity control the glucose-stimulated insulin secretion, by modulating the trafficking of insulin granules. Expression of PD-associated LRRK2 mutants, characterized by enhanced kinase-activity, increased basal insulin release, and decreased the glucose-stimulated secretion, thus affecting the animal's metabolic profile. These findings identify a new role of LRRK2 in the control of glucose homeostasis and support the idea that LRRK2 may contribute to PD development and/or progression also indirectly through modulation of glucose homeostasis and cellular energetics. Not surprisingly, drugs used in type 2 diabetes and intended to restore the glucose homeostasis are among the most promising treatments currently being considered as a possible new therapy for PD (Chapter II).

In the complex, our data indicate LRRK2 as a master regulator of secretory vesicles trafficking in both neuronal and endocrine cells of the pancreas and suggest the protein as important therapeutic target in multiple diseases.

1. Introduction - Chapter I

1.1 Parkinson ’s Disease: a general introduction

Parkinson’s disease (PD) is a chronic, progressive, late-onset neurodegenerative disease affecting about 2-3% of the population over 65 years of age and is the second most common neurodegenerative disorder of the human brain, after Alzheimer's disease (Poewe et al., 2017). The disease is clinically characterized by impaired motor function, often encompassing non-motor symptoms, and was first described two centuries ago by the English physician James Parkinson, who published an accurate description of it in 1817 named “An Essay on the Shaking Palsy”. The clinical spectrum of this disease was later described J. M. Charcot, who also changed its name to Parkinson's Disease (Dexter and Jenner, 2013; Lees et al., 2009; Parkinson, 2002; Titova et al., 2017). The selective degeneration of pigmented dopaminergic (DAergic) neurons in the substantia nigra pars compacta (SNpc) in the midbrain is responsible for the cardinal motor symptoms of the disease (Dauer and Przedborski, 2003) (Figure 1.1). When more than 50-60% of the neurons in this area are degenerated, symptoms of the disease appear. Surviving SNpc neurons often develop spherical eosinophilic cytoplasmic protein aggregates (composed of α-synuclein, parkin, ubiquitin, and neurofilaments), known as Lewy bodies (LBs) (Wakabayashi et al., 2013). The mechanisms leading to neuronal loss and LBs development are not fully elucidated, although great progress has been made in the understanding of PD causes.

The onset of PD occurs usually around 55-60 years of age, although in a small percentage (5-10% of all cases) may appear before the age of 40 ("early onset") or even under the age of 21 ("young onset") (Ferguson et al., 2016; Rizek et al., 2016). Currently, there is no cure for PD, although second-line therapies improve patients' quality of life (Hayes, 2019). The lack of treatment options to change the disease's progression, together with the ageing population, predict a significant increase in the incidence of the disease in the near future, with an important economic burden for patients and payers ($51.9 billion in 2017, estimated to be about $79.1 billion in 2037 in the U.S.)(Yang et al., 2020). PD’s aetiology is heterogeneous and multifactorial, and it is due to a combination of environmental and genetic factors. Exposure to toxicant chemicals and head injury may increase the risk of PD, genetic susceptibility factors may modify the effects of environmental exposures (Kim and Alcalay, 2017). Although known genes are responsible for a minority of PD cases (5-10%), understanding their pathological mechanisms may be useful for improving prognosis determination, patient care and for identifying new possible targets of pharmacological intervention.

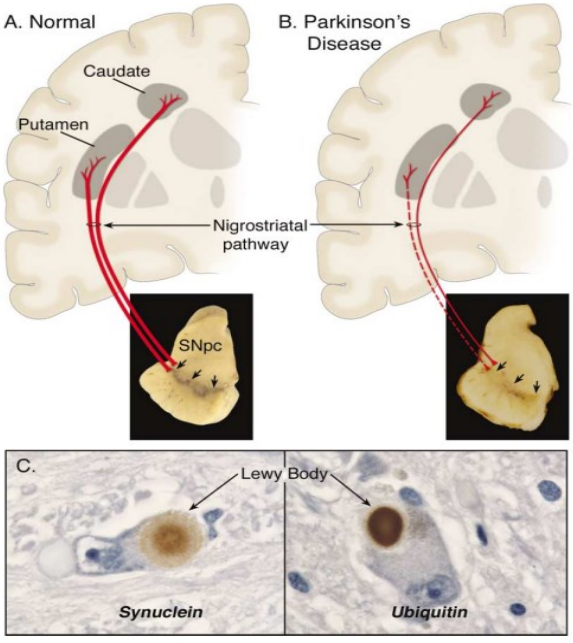

Figure 1.1. Schematic representation of the Nigrostriatal pathway*. (A-B) The nigrostriatal pathway (red) consists of dopaminergic neurons connecting the SNpc (substantia nigra pars compacta) with the dorsal striatum (putamen and caudate nucleaus) . A sever depigmentation is observed in the SNpc of Parkinson’s desease subjects, due to dopaminergic neuron loss. (C) The presence of Lewy bodies (LB) in neuronal bodies is the pathological hallmarks of the disease (Adapted from Dauer and Przedborski, 2003).*

1.1.1 The clinical and pathological features of Parkinson's disease

PD is a slowly progressive neurodegenerative disorder which has been divided into " pre-symptomatic" and "symptomatic" stages. The disease development process is "silent" and takes years until motor symptoms become evident (Sy and Fernandez, 2020) (Figure 1.2). The cardinal features based on motor symptoms, as described by Parkinson, still remain crucial for the clinical diagnosis of PD. Nevertheless, it has long been recognized there are several non-motor symptoms (NMS), which include autonomic and neuropsychiatric signs. Indeed, several autonomic function disorders may insidiously develop in the prodromal phase up to several years before the onset of motor features and may involve sleep disturbance, hyposmia (impaired sense of smell), and constipation. Such symptoms have been shown to go in association with a significantly increased risk of developing PD in differently healthy individuals in population-based cohort trials (Ishihara and Brayne, 2006; Ross et al., 2008; Savica et al., 2009; Shiba et al., 2000). Taken together, these results clearly indicate the presence of a PD stage in which affected subjects may be asymptomatic ('preclinical PD') or where they may exhibit an array of non-motor symptoms and/or subtle motor cues that do not satisfy existing diagnostic criteria ('prodromal PD') (Mahlknecht et al., 2015; A. H. V. Schapira et al., 2017; Stern et al., 2012). The duration of this prodromal phase is variable, as is the timeline of NMS onset. The rate of dopaminergic function decline (driven by dopaminergic neuron dysfunction and death) in PD can be variable (as shown by the blue shaded segment region in figure 1.2). The first clinical manifestation occurs in the middle phase of the pathological disturbance, when 50% or more of the dopaminergic neurons have degenerated into the substantia nigra (A. H. V. Schapira et al., 2017). This stage (ranging in duration from 4-12 years) typically encompasses the occurrence of some of the motor symptoms of the parkinsonism spectrum and may be associated with the emergence of additional NMS. The diagnosis may be preceded by emerging subtle motor characteristics unnoticed by the patient. If untreated, the movement disorder advances relatively quickly after diagnosis. The motor problems continue to develop during the course of the disease, coupled also with cognitive and autonomic features that become common in the later stages. The most frequent clinical features associated with PD are discussed in the following sections.

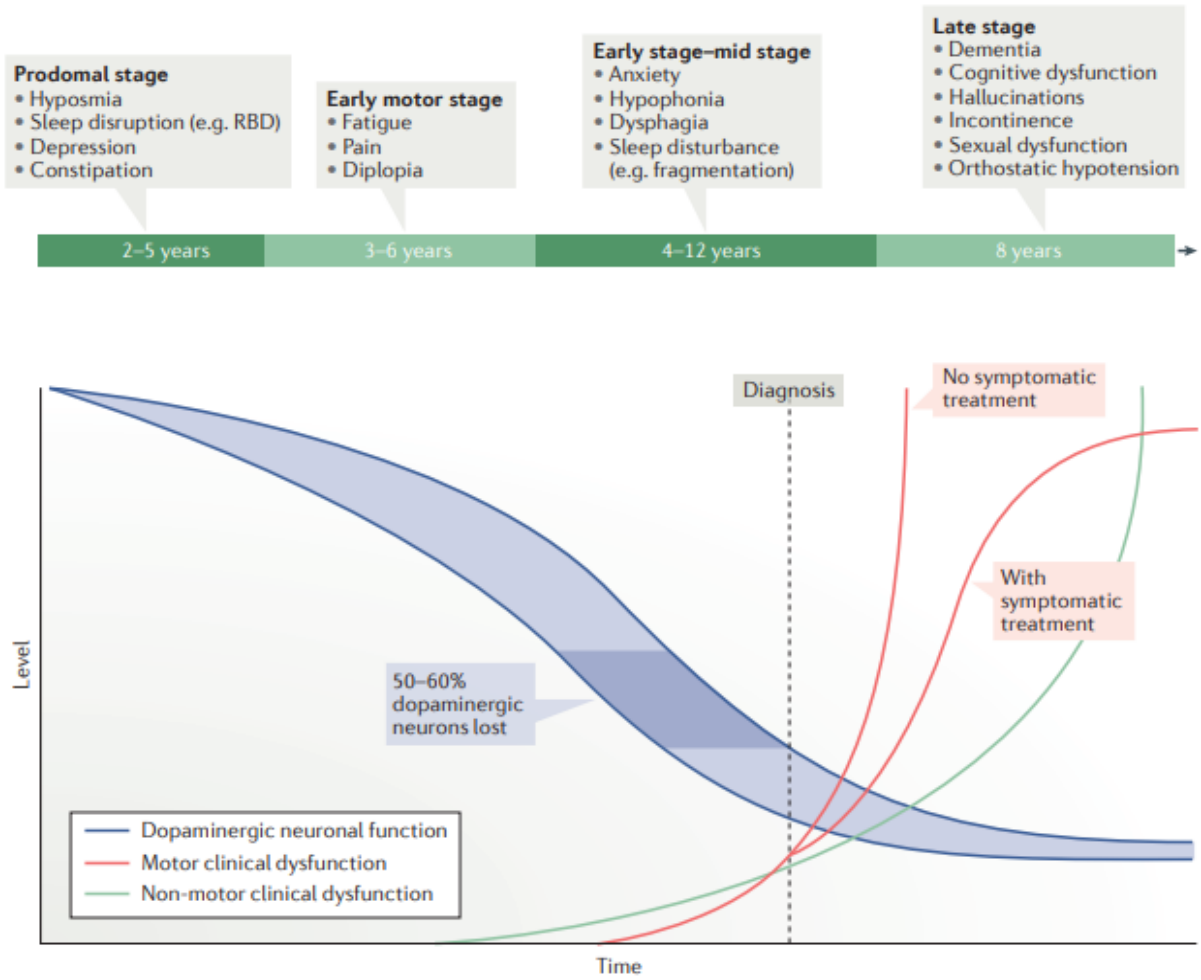

Figure 1.2. Time course of the manifestation of the motor and non-motor features of Parkinson's disease *(Adapted from Schapira AHV., 2017).*

1.1.1.1 The motor symptoms of Parkinson 's disease

The diagnosis of PD remains the greatest challenge for scientists and clinicians. It is based on clinical criteria, mainly related to the presence of bradykinesia in combination with one or more cardinal motor deficits (Radhakrishnan and Goyal, 2018). An additional criteria is the responsiveness to L-3, 4-dihydroxyphenylalanine (L-DOPA), a precursor of DA and the most effective pharmacological treatment for PD (it treats the clinical motor symptoms)(Poewe et al., 2017). Furthermore, the response to L-DOPA allows to differentiate PD from other diseases with similar clinical presentation (Jagadeesan et al., 2017).

The clinical syndrome known as *Parkinsonism*, is historically associated with the triad of motor dysfunction bradykinesia, rest tremor, and rigidity which may be also coupled with postural instability, often appearing with the progression of the disease (Kouli et al., 2018). Main features of each symptom are reported below.

Bradykinesia: refers to slowness of movements and impairment of voluntary motor control. This slowness encompasses reduction of performing automatic movements, difficulty with planning, initiating, and executing movements etc, and this translates into difficulty in performing everyday activities (Kouli et al., 2018).

Rest tremor: is characterized by a slow 4- to 6-Hz tremor, when the muscle is fully relaxed. It is an easily identified symptom and is present in 75% of patients. The tremor, with typically unilateral onset, often affects

the distal part of a limb. It mainly manifests with involuntary rotatory motions of hands and fingers called "pill-rolling" (Jankovic, 2008). Tremor is a symptom that disrupts patients' emotional stability, yet it is a minor contributor to patient disability as compared to the other manifestations of the disease.

Rigidity: presents as increased muscle tone or resistance to passive movement and it is experienced as a stiffness and inflexibility of the limbs, neck, or trunk. The rigidity is more pronounced when associated with an underlying tremor limb; when tremor is superimposed on rigidity, the resistance is ratchety and is known as the ‘‘cogwheel’’ phenomenon. The rigidity may be uncomfortable and is often associated with pain (Hess and Hallett, 2017; Jankovic, 2008).

Postural instability: is more common in patients in advanced stages of the disease. It is characterised by a shuffled gait, difficulty maintaining equilibrium and festination (a gait disturbance characterized by short, rapid, and accelerating steps and the inability to stop), leading to frequent falls and injury (Sveinbjornsdottir, 2016).

Similar to other neurodegenerative disorders, the onset of symptoms is insidious and very often nonspecific. The appearance of motor symptoms is often asymmetrical and may involve only one limb, in the following years, spread to one side of the body and later to both sides of the body, until the patient becomes almost deprived of autonomy (Miller-Patterson et al., 2018). Other secondary symptoms may be also present (freezing of gait, micrographia, dystonia, difficulty swallowing etc.), which do not occur in most cases (Sveinbjornsdottir, 2016). To date, no final diagnostic methods exist to identify patients with PD *in vivo*. In fact, definitive diagnosis of this disease can only be made by post-mortem, by detection of dopamine (DA) denervation in patients’ brain, linked to depigmentation of the substantia nigra and deposition of LBs in surviving neurons.

1.1.1.2 Non-motor symptoms of Parkinson ‘s disease

It has been long recognized that the neuropathology underlying PD includes also non-dopaminergic systems that are known to cause several NMS including sensory and autonomic dysfunction, cognitive decline, neuropsychiatric symptoms, and sleep disturbances (Amara and Memon, 2018; Poewe, 2008).

Sensory features: numerous alterations in sensation have been described, which increase in both prevalence and severity as the disease progresses. Alteration of the olfactory sense is probably one of the most widely recognized, but several problems with vision and pain also occur (Zhu et al., 2016).

Autonomic dysfunction: can be experienced during any stage of PD, and some features, such as constipation, can precede the onset of motor symptoms by years or even decades. Such symptoms include orthostatic hypotension, gastrointestinal and sexual dysfunction. However, sphincter symptoms are some of the most insidious. (Pfeiffer, 2020; A. H. V. Schapira et al., 2017).

Cognitive decline: progressive cognitive deficits may emerge in 75% of patients with PD, and can reach significant severity in about 20% of cases, leading to dementia (Williams-Gray et al., 2006). The ability to program, organize, and use problem-solving strategies, and adapt one's behaviour to different situations is the most impaired function in PD patients. In addition, patients with PD may experience attention disorders, difficulties in learning new information, and problems with both episodic and prospective memory (Roheger et al., 2018). When PD is associated with dementia, the decline in cognitive function can range from mild to very pronounced (A. H. V. Schapira et al., 2017).

Neuropsychiatric symptoms: they include symptoms such as depression, anxiety, apathy, and psychosis, and are experienced in most patients with PD. If such manifestations are present, they are difficult to manage and are associated with decreased quality of life (Aarsland et al., 2009).

Sleep disturbance: include the inability to fall asleep or sleep, with frequent nocturnal awakenings. In some cases, patients experience a reverse sleep cycle, sleep during the day, take several naps, and are awake at night. In some cases, patients experience a REM sleep disorder (RBD): they talk and gesticulate during REM sleep, acting out the content of their dreams. Such a patients have an approximately 80-90% risk of developing PD (Pfeiffer, 2016). Insomnia can be related to the pathological features of the disease, as well as to the use of dopamine-agonist drugs and L-DOPA (Louter et al., 2013; Stefani and Högl, 2020).

NMS may appear early in the disease and become evident with disease progression. They contribute significantly to overall disability and impaired quality of life in PD patients (Pfeiffer, 2016). The recognition that non-motor abnormalities may emerge during all phases of the disorder, including the premotor phase, has prompted their evaluation as possible biomarkers. Therefore, it is important to focus on treating non-motor features to improve PD patients' prognosis and quality of life (A. H. V. Schapira et al., 2017; Sveinbjornsdottir, 2016).

1.1.1.3 Neuropathological features of Parkinson ‘s disease

The pathological hallmark features of PD are the massive loss of DAergic neurons in the SNpc associated with the progressive accumulation of LBs. The loss of these neurons, which normally contain high levels of neuromelanin, leads to the classic SNpc depigmentation, typical neuropathological feature of this disease (Hayes, 2019). Dopamine-positive cell death in the SNpc is the principal cause of PD's classic motor symptoms. It is estimated that 50-60% of DAergic cells in the nigrostriatal system are lost before the onset of the cardinal motor characteristics of PD (DeMaagd and Philip, 2015). PD pathology extends not only to the nigrostriatal system but also affects various extranigral regions. LBs formation and neurodegeneration also takes place at the level of cholinergic (basal nucleus of Meynert, dorsal motor nucleus of vagus), noradrenergic (locus coeruleus), serotonergic (raphe nucleus), as well as in the cerebral cortex (particularly in the cingulate and entorhinal cortex), the olfactory bulb, and the autonomic nervous system (DeMaagd and Philip, 2015). Widespread loss of cells throughout these multiple non-DAergic neurotransmitter systems is thought to be responsible for the appearance of some of the non-motor symptoms of PD and do not respond well to dopamine replacement therapies (Kalia et al., 2013). However, the precise pathological mechanisms underlying PD and how LBs are related to the progression of the disease are still relatively unclear. Several mechanisms have been suggested to be implicated in the pathogenesis of PD including abnormalities in protein clearance, mitochondrial dysfunction, neuroinflammation, and oxidative stress (Rocha et al., 2018; Zhang et al., 2021).

1.1.2 The aetiology of Parkinson's disease

The aetiology of PD is multifactorial, complex, and in most patients is still unknown. It is determined by the interplay of both environmental and genetic risk factors.

1.1.2.1 Environmental risks

Early evidence that exposure to environmental toxins may cause parkinsonism came in 1980s, with the discovery of the MPTP (n-methyl-4-phenyl-1,2,3,6-tetrahydropyridine). The MPTP, which originates during synthesis of a meperidine analog, was found to be the cause of a rapidly progressive parkinsonian syndrome in intravenous drug users (Langston et al., 1983). In the brain, MPTP easily crosses the blood brain barrier (BBB) and is metabolised by monoamine oxidase B (MAO B) into MPP+ (1-methyl-4-phenylpyridinium), a potent mitochondrial complex I inhibitor. MPP+ displays a selective toxicity for DAergic neurons in SN, thereby replicating PD symptoms (Richardson et al., 2005). The discovery of the neurotoxin MPTP and its mechanism of action has led to the hypothesis that exogeneous toxins, causing the selective loss of DAergic neurons, mimic the clinical and pathological symptoms of PD. Another neurotoxin found to mimic parkinsonian symptoms is the 6-OHDA (6-hydroxydopamine), a hydroxylated analogue of the natural neurotransmitter DA (Schober, 2004), which is able to selectively induce degeneration of DAergic neurons, as a consequence of reduced mitochondrial complex I function and enhanced production of reactive oxygen species (ROS) (Schober, 2004).

Increased risk of developing PD is linked to rural livings and agricultural professions, probably for their higher incidence of exposure to pesticide or herbicide (Lai et al., 2002). Indeed, epidemiological studies suggest that long exposure to pesticides, most notably paraquat (herbicide) and rotenone (insecticide), can induce the typical PD phenotype (Betarbet et al., 2000; Sherer et al., 2003). Rotenone, analogous to 6-OHDA and MPTP, mimics symptoms and neuropathology of PD, *via* inhibition of mitochondrial complex I and subsequent degeneration of nigro-striatal DAergic neurons (Sherer et al., 2003). Paraquat is an herbicide that crosses the BBB and causes degeneration of DAergic neurons. Unlike the described neurotoxins, paraquat exerts its effects by oxidising the cytosolic form of thioredoxin (Trx), a class of small redox proteins, and activating the JNK/MAPK mediated, caspase-3-dependent, cell death (Ramachandiran et al., 2007). Administration of these neurotoxins and pesticides has been successfully used to generate experimental animal models of PD where to investigate the mechanisms leading to PD and evaluate new potential therapies (Bové and Perier, 2012).

Finally, other environmental risk factors are lifestyle and trauma. In this regard, several case-reports and epidemiological studies link traumatic head injuries with PD. It is possible that the high frequency and severity of the head injuries can lead to a progressive Parkinson's-like disorder. It is frequently observed among boxers, and called "pugilistic Parkinson's syndrome" (Gershanik, 2007; Lai et al., 2002).

1.1.2.2 The genetics of Parkinson's disease

PD has long been considered a non-genetic disorder of 'sporadic' origin caused by synergistic environmental factors. This concept changed when rare familial forms of parkinsonism and genetic mutations in specific genes were identified. Since the discovery of disease-causing mutations in the *Synuclein Alfa (*SNCA) gene in 1997 (Polymeropoulos et al., 1997), several additional PD-associated genes have been identified through linkage analysis, genome-wide association studies (GWAS), and family-based.

Over the past two decades, our understanding of the PD genetics has made significant progress. Genetic forms accounts only for approximately 5-10% of patients with PD, and about 5% have Mendelian inheritance

(Deng et al., 2018). To date, at least 23 chromosomal loci have been identified. They are termed "PARK", for their link to PD, and numbered according to the order in which they were first identified. 19 disease-causing genes for parkinsonism have been categorized by the HUGO Gene Nomenclature Committee (HGNC). Mutations in these genes cause PD in relatively small numbers of patients, except for the *Leucine-rich repeat kinase 2* (LRRK2). All known combined monogenic forms of PD explain only about 30% of familial cases and 3-5% of sporadic cases (Nalls et al., 2019). Mutations in PARK genes include 10 autosomal dominant (AD) and 9 autosomal recessive (AR) genes; in addition, various genetic risk loci and variants for sporadic PD have been identified by association studies, as summarized in Table 1.1 (Deng et al., 2018).

1.1.2.2.1 Autosomal dominant genes in PD

Mutations in three genes (*SNCA, LRRK2, VPS35*) are definitely established as causing AD forms of PD. Evidence regarding a fourth gene, *EIF4G1*, is still inconclusive. The heterozygous mutations in the *GBA* gene are an important risk factor for PD and widespread Lewy body disease (DLB) (Cherian and Divya, 2020). Mutations in genes associated to AD forms of PD can have different impacts on protein function. Neurotoxicity may derive from an "existing gain of function" in which PD protein activity is abnormally high (this is believed to underlie the pathogenic mechanism of the *LRRK2* mutants) or may occur for a "gain of a new function". This last mechanism has been suggested for α synuclein, which, when mutated, is prone to form oligomers and neurotoxic aggregates typical of PD.

1.1.2.2.2 Autosomal recessive genes in PD

Recessively inherited early-onset parkinsonism has been associated with mutations in *PARK2* (RBR E3ubiquitin protein ligase, commonly known as *Parkin*), *PINK1* (PTEN induced putative kinase 1) and *PARK7* (Parkinson protein7, commonly known as *DJ-1*). The mean age at onset is about 39 years, and the disease usually develops without atypical clinical signs. The most commonly mutated AR gene of PD is *Parkin*, which accounts for 8.6% of early-onset (< 50 years) PD cases, followed by *PINK1* (3.7%) and *DJ-1*(0.4%) (Cherian and Divya, 2020). Also, recessive mutations in *ATP13A2* (*ATPase type 13A2*) have been associated with the development of juvenile-onset, levodopa-responsive parkinsonism (Yang and Xu, 2014). Recently, other recessive mutations in *PLA2G6* (phospholipase A2, group VI*)*, *FBXO7* (F-box only protein 7), *DNAJC6* and *SYNJ1* were reported in patients with juvenile levodopa-responsive dystonia-parkinsonism (Nalls et al., 2019).

Locus (OMIM)	Location	Full Gene Name Approved by HGNC	HGNC Approved Gene Symbol (OMIM)	Inheritance	Disease onset	Lewy bodies
PARK1 (168601)	4q22.1	synuclein alpha	*SNCA* (163890)	AD	Early-onset, late-onset*	C
PARK2 (600116)	6q26	parkin RBR E3 ubiquitin protein ligase	*PRKN* (602544)	AR	Early-onset	NC
PARK3 (602404)	2p13	Parkinson disease 3	*PARK3* (Unclear)	AD	Late-onset	NC
PARK4 (605543)	4q22.1	synuclein alpha	*SNCA* (163890)	AD	Early-onset	C
PARK5 (613643)	4p13	ubiquitin C-terminal hydrolase L1	*UCHL1* (191342)	AD	Early-onset, late-onset	NC
PARK6 (605909)	1p36	PTEN induced putative kinase 1	*PINK1* (608309)	AR	Early-onset	NC
PARK7 (606324)	1p36.23	parkinsonism associated deglycase	*PARK7* (602533)	AR	Early-onset	NC
PARK8 (607060)	12q12	leucine rich repeat kinase 2	*LRRK2* (609007)	AD	Late-onset	C
PARK9 (606693)	1p36.13	ATPase 13A2	*ATP13A2* (610513)	AR	Early-onset	NC
PARK10 (606852)	1p32	Parkinson disease 10	*PARK10* (Unclear)	Unclear	Late-onset	NC
PARK11 (607688)	2q37.1	GRB10 interacting GYF protein 2	*GIGYF2* (612003)	AD	Late-onset	NC
PARK12 (300557)	Xq21-q25	Parkinson disease 12	*PARK12* (Unclear)	X-linked inheritance	Late-onset	NC
PARK13 (610297)	2p13.1	HtrA serine peptidase 2	*HTRA2* (606441)	AD	Late-onset, early-onset*	NC
PARK14 (612593)	22q13.1	phospholipase A2 group VI	*PLA2G6* (603604)	AR	Early-onset	NC
PARK15 (260300)	22q12.3	F-box protein 7	*FBXO7* (605648)	AR	Early-onset	NC
PARK16 (613164)	1q32	Parkinson disease 16	*PARK16* (Unclear)	Unclear	Late-onset	NC
PARK17 (614203)	16q11.2	VPS35, retromer complex component	*VPS35* (601501)	AD	Late-onset	NC
PARK18 (614251)	3q27.1	eukaryotic translation initiation factor 4 gamma 1	*EIF4G1* (600495)	AD	Late-onset	NC
PARK19 (615528)	1p31.3	DnaJ heat shock protein family (Hsp40) member C6	*DNAJC6* (608375)	AR	Early-onset	NC
PARK20 (615530)	21q22.1	synaptojanin 1	*SYNJ1* (604297)	AR	Early-onset	NC
PARK21 (616361)	20p13	transmembrane protein 230	*TMEM230* (617019)	AD	Late-onset, early-onset*	C
PARK22 (616710)	7p11.2	coiled-coil-helix-coiled-coil-helix domain containing 2	*CHCHD2* (616244)	AD	Late-onset, early-onset*	NC
PARK23 (616840)	15q22.2	vacuolar protein sorting 13 homolog C	*VPS13C* (608879)	AR	Early-onset	NC
	11p15.4	RIC3 acetylcholine receptor chaperone	*RIC3* (610509)	AD	Late-onset, early-onset*	NC

Table 1.1. List of Parkinson disease-associated loci and genes. *HGNC: HUGO Gene Nomenclature Committee, AD: autosomal dominant, AR: autosomal recessive,*: few cases, C: confirmed; NC: not confirmed (Adapted from Deng H., et al 2018).*

The discovery of mutated genes in PD and functional studies on their protein products have yielded new insights into the pathological events driving neurodegeneration. In particular, they have identified new, interlinked, molecular pathways that appear to be disrupted in all forms of PD. A better understanding of these events can pave the way for the design of targeted therapies, aimed at preventing and treating the disease. Here I will review LRRK2, which is the topic of my thesis.

1.2 Leucine-rich repeat kinase II

The genome-wide linkage analysis of a large Japanese family in 2002 identified a new locus for PD, termed *PARK8*, on chromosome 12 (12p11.2-q13.1) (Funayama et al., 2002). In 2004, two different groups identified missense mutation within a large gene segregating with *PARK8*-linked PD (Paisán-Ruíz et al., 2004; Zimprich et al., 2004). The gene was named *LRRK2* (Leucine-Rich Repeat Kinase 2) and the encoded protein LRRK2 or dardarin (from the Basque term dardara, meaning tremor). Analysis of 133 families worldwide reported that the frequency of *LRRK2* mutations was found in 4% of hereditary PD and 1% of idiopathic PD patients (Healy et al., 2008), comprising the most common genetic causes of both familial and sporadic PD.

1.2.1 LRRK2 multidomain structure

The gene encoding for LRRK2 maps to chromosome 12 at position q12, consists of 51 exons and is transcribed into a 9kb mRNA. LRRK2 is a large protein consisting of 2527 amino acids, whose molecular weight is about 280 kDa and has the following structural domains (Guo et al., 2006; Mata et al., 2006) (Figure 1.3):

- An “armadillo repeats” domain (ARM).
- An “ankyrin repeats” domain (ANK).
- A leucine-rich repeats (LRR) domain.
- A Roc domain with GTPase activity (ROC).
- A carboxy terminal of Roc domain (COR).
- A Kinase domain, homologous with MAP-kinase-kinase-kinase (MAPKKK).
- A C-terminal WD-40 repeat domain (WD40).

LRRK2 is classified as member of the Roco family of proteins, it is characterized by the presence of a Ras-like G domain, called Ras of complex proteins (Roc), which always occurs in tandem with the characteristic C-terminal of Roc (COR) domain. The Roc-COR domain is then followed by a kinase domain belonging to the mitogen- activated protein kinase kinase kinase (MAPKKK) subfamily at the C-terminal. In addition to the Roc-COR-kinase catalytic core in the centre of the protein, Roco proteins are flanked by a large variety of additional C- and N-terminal domains involved in protein-protein interactions. The N- terminal part of LRRK2 consists of armadillo (ARM), ankyrin (ANK), and leucine rich repeat (LRR) domains, while a WD40 domain is present at the C-terminus of LRRK2 (Wauters et al., 2019).

The protein exists in both a monomeric and dimeric form, the former is mainly cytosolic and thought to be inactive, the latter is enriched in membrane fractions and expected to be active (Civiero et al., 2012; Greggio et al., 2008; Guaitoli et al., 2016; Berger et al., 2010).

The pathologic mutations are clustered inside the enzyme core of the GTPase (R1441C/H/G, Y1966C, N141437H) and kinase (G2019S, I2020T, I2012T) domains. G2385R and R1628P risk variants reside in the ROC and WD40 repeat regions, respectively.

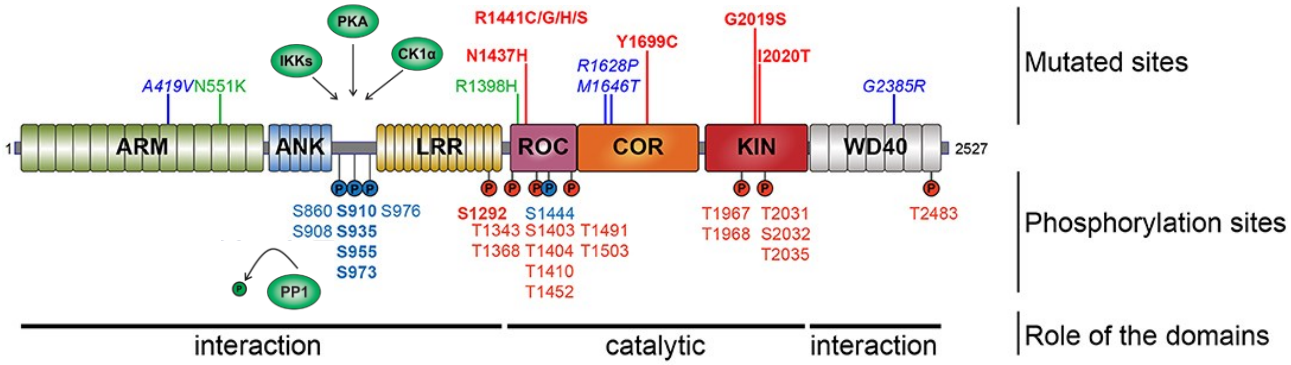

Figure 1.3. Schematic of LRRK2 functional domains, phosphorylation sites and the pathogenic mutations associated with PD. *ARM, armadillo; ANK, ankyrin repeat; LRR, leucine-rich repeat; ROC, Ras of complex proteins: GTPase; COR, C-terminal of ROC; WD40, WD-40 domain. In the upper part, pathogenic mutations are indicated in red, and risk variants are shown in blue. In the lower part, the phosphorylation sites are shown; the heterologous phosphorylation sites are indicated in blue and the sites of autophosphorylation are in red. The most described and studied sites are indicated in bold. To date, IKKs, PKA, and CK1α have been reported to phosphorylate LRRK2 at S910, S935, S955, and S973 while PP1 dephosphorylate them. 14-3-3 protein has been reported to bind to phosphorylated S910, S935. (Adapted from Marchand A., et al 2020).*

1.2.1.1 LRRK2 Domains

LRRK2 is a complex protein that carries a dual, GTPase and kinase, enzymatic activity.

The Roc domain encompasses a small fraction (residues 1335-1510) of the full-length LRRK2 protein (~7% of the total) and possesses GTPase activity. The structure shares sequence homology with the Ras-related GTPase superfamily. To work properly, the Ras-related GTPase requires the involvement of proteins called 'Guanine Nucleotide Exchange Factors' (GEFs) and 'GTPase-Activating Proteins' (GAPs). The coordinated activity of the GEFs and GAPs proteins enables the molecular switch from the GDP-bound 'off' state to the GTP-bound 'on' state, prompting the activation of the intrinsic GTPase function of the Roc domain (Bosgraaf and Van Haastert, 2003; Nguyen and Moore, 2017; Tsika and Moore, 2013). In particular, the ROC domain of LRRK2 binds a GDP molecule, while the protein is inactive. The binding to GTP is regulated by the interaction with GEFs: the GEF protein binds the ROC domains of two distinct LRRK2 proteins, yielding a homodimer. This enables the GDP-GTP exchange, which induces activation of the intrinsic GTPase function of the ROC domain, triggering the protein autophosphorylation and the activation of the kinase function (Biosa et al., 2013; Gilsbach et al., 2018). Crystallographic studies of the tandem Roc-COR domain of the Roco protein from *Chlorobium tepidum* confirm that dimerization is mediated through COR domains (Deyaert et al., 2017; Gotthardt et al., 2008). Thus, the dimerization represents a critical step for LRRK2 membrane localization and for the regulation of its enzymatic activities. Interestingly, a large number of familial mutations cluster within the Roc-COR tandem domain and impair GTPase activity. Pathogenic mutations (R1441 and I1371) disrupt the ROC dimer resulting in decreased GTPase activity. The pathological mutations R1441C/G/H and Y1699C in the GTPase domain, disrupt both the GTP binding and hydrolysis rate compared to wild-type LRRK2 (Daniëls et al., 2011; Deng et al., 2008; Li et al., 2007; Liao et al., 2014) which subsequently alters the downstream enzymatic activity of the protein. Hence, GTPase activity is clearly important for LRRK2 function, regulation of kinase activity, and development of PD.

The MAPKKK domain is positioned at the C-terminal of the COR domain and is organized in two lobes: a minor lobe, at the N-terminal portion, and a major lobe, at the C-terminal portion. This particular conformation leads to the formation of a gap between the two lobes, where are located the amino acid residues necessary for the binding of the enzyme to ATP and its substrates (Mata et al., 2006). The kinase activity of LRRK2 is regulated by the autophosphorylation of three residues located in the kinase activation loop and identified by *in vitro* assays (Marchand et al., 2020). Other autophosphorylation sites have been identified within the different domains of LRRK2, many of them are clustered around the central ROC domain. As mentioned above, auto-activation of the ROC domain, in turn induces the kinase activity of LRRK2, suggesting a complex and reciprocal regulation between the two enzymatic activities of the protein (Berwick et al., 2019; Greggio et al., 2008; Marchand et al., 2020). The most common pathogenic variant, G2019S, falls within this domain and exhibits enhanced kinase activity. This prompted to the hypothesis that all disease-related mutations are gain-of-function and induce neuronal toxicity in a kinase-dependent manner, through hyperphosphorylation of substrate proteins.

1.2.1.2 LRRK2 protein-protein interaction domains

LRRK2 encompasses several domains involved in protein-protein interactions, namely the ARM, ANK and LRR repeats at the N-terminus as well as the WD40 repeats at the C-terminus.

The Trp-Asp-40 (WD40) domain consists of ~40 amino acids repeating motifs that terminate frequently with a conserved glycine-histidine and the tryptophan-aspartate dipeptide motif. Each motif is arranged in 4 antiparallel β-sheets that form a donut shape. Seven of these motifs are disposed to form a positively charged

arginine residue-rich structure that allows the WD40 domain to interact with negatively charged structures such as phospholipids or nucleic acids (M. Schapira et al., 2017). The WD40 domains typically act as a scaffold, often within large multiprotein complexes, has been implicated in the interaction with microtubules and synaptic vesicles (Carrion et al., 2017; Piccoli et al., 2014; Zhang et al., 2019) and it is required to induce LRRK2-mediated neurotoxicity (Jorgensen et al., 2009). The G2385R missense mutant within the C-terminal WD40, associated with increased risk of developing idiopathic PD (Tan, 2006; Xie et al., 2014), impacts on the WD40 domain folding and binding properties and affects synaptic vesicle dynamics, thus supporting a key role of this domain in the control of the synaptic function (Piccoli et al., 2014).

The leucine rich repeat (LRR) domain is upstream the ROC domain and comprises 13 repeats, each of which consists of repeating 20-30 amino acid stretches. The following motif is present in the repeats: LxxLxLxxN/CxL, where L indicates a leucine, valine, or isoleucine, N indicates an asparagine, threonine, or serine, and the x refers to an acidic amino acid residue. This domain is structurally formed by a β-sheet followed by an α-helix folded to make an arch. This concave arch segment is enriched with positively charged amino acids and provides an interaction surface (Mills et al., 2014).

The ankyrin repeat (ANK) domain comprises seven repeats which form a slightly curved structure. Each repeat consists of 33 amino acid residues organized into two α-helices, separated by loops. ANK is a highly conserved domain, found in several bacterial and eukaryotic proteins, it mediates protein-protein interactions and has been involved in several functions, ranging from transcriptional initiators to cytoskeletal and cell cycle regulators (Mosavi et al., 2004).

The armadillo (ARM) domain, located at the N-terminal terminus of the protein, consists of 13 repeated units of 42 amino acid stretches. It is organized in three α-helices each (named H1-H3), to which is interposed a groove flanked by positively charged residues, mainly histidine. The H1 is the shortest helix and contains two loops. The H2 and H3 helices consist of about three and four loops, respectively. The helices H2 and H3 both share large hydrophobic interactions and are antiparallel in orientation, whereas H1 stands almost perpendicular to the other helices. Together, these helices are arranged in a super-helical structure that defines a protein-binding groove. All the repeats are merged in a single protein with a hydrophobic elongated core (Striegl et al., 2010). The ARM domain was first identified in the segmental polarity protein armadillo from *Drosophila melanogaster*, the mammalian homologue of β-catenin, which is essential for cadherin-based cell adhesion and Wnt/Wingless growth factor signaling. In addition, it serves to link the cytoplasmic cadherin domain to α-catenin and the actin cytoskeleton. The armadillo repeats are folded together to form a superhelix, which provides a versatile scaffold for multiple protein interactions (Tewari et al., 2010). The N-terminal ARM domain is involved in LRRK2 supra-molecular organization (Guaitoli et al., 2016) and mediates the LRRK2 interaction with FADD, a key factor in the triggering of LRRK2-related toxicity (Antoniou et al., 2018). More recently, by exploiting a combination of homology modelling, mutagenesis, pulldown, and fluorescence-based assays, it has been found that a negatively charged loop in the ARM domain is involved in the binding of LRRK2 with Rab32 GTPases (Rab32 and Rab38) (McGrath et al., 2021).

It remains poorly understood how the kinase, GTPase, and protein-protein interaction domains of LRRK2 govern cellular processes under physiological conditions and consequently how pathogenic mutations affect the enzymatic activity and in general the functional output of LRRK2 on these processes.

1.2.2 Cellular functions of LRRK2

So far, all available results strongly suggest a critical role of LRRK2 in the pathological processes underlying inherited and sporadic PD. A wide range of studies have been performed in recent years using both cellular and animal models, but a definitive pathophysiological role for LRRK2 remains to be clarified. Expression of LRRK2 in astrocytes, microglia, neurons, endothelial cells, and peripheral immune cells (Kluss et al., 2018; Marchand et al., 2020) suggests the protein involvement in signalling pathways that may be either cellular- or context-specific. A convincing body of evidence establishes that LRRK2 is involved in the control of cellular processes such as vesicular trafficking, organization of the cytoskeleton, control of the autophagic process, endocytosis, modulation of mitochondrial functions, protein aggregation, translation, and inflammation (Berwick et al., 2019; Kluss et al., 2018) (Figure 1.4). Such a wide range of functions further challenges the understanding of LRRK2's role in the disease. In the next sections I will highlight the function of LRRK2 on vesicular trafficking, since it was one of the aspects investigated during my thesis work.

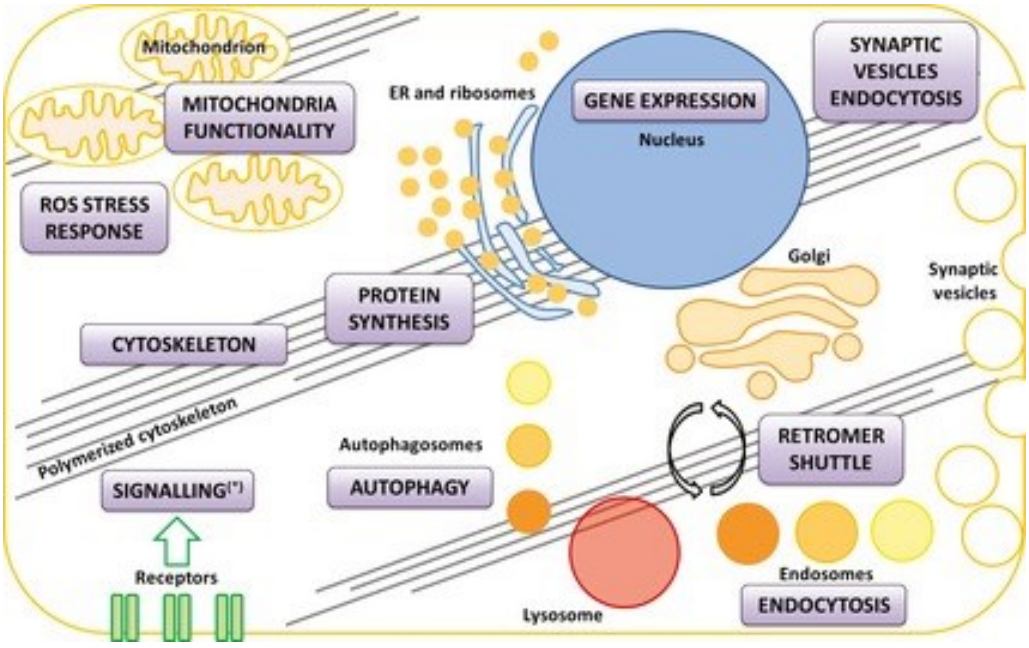

Figure 1.4. The cellular pathways that have been linked to LRRK2 functionality in physiology and/or disease over time *(Adapted from Wallings et al., 2015).*

1.2.2.1 LRRK2 and vesicular trafficking

Impairment of vesicle trafficking appears to represent a common pathological mechanism in PD. Various pieces of evidence support a role for LRRK2 as a regulator of membrane trafficking, from vesicle generation to movement along the cytoskeleton and, eventually, to vesicle fusion with the cell membrane and recycling. Of interest, expression of disease associated *LRRK2* mutants disrupts the dopamine D1 receptor (DRD1) trafficking in both animal and cellular models. In particular, the expression of G2019S *LRRK2* impairs DRD1 internalization and causes its membrane enrichment, leading to alteration in signal transduction (Migheli et al., 2013; Rassu et al., 2017).

LRRK2 has been implicated in synaptic vesicles endocytosis, *via* association with Rab5b, a regulator of vesicle trafficking from the plasma membrane to the first endosomal compartments. siRNA knock-down of LRRK2 as well as overexpression of LRRK2 markedly reduced synaptic vesicle endocytosis, and this altered phenotype is rescued by the introduction of Rab5b (Shin et al., 2008). More recent studies demonstrated that Rab5b is

a substrate of LRRK2 kinase activity *in vitro* and its GTPase activity is enhanced after phosphorylation (Yun et al., 2015).

LRRK2 also interacts physically and functionally with many proteins that are critical facilitators of endocytic vesicle trafficking, including Auxilin (*DNAJC6*) and EndophilinA (EndoA). Auxilin recruits Hsc70 to clathrin-coated vesicles to initiate their uncoating. The S627 residue of auxilin is important for regulating its binding to clathrin. Interestingly, LRRK2 phosphorylates auxilin at S627 residue, thereby inhibiting its binding to clathrin and leading to impaired vesicles recycling (Erb and Moore, 2020).
Studies in *Drosophila* showed that LRRK2 phosphorylates EndoA, a protein involved in vesicle formation, at Ser-75, thus reducing its affinity for membranes and thereby affecting EndoA-dependent membrane tubulation (Wallings et al., 2015). In mammalian cells, LRRK2 phosphorylates the neuron specific EndoA1, supporting the idea that the signaling cascade governing synapse function translates from fly to mammalian neurons (Arranz et al., 2014).

Among LRRK2 substrates, it was found to interact also with Rab7L1 (also called Rab29), which is associated with the *trans*-Golgi network and mediate the retrograde trafficking. Studies showed how Rab7L1 interacts with LRRK2 to regulate retromer function and lysosomal pathways to modify intraneuronal protein sorting and PD risk (MacLeod et al., 2013). In addition, genome-wide association studies (GWAS) highlight a genetic interaction between Rab7L1 and LRRK2 (Beilina et al., 2014).

LRRK2 has been also proposed to modulate the exo- and endo-cytic pathways by regulating the soluble NSF attachment protein receptor (SNARE) complex dissociation *via* phosphorylation of NSF (N-ethylmaleimide-sensitive factor). Following vesicle fusion with the membrane and exocytosis, NSF is able to associate with SNAREs *via* SNAP25 (synaptosomal-associated protein 25) and, through its ATPase activity, to induce disaggregation of the SNARE complex (Ryu et al., 2016). LRRK2-mediated phosphorylation of NSF enhances its ATPase activity and increases the rate of SNARE complex disassembly *in vitro* (Belluzzi et al., 2016). Snapin, a SNAP-25 binding protein associated with the SNARE complex, is another LRRK2 kinase substrate. Thus, inhibition of snapin and SNAP25 interaction blocks the association of the SNARE complex with synaptotagmin. Snapin null mice show impaired calcium-mediated exocytosis and disrupted SNAP25-Synaptotagmin1 binding. LRRK2 both interacts with and phosphorylates Snapin at Thr117. The phosphorylation rate is higher with the pathological *LRRK2* G2019S mutation as well as with the phosphomimetic Snapin-T117D and, in either case, causes decreased association of synaptotagmin1 with SNARE proteins, suggesting the involvement of LRRK2 in neurotransmitter release (Hur et al., 2019).

LRRK2 binds to various synaptic proteins through its WD40 domain (Piccoli et al., 2014), among them the synapsin I, an important SV-associated phosphoprotein. Synapsin I anchors SV to the actin cytoskeleton in a reversible manner, thereby controlling the number of vesicles that are at the active zone and ready for fusion (Cesca et al., 2010). The G2385R variant within the C-terminal WD40 domain (Tan, 2006; Xie et al., 2014) binds less efficiently to synapsin I and increases the synaptic vesicle trafficking (Carrion et al., 2017). Recently, it has been demonstrated that synapsin I is phosphorylated by LRRK2 and this phosphorylation plays a pivotal role in regulating the glutamate release at pre-synaptic sites (Marte et al., 2019).

These results confirm that LRRK2 is involved in a complex range of cellular functions including vesicle dynamics, *trans*-Golgi networks, and lysosomal homeostasis. Yet is very challenging to bring together various results from different models and combine them into a comprehensive description of the underlying molecular mechanism supported by LRRK2.

1.2.2.1.1 Rab GTPase as LRRK2 target

Our understanding of LRRK2 functions has significantly evolved since the discovery of a subset of small GTPases (Rabs) as physiological substrates of the enzyme. Rab proteins are distributed among specific membrane-bound compartments, and act as key regulators of vesicular trafficking, coordinating multiple aspects such as vesicle formation, maturation, transport, binding, and fusion. Rab GTPases represents by far the largest subgroup of the Ras-like GTPase superfamily and, in the human genome, embrace more than 60 members (Figure 1.5). These proteins shift cyclically from a GTP-bound to a GDP-bound form, and they transition between states either through GDP release (a slow and limiting step) or by hydrolysis of the bound GTP (as well slow). With the intrinsic slowness of GDP release and GTP hydrolysis, therefore, the transition from the active GDP-bound form to the inactive GDP-bound form is facilitated by secondary proteins called guanine nucleotide exchange factors (GEFs) and GTPase activating proteins (GAPs), which both enhance the rates of these reactions and are rather specific regarding their corresponding Rab substrates. Rabs, in their GTP-bound form, recruit effector proteins from the cytosol, which establish the functional membrane domains, allowing SNARE proteins to interact and drive membrane fusion. GDP-bound Rab becomes a substrate of the GDP dissociation inhibitor (GDI), which pulls Rab out of the membrane. GDI-bound Rab is then able to be reintegrated into the membrane to begin the cycle again (Hutagalung and Novick, 2011; Stenmark, 2009). The link between LRRK2 and Rab GTPases was first established genetically (MacLeod et al., 2013), then many lines of evidence identified a number of RAB GTPase as LRRK2 substrates both *in vitro* and *in vivo*. An investigation of LRRK2 substrates analysis based on large-scale phosphoproteomic screening has generated substantial evidence for LRRK2-mediated phosphorylation of a subset of RAB GTPases: Rab3A/B/C/D, Rab8A/B, Rab10, Rab12, Rab 29, Rab35, and Rab43 (Steger et al., 2017). The phosphorylation takes place at a conserved Thr/Ser residue located within the switch-II binding effector motif, which mediates the binding to interactors responsible for vesicle transport (Jeong et al., 2018). Thereafter, additional groups have similarly reported that Rab8, Rab10, and Rab29 interact as outstanding substrates of LRRK2 in cells (Fujimoto et al., 2018; Liu et al., 2018; Madero-Pérez et al., 2018). Most importantly, PD-associated *LRRK2* mutations characterized by increased kinase activity commonly result in increased Rab GTPases phosphorylation (Fujimoto et al., 2018; Liu et al., 2018; Steger et al., 2017), prompting the hypothesis that Rab hyperphosphorylation may be involved in PD pathogenesis.

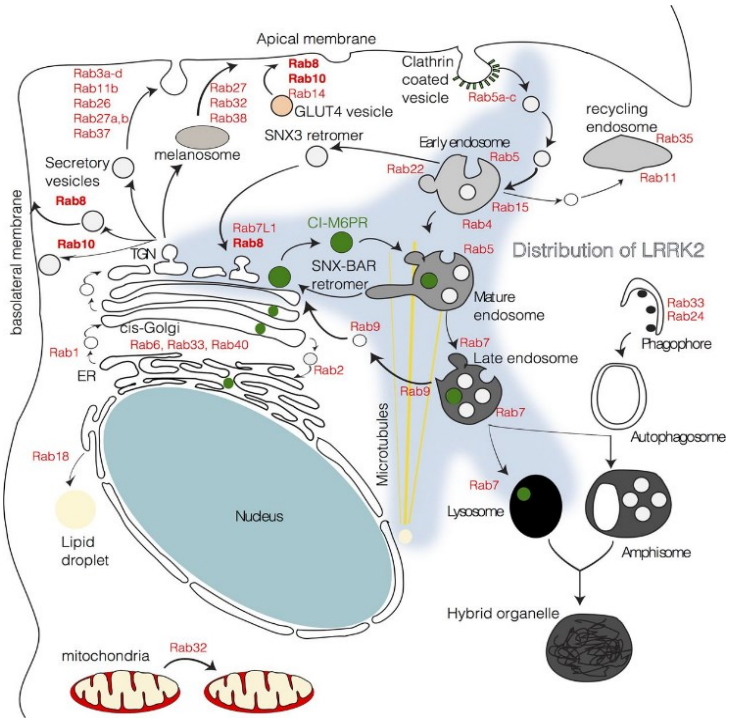

Figure 1.5. Schematic view of LRRK2-associated cellular pathways in association with Rab GTPases. *Some of the key vesicular trafficking events illustrated by curved arrows between labelled organelles. Some of the Rab GTPases are enlisted in red showing their approximate positions. LRRK2 distribution is shown as a shadow across multiple organelle compartments (Adapted from Roosen and Cookson, 2016).*

1.2.3 LRRK2 localization

LRRK2 is widely expressed in different tissues and organs including kidneys, liver, lung, heart, and in the brain within neurons, astrocytes, and microglia. This ubiquitous pattern of expression hints a role of the protein in multiple intracellular pathways. In the brain, LRRK2 is expressed in a variety of neuronal populations, in regions of the human brain directly implicated in the neuropathology of PD. Accordingly, post-mortem human brain tissue of PD patients demonstrates LRRK2 localization in the cerebral cortex, caudate-putamen and, at low-grade levels, in substantia nigra pars compacta (Higashi et al., 2007). Furthermore, LRRK2 is reported to be associated with LBs (Zhu et al., 2006) and Lewy neurites (LNs) (Giasson et al., 2006), however not as a principal component of these inclusions.

In the cell, LRRK2 is prevalently located in the cytoplasm, but it can be recruited to membrane-containing or membrane-associated fractions, including mitochondria (Singh et al., 2019), the endolysosomal system (Erb and Moore, 2020), the endoplasmic reticulum (ER) (Vitte et al., 2010), and the trans-Golgi (Piccoli and Volta, 2021). The LRRK2 recruitment to membrane domains is controlled by interaction with 14-3-3 proteins and it is relevant to promote LRRK2 dimerization and activation (Berger et al., 2010; Deng et al., 2008; Greggio et al., 2008; Sen et al., 2009). Indeed, LRRK2 exists as monomer and dimer, monomeric LRRK2 is predominantly cytosolic, with lower kinase activity, while dimeric forms are enriched on intracellular membranes and possess enhanced kinase activity (Berwick et al., 2019).

1.2.4 LRRK2 phosphorylation control both LRRK2 localization and activity

The phosphorylation of a protein is widely known to be a key mechanism governing protein function, and in LRRK2 controls its localization and activation. Under physiological conditions, LRRK2 is highly phosphorylated (Reynolds et al., 2014) and the balance between auto- and hetero-phosphorylation of the LRRK2 protein appears to be crucial in fine-tuning several cellular functions. Two groups of phosphorylable residues can be identified in LRRK2: autophosphorylation sites, which are phosphorylated by the LRRK2 kinase itself and heterologous phosphorylation sites, whose phosphorylation is carried out by other kinases (De Wit et al., 2018) (Figure 1.3). More specifically, about 60% of the identified protein phosphorylation sites are autophosphorylation sites and 36% are heterophosphorylation sites, whereas the remaining 4% are both targets of autophosphorylation and phosphorylation. In general, phosphorylation sites of LRRK2 mostly include serines (59%), followed by 37% threonines and some tyrosines (4%) (Marchand et al., 2020).

LRRK2 autophosphorylation sites are found across the protein, with various modification sites located within the catalytic core of the protein (most reside in the ROC domain, with only a few in the COR and kinase domains). Of note, a few of the autophosphorylation sites are undetectable *in vivo*, but they mostly map *in vitro,* by incubating ATP with purified LRRK2 (Wallings et al., 2015). Within the cellular context or *in vivo*, autophosphorylation occurs at residues T1410, T1503 and Ser1292, and the latter has been suggested to be the physiological readout for LRRK2 kinase activity *in vivo* (Kluss et al., 2018; De Wit et al., 2018; Pungaliya et al., 2010).

Looking over the distribution of phosphorylated residues throughout the LRRK2 protein, a cluster of serines lying between the ANK and the LRR domain, including Ser910, Ser935, Ser955, and Ser973, appears to be constitutively phosphorylated; however, these sites are phosphorylated by other kinases rather than LRRK2 itself (Marchand et al., 2020; Wallings et al., 2015). Different kinases can target LRRK2 phosphorylation; among them cAMP-dependent protein kinase A (PKA) (Muda et al., 2014), casein kinase 1α (CK1α) (Chia et al., 2014), IκB kinases (IKKs) (Dzamko et al., 2012), and protein kinase C (PKC) (Zach et al., 2010) are the most noted as upstream regulators of LRRK2 phosphorylation.
The rapid induction of LRRK2 dephosphorylation after LRRK2 kinase inhibition also suggests the involvement of protein phosphatases. Indeed, the dephosphorylation of the heterologous phosphorylation sites of LRRK2 is mediated by the protein phosphatase 1 (PP1) (Lobbestael et al., 2013). Curiously, although these residues are not phosphorylated by LRRK2, their level of phosphorylation is affected by pathogenic mutants of LRRK2 in the ROC/COR/kinase domains (N1437H, R1441C/G/H, Y1699C, I2020T, and risk factor G2385R and by LRRK2 kinase inhibition, thus suggesting that the LRRK2 kinase activity indirectly controls LRRK2 phosphorylation in some way.

Protein-protein interaction studies from several groups have established a functional significance for Ser910, Ser935, phosphosites present within the ANK-LRR interdomain, and have shown that they are essential for interaction with proteins 14-3-3. Consistent with this evidence, disruption of LRRK2 phosphorylation, either by phosphor dead Ser910Ala or Ser935Ala LRRK2 mutants, or by applying LRRK2 kinase inhibitors, impairs its interaction with 14-3-3 proteins and subsequently affects the downstream signaling (Doggett et al., 2012; Dzamko et al., 2017; Lobbestael et al., 2013; Mamais and Cookson, 2014; Nichols et al., 2010; Perera et al., 2016). The interaction with 14-3-3 recruits LRRK2 to membrane domains, where the protein dimerizes and becomes activated. In line with this possibility, the absence of LRRK2 binding to 14-3-3 causes the punctate cytosolic accumulation of the protein, and failure to relocate LRRK2 at the plasma membrane (Doggett et al., 2012; Nichols et al., 2010).

As above reported, several protein kinases can phosphorylate LRRK2, at least *in vitro*. As LRRK2 phosphorylation is implicated in LRRK2 recruitment to the plasma membrane and activation, therefore is great interest in understanding S910/S935/S955 and S973 phosphorylation.

Dephosphorylation is promoted by protein phosphatase 1 (PP1), which thereby boosts dissociation of 14-3-3 protein from LRRK2 (Lobbestael et al., 2013). Enhanced binding of LRRK2 to PP1 and consequently, decreased Ser910/Ser935 phosphorylation as well as reduced binding to 14-3-3 was observed in LRRK2 PD-mutants as compared to wild-type protein (Lobbestael et al., 2013; Doggett et al., 2012; Nichols et al., 2010). Dephosphorylation at residue S935 not only abrogates LRRK2-14-3-3 interaction but also lead to ubiquitination and degradation of a relevant fraction of the protein (Zhao et al., 2015).

Interestingly, recent studies indicate reduced phosphorylation of LRRK2 protein at Ser935 and Ser910 sites within the neuronal tissue of patients with both sporadic and familial Parkinson's disease (Dzamko et al., 2017), raising the possibility that altered LRRK2 phosphorylation is involved in the development of the disease.

1.2.5 Mutations in LRRK2 gene and their implication in Parkinson's disease

More than 80 PD-associated mutations in the LRRK2 gene have been reported, and yet, only eight mutations in *LRRK2* (N1437H, R1441 G /H/ C, Y1699C, I2012T, G2019S, and I2020T) have been confirmed as pathological variants by large family segregation studies (Chen and Wu, 2018). Mutations in LRRK2 are associated with autosomal dominant PD of incomplete penetrance, since a large number of putative pathogenic carrier mutations are disease-free.

PD-linked pathogenic LRRK2 mutations are clustered inside the catalytic core; R1441C/G/H, N1437H in the ROC domain, Y1699C in the COR domain, and G2019S, I2020T, and I2012T in the kinase domain (Hur and Lee, 2021). Many of these LRRK2 pathogenic mutants exhibit increased kinase activity as compared with wild-type (WT) LRRK2, and genetic or pharmacological inhibition of kinase activity could relieve the neurodegeneration caused by LRRK2 pathogenic mutants (Lee et al., 2012), hinting that aberrant kinase activity plays a critical role in the pathogenesis of PD (Smith et al., 2006; West et al., 2005).

Other mutations, G2385R and R1628P risk variants, reside in the ROC and WD40 repeat regions, respectively (Hur and Lee, 2021). A brief description of the pathogenic LRRK2 mutations is reported below.

1.2.5.1 PD-linked pathogenic LRRK2 mutation in the ROC-COR domain

The frequency of LRRK2 mutations carriers among PD patients varies in different ethnicity. The *LRRK2* R1441G mutation, within the Basque population, has a frequency of 2.5% and 46% in sporadic and familial PD, respectively. This mutation is rarely found in other European populations, including other regions of Spain, or in North and South America (Deng et al., 2006). In the contrary, the R1441C mutation accounts for the second most common LRRK2 mutation found in Europe, being the principal genetic cause of PD among Belgian patients with PD (Nuytemans et al., 2008). While R1441G/C mutations have not been described among Asian patients with PD, the R1441H mutation has been reported in Asia, Europe, and North America (Ross et al., 2011, 2009).

For several protein kinases, dimerization is a prerequisite for catalytic activity. Indeed, also in the case of LRRK2, a functional correlation between dimerization and kinase activity seems to exist as well (Greggio et al., 2008; Sen et al., 2009). The pathogenic mutants in the ROC (R1441C/G/H) and COR (Y1699C) domains

were related to impairments in dimerization properties. In the PD-linked R1441C/G/H mutants, a structure-based model of ROC revealed that mutations most probably decrease GTPase activity while enhancing the ability to bind GTP by disrupting ROC dimerization (Deng et al., 2008; Liao et al., 2014). It has been showed that GTP binding to the Roc domain regulates the kinase activity of LRRK2, and R1441C/G/H were demonstrated to up-regulate kinase activity (Liao et al., 2014; West et al., 2005). Additional studies have prompted that the Y1699C mutation impairs the dimerization of LRRK2, thereby reducing the activity of the GTPase. The authors found that the intra-molecular ROC:COR interaction is favoured over ROC:ROC dimerization. The pathogenic Y1699C mutation, situated at the ROC:COR interface, strengthens the intramolecular ROC:COR interaction, weakening the dimerization of LRRK2 at the ROC-COR tandem domain and resulting in decreased GTPase activity (Daniëls et al., 2011). It is noteworthy that mutations arising outside the ROC-COR region have been rarely found to directly abrupt LRRK2 dimerization. In line with this, in the isolated ROC-COR bidomain (Roco fragment), all 4 of these mutants demonstrated reduced self-interaction as compared to WT fragment (Klein et al., 2009).

Among the mutations within the COR domain is *LRRK2* R1628P, which was identified as genetic risk factor for PD especially among Han-Chinese's ethnic (Zhang et al., 2016). It was shown that R1628P substitution enables Cdk5 (Cyclin Dependent Kinase 5) phosphorylation of LRRK2 and upregulates its kinase activity (Shu et al., 2016).

1.2.5.2 PD-linked pathogenic LRRK2 mutation in the Kinase domain

The G2019S substitution of the MAPKKK domain of LRRK2 is the most common disease-causing mutation. It account for 4-5% of familial PD cases, but it is also a common mutation (approximately 1%) in sporadic PD (Gorostidi et al., 2009; Healy et al., 2008; Latourelle et al., 2008; Lesage et al., 2005; Marder et al., 2015). The frequency map of G2019S mutations in different population is very different. *LRRK2* G2019S mutation carriers account for 20-40% of all familial PD cases and 10-30% of sporadic cases in Morocco, Algeria, Tunisia, and Ashkenazi Jews (Alcalay et al., 2013; Bouhouche et al., 2017; Hulihan et al., 2008; Ishihara and Brayne, 2006; Lesage et al., 2005). On North Americans of European descent, nearly 2% of familial PD patients are carriers of G2019S, whereas up to 9% of sporadic cases have the allele (Cilia et al., 2014; Ferreira et al., 2007; Saunders-Pullman et al., 2011; Sierra et al., 2011; Yescas et al., 2010).

Regarding the biological feature of the G2019S mutation, i*n vitro* kinase assay using the full length recombinant LRRK2 protein have reported a 2- to 3-fold increase in the kinase activity (both autophosphorylation and phosphorylation of exogenous kinase substrates) (West et al., 2005). This 'gain-of-function' mechanism is suggested to be associated with the toxicity of the *LRRK2* G2019S mutation. Elevated levels of αSyn and tau proteins, mitochondrial dysfunction, disruption of synaptic vesicle transport, abnormal activation of Erk, c-Jun, and Akt signaling pathways have been observed after overexpression of the G2019S mutant, thus resulting in disruption of apoptotic regulation, hyperautophagy and reduce neurite outgrowth (Howlett et al., 2017; Litteljohn et al., 2018; Qing et al., 2009; Ren et al., 2019; Vermilyea and Emborg, 2018).

Two adjacent mutations (I2012T and I2020T) (Lu et al., 2005) were also mapped to the same domain, but are less frequent in the worldwide population. Recent extensive biochemical characterization of I2020T *LRRK2* reveals that this mutation causes increase kinase activity, *via* stabilization of the active state conformation, and increase rate of phosphoryl transfer (Ray et al., 2014). These data strongly suggest the relevance of the kinase domain for LRRK2-related disease.

1.2.5.3 PD-linked pathogenic LRRK2 mutation in the N- and C-terminus domain

Genetic studies have identified pathological relevant variants in domains outside the catalytic core. LRRK2 encompasses several domains involved in protein-protein interactions, namely the armadillo and LRR repeats at the N-terminus as well as WD40 repeats at the C-terminus (Marín, 2006). Through these domains, LRRK2 acts as a hub orchestrating various protein complexes involved in specific cellular functions.

Multiple amino acid variants have been found in the WD40 domain, and one, G2385R, showed an increased risk of developing idiopathic PD in Han Chinese and Korean ethnicity (Funayama et al., 2007; Tan et al., 2009; Xie et al., 2014). Studies suggest that the G2385R variant abolishes the physiological activity of LRRK2 and, therefore behaves as a partial loss-of-function mutation (Carrion et al., 2017; Rudenko et al., 2012), suggesting a pathogenetic mechanism different from the above reported LRRK2 kinase-activating mutations.

Recently a novel variant harboured within the N-terminal domain, E193K, was identified in an Italian family and the functional and molecular consequences of this variant characterized in cellular models (Perez Carrion et al., 2018). *In silico* prediction as well as *in vitro* evidence suggest that the E193K substitution impacts on N-terminal domain folding and therefore might alter its biochemical features (Perez Carrion et al., 2018). Since the *LRRK2* E193K variant was the focus of my investigation, a short description is given below.

1.2.5.1.1 The E193K mutation

The E193K *LRRK2* variant, consisting in an exchange of a glutamic acid into a lysine at position 193, was identified in an Italian family with people affected by early onset PD. The whole-exome sequencing was performed in the three, out of 10, siblings affected by PD (Figure 1.6). In all the three brothers the E193K substitution was present in the heterozygous state. The clinical symptoms were characteristic of idiopathic PD, with onset around 46-48 years of age, showing slow progression, and no cognitive decline, in all three affected siblings. The variant was also tasted in the other relatives: the same variant transition was also detected in two healthy relatives, suggesting incomplete penetrance as reported for other LRRK2 mutations. This variant is absent from the public mutation databases (GnomAD Browser) and ethnically matched controls (about 1800 Italian exomes) (Perez Carrion et al., 2018).

A

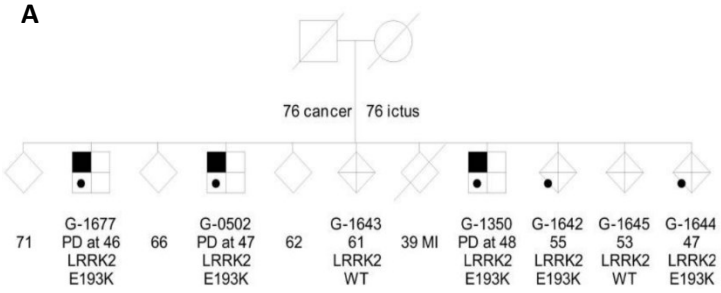

B

patients	age of onset	UPDRS score	clinical signs
G-0502	47	11 10yrs 36 16yrs	resting tremor, bradikinesia and rigidity of the arm at diagnosis; dyskinesias at 10 yrs of disease; cognitive function preserved; depression,apathy and sleep problems
G-1350	48	11 5yrs	resting tremor, bradikinesia and rigidity of the arm at diagnosis;
G-1677	46	22 22yrs	left leg stiffness and bilateral resting tremor at diagnosis; severe motor fluctuations and dyskinesias at 14 yrs of disease

C

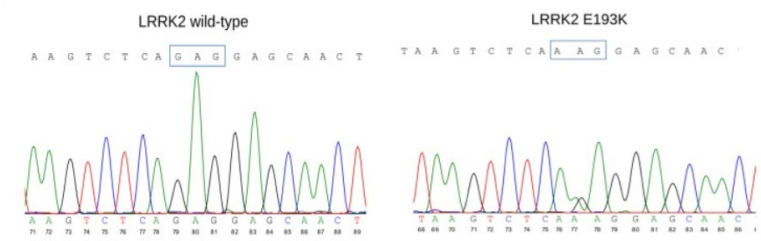

***Figure 1.6. Simplified genetic representation of the analysed family**. (**A**) Symbols with black upper corner indicate individuals affected by Parkinson's disease (PD). The result of leucine-rich repeat kinase 2 (LRRK2) genetic screening for the mutation was either wild type (WT) or heterozygous carrier (E193K). (**B**) The table summarizes clinical features of the three E193K carriers. (**C**) Sequencing of PCR product from exon 6 of WT and mutant alleles. The left chromatogram of the portion of the sequencing gel shows the wild allele and the right the heterozygous mutant allele (Adapted from Perez Carrion et al., 2018).*

1.2.6 The kinase activity of LRRK2: a boost into new drug therapies

As widely discussed above, mounting evidence strongly pointed to the fact that LRRK2 kinase activity is critical for the mutant *LRRK2*-induced PD phenotypes. Additionally, kinase-dead mutant versions of LRRK2 were found to be less toxic than their kinase-active counterparts in many cellular and animal models. Hence, modulation of LRRK2 kinase activity *via* selective small-molecule inhibitors has been brought forward as a potentially valid treatment for PD. Over the past decade, drugs discovery studies have identified many compounds able to successfully suppress LRRK2 kinase activity. So far, four generations of drugs have been developed (West, 2017).

The so-called "0" generation comprises early compounds; among them H-1152, GW5074, staurosporine, and sunitinib, and are mostly non-selective kinase inhibitors. They have relatively poor efficacy and poor blood-brain barrier (BBB) permeability.

The limitations of these compounds in clinical and research applications have prompted the further development of new, more favourable compounds (Zhao and Dzamko, 2019). LRRK2-IN-1 (Deng et al., 2011), CZC-54252, CZC-25146 (Ramsden et al., 2011), and TTT-3002 (Yao et al., 2013) were the first generation of selective LRRK2 kinase inhibitors, with better potency. Unfortunately, none of these compounds can traverse the BBB, and therefore, they were less favourable for clinical applications. Instead, they represent *in vitro* helpful tools to accelerate the comprehension of LRRK2 biology and pharmacology.

The second generation of LRRK2 kinase inhibitors included small compounds with increased BBB permeability, greater potency and selectivity, and less off-target effects. HG-10-102-1 was the first compound shown to penetrate the BBB and suppress LRRK2 activity in mouse brain (Choi et al., 2012). Later, GSK2578215A (Reith et al., 2012) and GNE group (GNE-7915, GNE-0877; GNE-9605) were developed (Estrada et al., 2012; Estrada and Sweeney, 2015).

The latest LRRK2 inhibitors belonging to the third generation are PF-06685360 (Andersen et al., 2018) and MLi-2 (Fell et al., 2015). MLi-2 exhibited excellent *in vitro* potency and showed dose-dependent reduction of LRRK2 kinase activity in mice either peripherally or centrally. Additionally, it appeared well tolerated for up to 15 weeks when administered daily at 30 mg/kg (Fell et al., 2015). These two inhibitors are in active preclinical development (Tolosa et al., 2020).

Currently, there are two LRRK2 kinase inhibitors, known as DNL201 and DNL151, which are under clinical development. The phase I study established the safety and the target engagement of DNL201 in healthy people. Global Phase II testing started in 2020 and is already ongoing (Tolosa et al., 2020).

A critical point for translating LRRK2 inhibitors into clinical practice is a comprehensive understanding of any potential safety implications of such compounds. Since the ATP-binding sites are highly conserved across kinases, the inhibitors of LRRK2 kinase deal with the risk of unwanted inhibition of unknown kinases in the

cell. Moreover, LRRK2 is not a brain-specific protein, being also highly expressed in peripheral tissues (notably in kidney, lung, and immune cells) (Marchand et al., 2020). The toxicology of LRRK2 kinase inhibition in preclinical studies has so far revealed adverse effects affecting lungs and kidneys (Herzig et al., 2011). Accordingly, an appropriate inhibition level of LRRK2 necessary to accomplish a therapeutic benefit by preventing any potential toxic effects must be established.

1.3 Aims

LRRK2 encompasses several domains involved in protein-protein interactions, namely the armadillo and LRR repeats at the N-terminus as well as WD40 repeats at the C-terminus (Marín, 2006). The identification of *LRRK2* as a PD causative gene boosted the interest on its GTPase and kinase domains, and the possible link of the modified enzymatic activities to the pathological cascade (Rosenbusch and Kortholt, 2016). However, genetic studies have identified pathological relevant variants in domains outside the catalytic core. Therefore, to better understand the role of this protein in pathophysiological conditions, studies are gaining deep insight into the functional role of the LRRK2 interactome due to these LRRK2 domains (Harvey and Outeiro, 2019). In our laboratory, we focused on the functional characteristics attributed to LRRK2 by its N- and C-terminal domains. In previous works, our group and others have contributed to clarify the functional and molecular features conferred by the C-terminal WD40 domain and a variant bearded within this domain, G2385R (Carrion et al., 2017; Piccoli et al., 2014). In order to further research on this issue, the objective of my work was to investigate the N-terminal domain function, which is less explored.

It is recognized that this domain is involved in LRRK2 supra-molecular organization (Guaitoli et al., 2016). Since LRRK2 is notably involved in vesicular trafficking, the aim for the proposed study was to investigate the role as a scaffold of the N-terminal domain of LRRK2 and its functional impact on synaptic vesicle (SV) dynamics. Recently, a novel variant carried within the N-terminal domain, E193K, was identified in an Italian family and we characterized its functional and molecular impact on vesicle dynamics (Perez Carrion et al., 2018). As reported in the introduction, the LRRK2 N-terminal domain encompasses several serine residues that undergo phosphorylation, thus potentially influencing LRRK2 function. Looking at the distribution of N-terminus LRRK2 phosphorylated residues, most interest has focussed on the serine 910/935, which are expected to interact with the 14-3-3 proteins and modulate subcellular distribution of LRRK2 (Marchand et al., 2020; Nichols et al., 2010; Zhao et al., 2015). With this in mind, we sought to investigate if the localization of the phosphorylation-dead mutant *LRRK2* S935A is modified and what are the consequences of this mislocalization on SV dynamics.

Elucidating the role of the protein-protein interaction domains of LRRK2 is fundamental for a better understanding of LRRK2 function in physiology and pathology.

2. Results and Discussion – Chapter I

As previously discussed, the purpose of this first part was primarily to investigate the interactome and the functional impact of the N-terminal domain of the LRRK2 on SV dynamics. Second, since a serine cluster (S910 and S935) is located between the armadillo and the LRR repeats in the N-terminus, we aimed to assess the role of these phosphorylation residues on the protein's functional activity.

The study was performed in the N2a neuroblastoma (ATCC CCL-131) cell line, which endogenously expresses the LRRK2 protein at a very low extend. In order to perform biochemical and functional experiments, cells were transfected with a panel of Red Fluorescent Protein (RFP)-tagged LRRK2 derived constructs.

2.1 The N-terminal domain influences LRRK2 interactions and impacts on vesicle trafficking

LRRK2 N-terminal Armadillo, LRR, and Ankyrin repeats as well as the C-terminal WD40 domain have been predicted to be involved in protein complex interactions (Guaitoli et al., 2016; Mills et al., 2014). There is evidence that LRRK2 directly binds SV proteins of and modulates vesicles trafficking. Using pull-down experiments, we first exploited the possibility that the N-terminal domain could interact with vesicle-associated proteins (synapsin I) and cytoskeletal proteins (actin and tubulin) which are known partners of LRRK2 (Carrion et al., 2017; Piccoli et al., 2011, 2014). To assess the role of the LRRK2 N-terminal domain in such interactions, we expressed Strep-FLAG full-length LRRK2 and Strep-FLAG LRRK2ΔN-term (lacking the first 913 amino acids) in N2a cells. Upon streptavidin-pull-down, we eluted the interacting proteins and analysed them by western-blotting (Fig. 2.1A).

Both the analysed constructs (LRRK2 and LRRK2ΔN-term) can interact with the investigated proteins, although with a different affinity (Fig. 2.1A). Indeed, we found that the interaction with synapsin I, α-tubulin, and β-actin was significantly decreased in the LRRK2ΔN-term variant (Fig. 2.1B), suggesting that the N-terminal domain plays a role in the control of LRRK2 interactome.

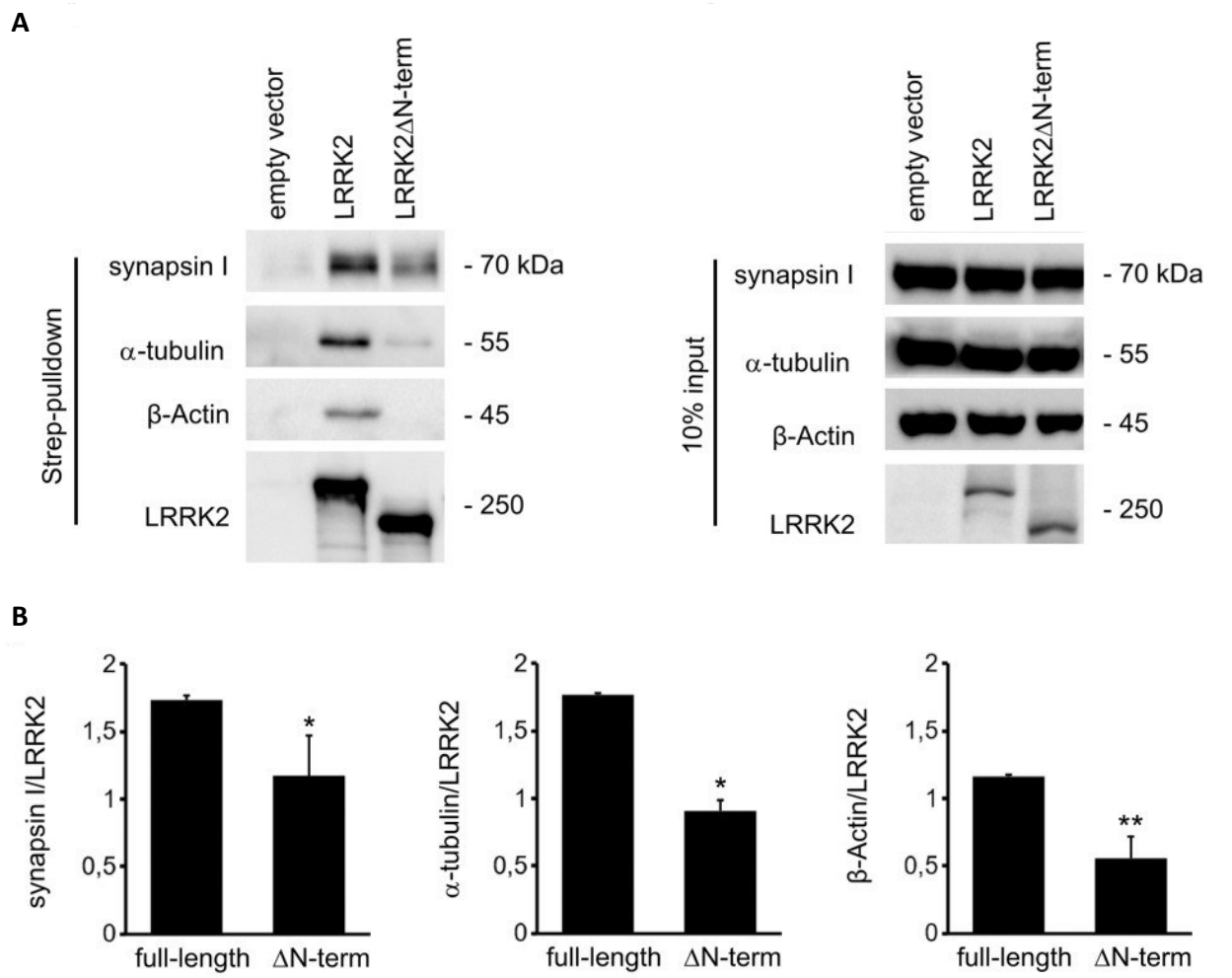

Figure 2.1. LRRK2 interacts with proteins involved in vesicle trafficking. *(**A**) We isolated on streptavidin resin full-length Strep-FLAG-LRRK2 and Strep-FLAG-LRRK2ΔN-terminus proteins from N2A over-expressing cells. Interacting proteins were resolved by western blotting. (**B**) We evaluated the extent of Synapsin I, α-tubulin and β-Actin bound to the different LRRK2 variants. Data are expressed as optical density and normalized versus amount of precipitated LRRK2 protein. Graphs reports mean ± SE, *p < 0.05, **p < 0.01 Student's T-test, n = 4 independent experiments.*

We then addressed our studies to the functional impact of the N-terminal domain. Since the proteins found to interact with the N-terminal domain are implicated in the control of neurotransmitter release and many reports correlate LRRK2 to synaptic functions (Matta et al., 2012; Piccoli et al., 2011; Shin et al., 2008), we investigated whether the N-terminal domain is involved in vesicular trafficking by means of the sypHy reporter coupled to total internal reflection fluorescence microscopy (TIRFM). SypHy is a fusion protein between synaptobrevin (VAMP2) and a pH-sensitive variant of the Green Fluorescent Protein (GFP) (Daniele et al., 2015). The protein is switched off when present in the vesicles, because of the low luminal pH (pH~5.6), but when the vesicles fuse with the plasma membrane and meet the neutral extracellular space (pH~7.4), the fluorescence signal rapidly appears. Therefore, every discrete spot-like signal represents a vesicle fusion event. We recorded the cells by TIRFM, a particular fluorescence microscopy technique which enables the selective visualization of events taking place at the plasma membrane or immediately beneath it, thus providing the spatio-temporal resolution necessary to follow vesicle dynamics. Counting the number of fusion events occurring in the cells, in the time course of the experiments, we can evaluate the impact of LRRK2 mutants on vesicle dynamics.

To perform the functional experiments, we over-expressed in N2a neuronal line the sypHy reporter together with a panel of RFP-tagged LRRK2 derived constructs: LRRK2 full-length, LRRK2 lacking the first 913 amino acids (hereinafter LRRK2ΔN-term) as well as a complementary deletion construct LRRK2 aa 1–983, containing the N-terminal Armadillo and Ankyrin domains (hereinafter N-terminal domain) (Fig. 2.2A). Since the trafficking of synaptic vesicles can be influenced by the relative expression of LRRK2 constructs and the sypHy reporter, firstly, by western-blotting analysis we verified that different LRRK2 constructs show similar expression yield and do not overtly influence the level of sypHy within cells (Fig. 2.2B-D).

Next, we analysed the impact of the N-terminal armadillo domain on vesicles dynamics. At 48 hours following co-transfection of LRRK2-derived constructs and sypHy, real-time recordings of vital cells visualized in TIRF microscopy were performed for 30 seconds, at a 1 hertz frequency. We aimed to evaluate the number of fusion events and the change in the fluorescence intensity produced by the fusion of all vesicles with the plasma membrane in cells transfected with the various LRRK2-derived constructs. Given that number of the recorded events across the cell is also dependent on cell dimensions, we normalized the data to cell area. Upon over-expression, full-length wild-type LRRK2 significantly increased the number of spontaneous fusion events (Fig. 2.2G,H) without changing single peak intensities (Fig. 2.2E,F). The expression of the isolated LRRK2 N-terminal domain did not elicit changes in SV dynamics as judged by the quantification of number of events, total fluorescence intensity (Fig. 2.2E,G,H) or increase in peak fluorescence intensity (Fig. 2.2F). To further characterize the functional role of LRRK2 N-terminal armadillo domain, we studied SV trafficking upon expression of LRRK2 construct lacking the N-terminal armadillo domain (LRRK2ΔN-term). Interestingly the expression of LRRK2 ΔN-term increased the frequency of fusion events and the total fluorescence elicited (Fig. 2.2E-H), thus indicating massive SV release.

Together, our findings indicate that the N-terminal domain (i.e., containing the Armadillo and Ankyrin domains) is a critical effector of LRRK2 function on SV dynamics.

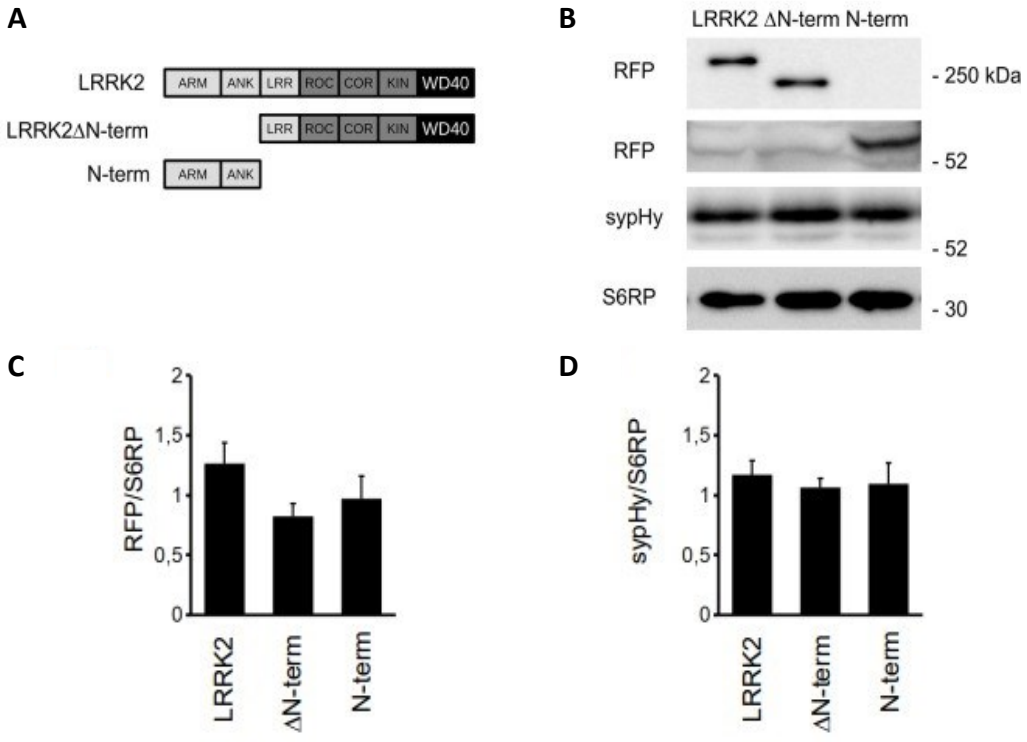

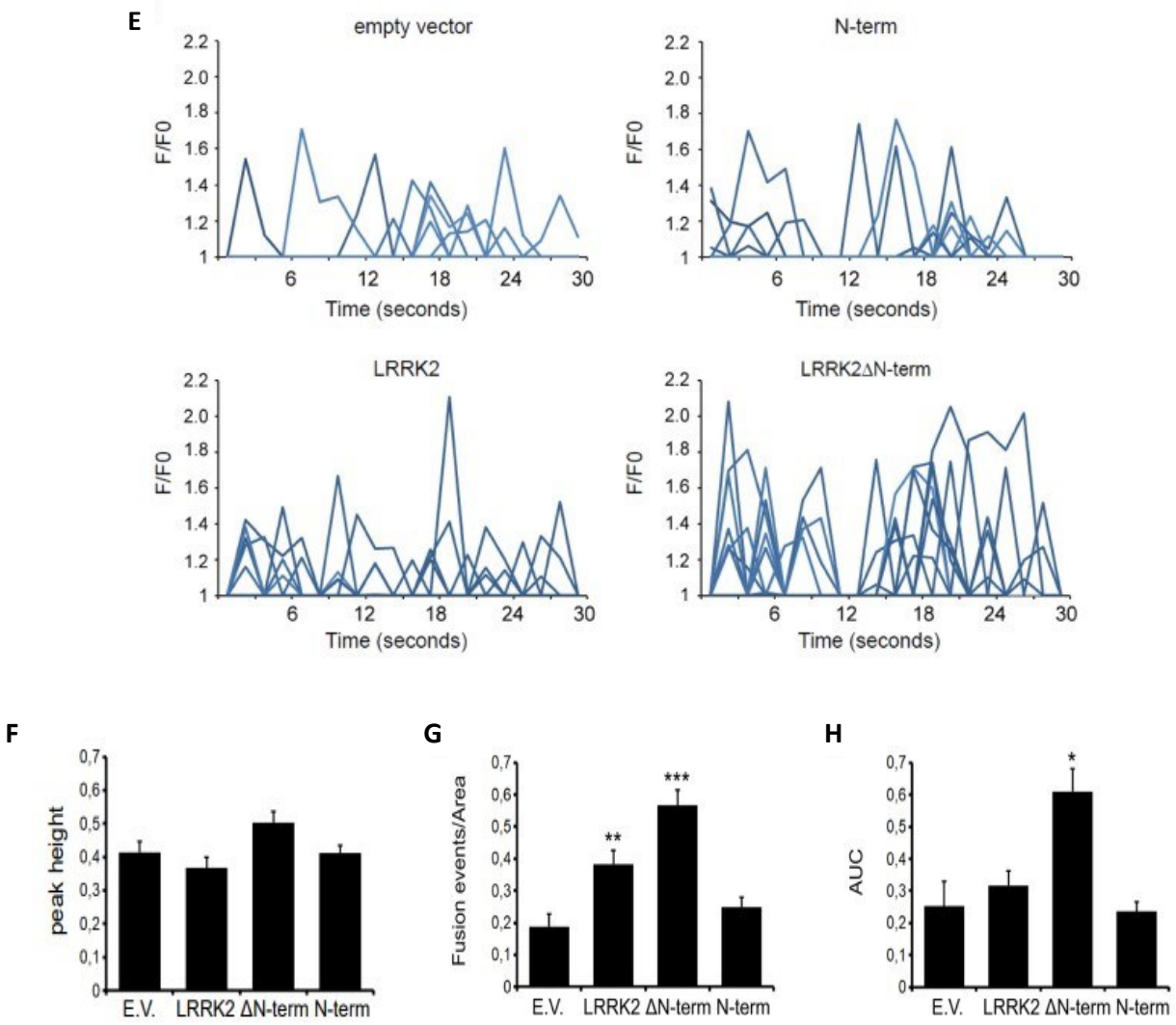

Figure 2.2. Domain-wise dissection of LRRK2 impact on vesicle trafficking. *(**A**) Schematic representation of RFP-LRRK2 derived constructs. The distinct LRRK2 domains are indicated. Protein-protein domains: ARM, armadillo repeats; ANK, ankyrin repeats; LRRs, leucine-rich repeats; WD40, WD40 repeats; Roc, Ras of complex proteins; COR, C-terminal of ROC; Kin, kinase domain. (**B**) Western blotting analysis of cells expressing synaptopHluorin reporter (sypHy) together with RFP-LRRK2 derived constructs. (**C**) The graphs show RFP-LRRK2 derived construct (**D**) and sypHy optical density normalized upon S6 ribosomal protein (S6RP) level as detected by western blotting. Data are expressed as mean ± SE, n=5. (**E**) Time course analysis of fusion events occurring in N2A cells transfected with the different LRRK2 derived constructs. N2a cells were co-transfected with sypHy reporter and empty vector (E.V.) or the indicated RFP-LRRK2 derived constructs. TIRFM imaging was performed 48 h after transfection. Peaks of fluorescence intensity correspond to single fusion events. Fluorescence data are expressed as F/F0. (**F**) The graph shows the average peak height of the synaptic events for the different constructs. Data are expressed as mean ± SE of up to 20 cells per construct. The graphs show the total number of fusion events (**G**) and the resulting fluorescence changes (**H**) expressed as Area Under Curve (AUC) for each construct. Data are normalized for the cell area and are expressed as mean ± SE; n = 20 cells per construct, in three independent experiments. *p < 0.05, **p < 0.01, ***p < 0.001 vs empty vector, ANOVA.*

These observations bring further support to the model describing LRRK2 as a key player in SV dynamics (Piccoli et al., 2011). We believe that this function arises, at least in part, from the binding of LRRK2 to proteins involved in SV mobilization such as α-tubulin, β-actin, and synapsin I. Previously we reported that also the WD40 domain interacts with SV-associated proteins and SV itself (specifically, the isolated WD40 domain directly binds to SV and harbours interactions with α-tubulin, β-actin, and synapsin I) (Piccoli et al., 2014).

This result, however, is only apparently in conflict with our data on the N-terminal domain. Indeed, LRRK2 is reported to be a dimer characterized by a complex architecture in which distant interdomain contacts. In particular, a model of the dimeric LRRK2 holoenzyme generated by combined homology models, molecular docking and experimental constraints disclosed a compact folding of the LRRK2 dimer in which the C-terminal WD40 domain is in close proximity to the N-terminal domains (Guaitoli et al., 2016). Together, our data support this model and suggest that probably the N-terminal and C-terminal domains operate together in structuring the interaction site for SV and SV-associated proteins.

2.2 The E193K variant alters LRRK2-binding properties and affects vesicle trafficking

Through whole-exome sequencing performed in an Italian family with three siblings affected by early-onset PD, a variant E193K, consisting in the exchange of a glutamic acid to a lysine at position 193 of the LRRK2 protein, was identified (Perez Carrion et al., 2018). Interestingly, this variant falls within the N-terminal armadillo repeat structure, reinforcing the physiological importance of the N-terminal domain of LRRK2 and suggesting the possibility that this variant may impact on the domain function. *In silico* prediction as well as *in vitro* evidence suggest that E193K variant impact on N-terminal domain folding and therefore might alter its biochemical features (Perez Carrion et al., 2018). Moreover, the substitution of a negatively charged residue with a positively charged one is strongly expected to influence the biochemical characteristics of the N-terminal armadillo domain of LRRK2. Therefore, we first sought to find out whether the E193K variant has an impact on the binding properties of LRRK2. To address this question, we analysed the binding properties of LRRK2 wild-type and E193K variant. We expressed Strep-FLAG full length LRRK2 and Strep-FLAG E193K in N2a cells. Upon streptavidin-pull-down, the eluted proteins were subsequently resolved by western blotting. As shown in the image (Fig. 2.3A), both the analysed constructs (LRRK2 wild-type and LRRK2 E193K) can interact with the investigated proteins. Intriguingly, our results showed that the E193K variant significantly reduces the affinity of LRRK2 towards synapsin I, α-tubulin, and β-actin (Fig. 2.3B).

We already described that the N-terminus domain has an impact on vesicles trafficking. Since we found that the E193K variant disrupts the biochemical binding properties of LRRK2, we questioned whether the E193K variant perturbs the interaction between LRRK2 and SVs itself. To test this hypothesis, in collaboration with Dr. Franco Onofri from University of Genova, we tested the amount of LRRK2 binding to SVs *via* a high-speed sedimentation assay. Purified full-length *LRRK2* WT or E193K RFP-fusion proteins from N2a transfected cells were incubated with purified SVs. Then, SVs were isolated by high-speed centrifugation and the fraction of LRRK2 bound to SVs was revealed by electrophoresis and immunoblotting with an anti-RFP antibody. Data clearly revealed that the LRRK2 E193K binds less efficiently to purified SV than LRRK2 wild type (Fig. 2.3C,D).

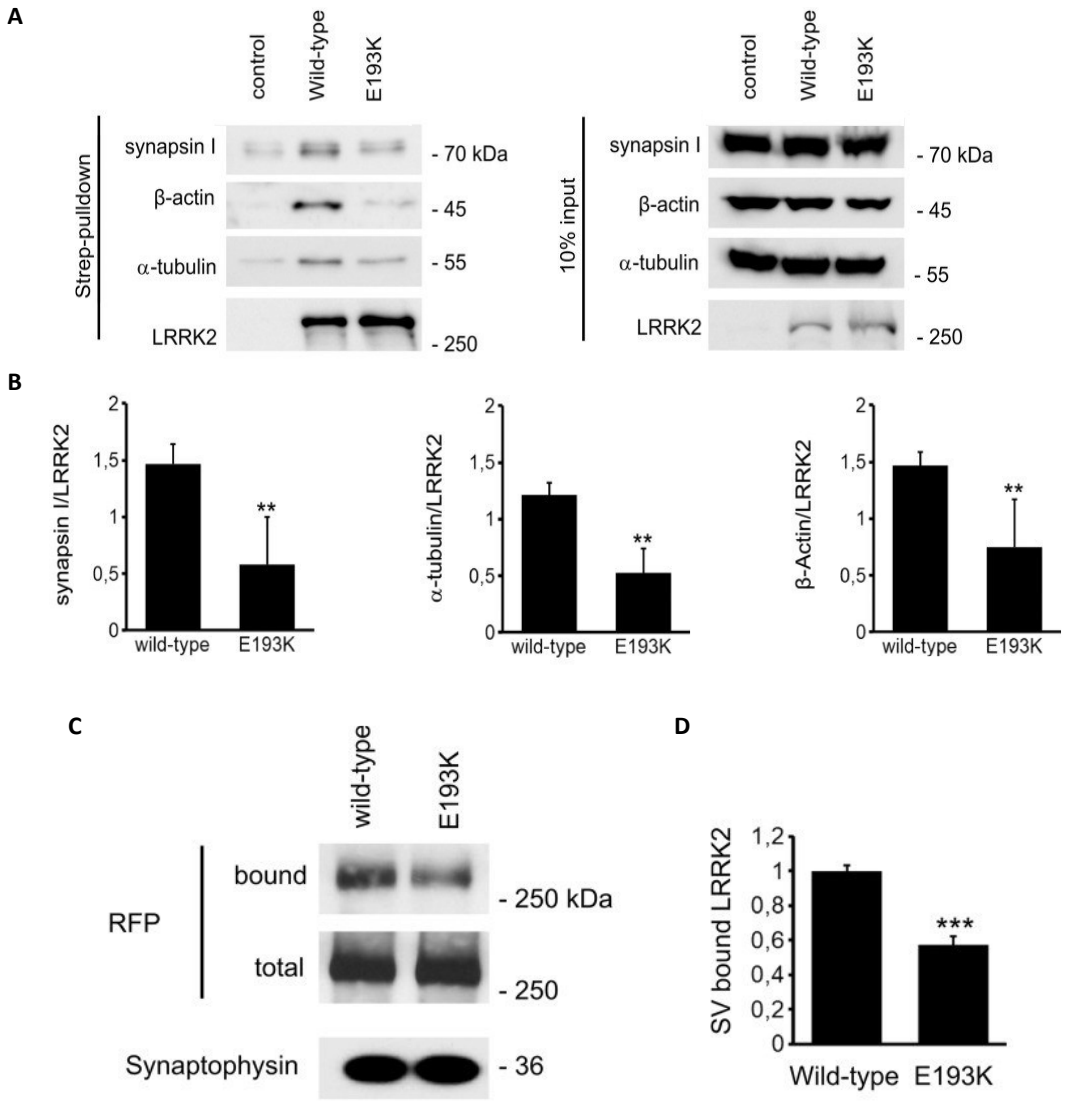

Figure 2.3. E193K mutation affects LRRK2 binding properties. *(**A**) We isolated on streptavidin resin full-length FLAG-LRRK2 wild-type and FLAG-LRRK2 E193K proteins from N2a over-expressing cells. Interacting proteins were resolved by western blotting. (**B**) We evaluated the extent of synapsin I, α-tubulin, β-Actin bound to the different LRRK2 variant. Data are expressed as the ratio over LRRK2 wild type. Graphs reports mean ± SE; n = 4. **p < 0.01, Student's T-test. (**C**) We measured the extent of LRRK2 and SV binding by ultracentrifugation sedimentation assay. We incubated purified RFP-LRRK2 wild type and E193K variant with isolated SV (10 µg protein/sample). Bound RFP-LRRK2 was separated from free RFP-LRRK2 by high-speed centrifugation. We appreciated SV-bound LRRK2 by immunoblotting with anti-RFP antibody. The recovery of SV in the pellet was evaluated based on synaptophysin immunoreactivity. (**D**) The binding of RFP-LRRK2 wild type and E193K to SV was calculated as the ratio of total RFP-LRRK2 and expressed as mean ± SE, n = 6, ***p < 0.001, Student's t-test.*

Since synapsin and actin play an important role in the binding and restraining of SV to the actin cytoskeleton (Fdez and Hilfiker, 2007), we speculated that the E193K mutation may increase the redistribution of vesicles from the reserve pool towards the membrane, thus impinging the vesicle density in the ready-releasable pool. To test this possibility, we manifested the total pool of sypHy vesicles *via* NH_4Cl basification. Under epifluorescence microscopy, cells expressing wild type or *LRRK2* E193K showed similar vesicles density, suggesting that cells present the same total number of SV. Instead, underby TIRFM (i.e. within a range of up to 100 nm away from the plasma membrane where the ready releasable pool is located) the number of sypHy clusters were significantly increased in cells expressing *LRRK2* E193K (Fig.2.4A,B).

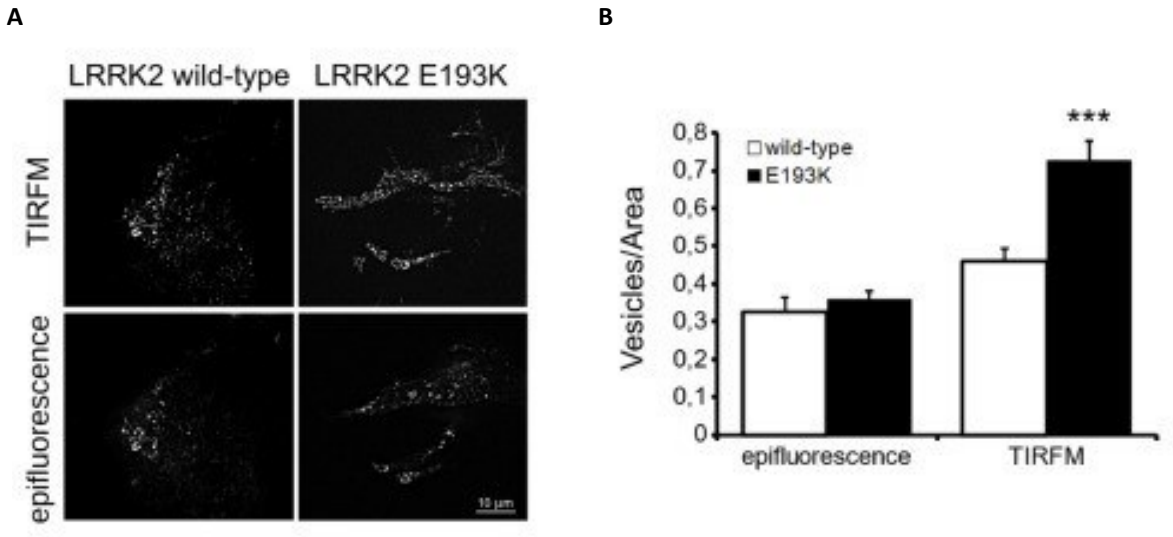

Figure 2.4. E193K mutation affects the SV number in the TIRF zone. *(**A**) Vesicle density in the TIRFM zone after NH_4Cl treatment. The cells were incubated with the membrane permeant NH_4Cl solution for 5 minutes, to label all sypHy positive clusters. Then, cells were fixed and imaged by epifluorescence or TIRFM to visualize vesicles docked to the plasma membrane. Each spot corresponds to a sypHy positive cluster. Scale bar = 10 µm. (**B**) The graph reports the number of sypHy positive clusters visualized in the same cell under epifluorescence or TIRFM. Data are normalized for the cell area and are expressed as mean ± SE; n = 15 cells for construct. ***p < 0.001, Student's T-test.*

Data confirm the hypothesis that the structural alterations induced by the E193K substitution functionally modify LRRK2 binding properties, thereby lowering its interaction with SVs and a specific subset of vesicular and cytoskeletal proteins responsible for their restrain in the reserve pool. This in turn, is expected to redistribute vesicles towards the membrane and, eventually, promote their fusion.

To test this possibility SV trafficking was measured in N2a cells expressing the wild type LRRK2 protein or the LRRK2 protein bearing the E193K mutation (Fig. 2.5A). By western blotting analysis we confirmed that the level of expression of LRRK2-derived constructs in the two clones were comparable and that the sypHy reporter level was not significantly affected by overexpression of the two constructs (Fig. 2.5B-D). We than analysed the impact of the E193K variant on sypHy vesicles trafficking by the same experimental strategy above reported (sypHy overexpression coupled to TIRFM). Detailed analyses of sypHy-positive SV dynamics revealed an increased number of fusion events in clones overexpressing *LRRK2* E193K with respect to *LRRK2* WT (Fig. 2.5E-G). No changes in single peak fluorescence were observed (Fig. 2.5H). A similar effect was detected in cells overexpressing the *LRRK2* ΔN-term construct, thus suggesting that the E193K variant might have abolished the physiological function of the N-terminal armadillo domain. Interestingly, previous findings showed that acute depletion of endogenous LRRK2 by siRNA correlates with an increase in SV fusion (Piccoli et al., 2011), due to greater sypHy clusters in the TIRF region (Carrion et al., 2017). Collectively, these data suggest that either LRRK2 acute silencing or *LRRK2* E193K overexpression have a similar impact on the trafficking and distribution of sypHy-positive vesicles near the membrane, suggesting that the E193K variant behaves as a loss-of-function mutation.

We attempted to rescue the E193K phenotype on vesicle trafficking by overexpressing the isolated N-terminal domain of LRRK2 in the *LRRK2* WT or E193K clones, together with the sypHy reporter (Fig. 2.5A). 48 hours post-transfection, western blotting analysis confirmed that LRRK2-derived constructs were expressed in a similar extent and did not affect significantly sypHy levels (Fig. 2.5B-D). However, the co-expression of the *LRRK2* N-terminus abolished the increase in the frequency of fusion events and the associated change in

total fluorescence detectable upon *LRRK2* E193K expression (Fig. 2.5E–H). These findings further prove that the E193K abrogates the physiological activity of LRRK2 and behaves as a partial loss-of-function mutation.

Loss-of-function mutations are usually recessively inherited, whereas LRRK2 mutations, despite incomplete penetrance, are well recognized as dominant (Monfrini and Di Fonzo, 2017). A recent biochemical characterization of LRRK2 dimers, comprising wild type/wild type, wild type/mutant, or mutant/mutant proteins, indicate that the hetero dimers of WT and mutant LRRK2 behave as wild type homodimers, suggesting that a key event in disease pathogenesis may be the gradual formation of mutant LRRK2 homodimer (Leandrou et al., 2019). In this scenario, the age-dependent accumulation of dysfunctional *LRRK2* E193K homodimers might influence synaptic transmission in a dominant-negative manner.

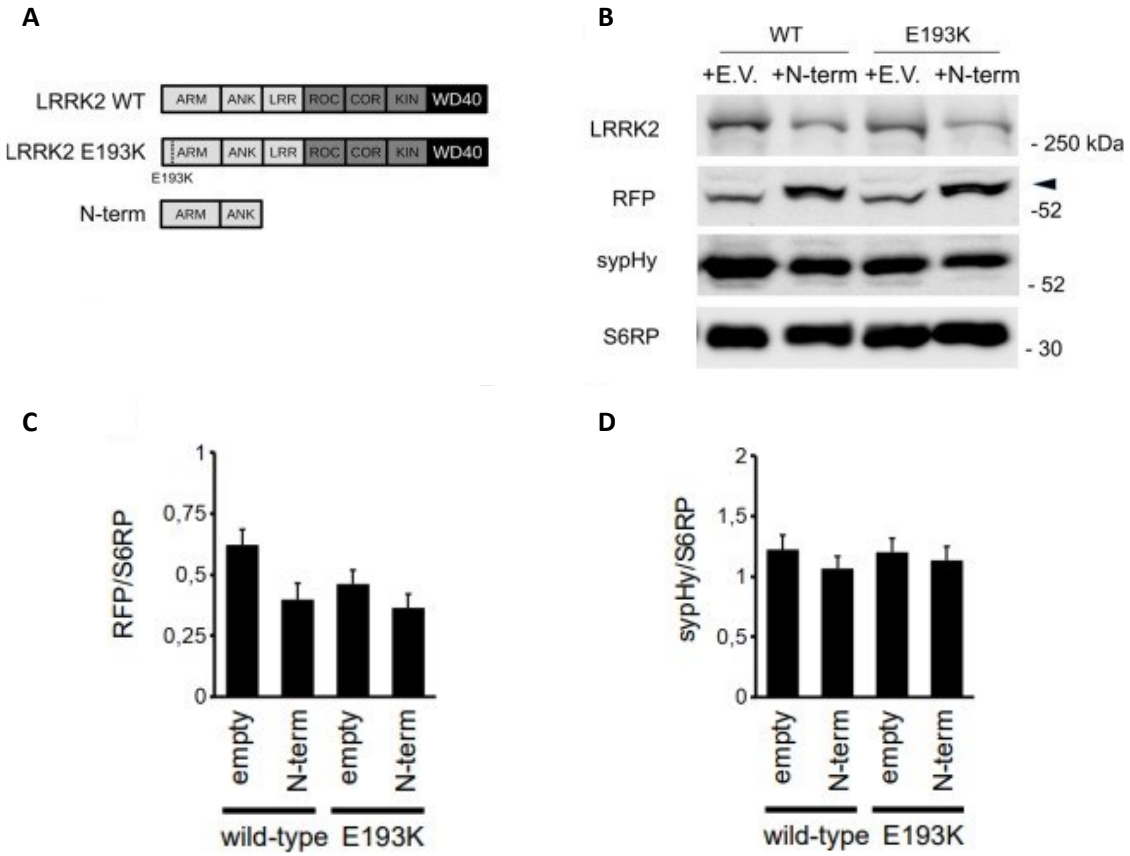

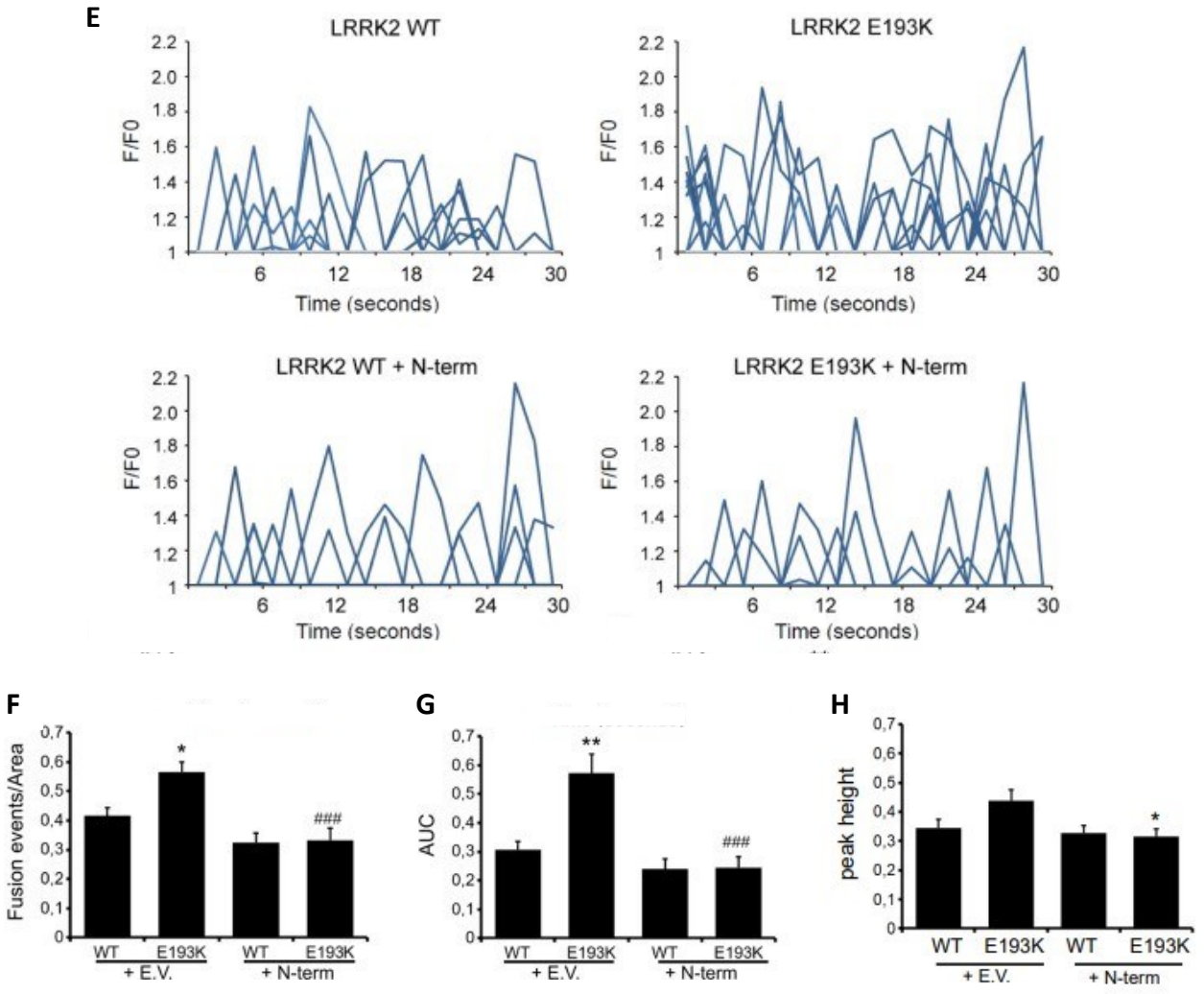

Figure 2.5. E193K variant affects vesicle trafficking. *(**A**) Schematic representation of LRRK2 wild type, E193K variant and N-terminus domain. The distinct LRRK2 domains are indicated. (**B**) Western-blotting analysis of WT and E193K N2a clones expressing sypHy reporter together with empty vector or RFP-LRRK2 N-terminus constructs. Arrowhead indicates the specific RFP positive band detected by the anti-RFP antibody. (**C**) The bars show the optical density of RFP-LRRK2 derived constructs (**D**) and sypHy detected by western blotting. Data are normalized on S6 ribosomal protein (S6RP) level and are expressed as mean ± SE; n=5. (**E**) Time course analysis of synaptic events occurring in N2a clones expressing wild type (WT) LRRK2 or E193K LRRK2 and transfected with the empty-vector or with the isolated N-terminal domain together with the sypHy reporter. Transfected cells were imaged by TIRFM 48 h later. Fluorescence data are expressed as F/F0. Peaks of variable fluorescence intensity correspond to single fusion events. The graphs show the total number of fusion events (**F**) and the resulting fluorescence changes (**G**) expressed as Area Under Curve (AUC) for each construct. Data are normalized for the cell area and are expressed as mean ± SE of up to 20 cells per construct, in three independent experiments. *p < 0.05, **p < 0.01 compared to LRRK2 wild type, ###p < 0.001 compared to empty vector transfected clones. (**H**) The graph shows the average peak height of the synaptic events for the different constructs. Data are expressed as mean ± SE of up to 20 cells per construct; *p<0.05 vs E193K.*

Collectively, these findings confirm the key role of the N-terminal domain in the contest of vesicle dynamics and support a possible pathological relevance of the *LRRK2* E193K variant. Even though the mutation is very rare and likely a private mutation, we believe that an extensive functional characterization of this variant could help in elucidating LRRK2 tasks.

2.3 LRRK2 phosphorylation on Ser-935 control both LRRK2 localization and activity

Under physiological conditions, LRRK2 is highly phosphorylated within the cell. There is great interest in understanding the role of LRRK2 phosphorylation as several pathological variants of the protein are characterized by a significant reduced state of phosphorylation, thus suggesting that phosphorylation plays a role in the development of PD (Dzamko et al., 2017; Zhao et al., 2015). Most interest has focussed on serine 910 and 935, which are located in the N-terminal domain, between the armadillo and the LRR repeats (Marchand et al., 2020).

Literature data indicate that phosphorylation of Ser-935 controls the LRRK2 binding to 14-3-3 proteins, an interaction required to target the kinase to the plasma membrane where the protein is predicted to dimerize and become activated. Mutations in Ser-910 and Ser-935 lead to loss of interaction of LRRK2 with 14-3-3 proteins and result in its accumulations in cytoplasmic aggregates (Nichols et al., 2010; Zhao et al., 2015) (Marchand et al., 2020). Curiously, this phosphorylation site falls in the N-terminal domain, which we are aiming to characterize, and once again influences LRRK2 interactome because, firstly, it impacts the binding to 14-3-3 proteins.

Considering the relevance of the Ser-935 LRRK2 phosphorylation site in the subcellular distribution of the kinase, we generated a mutant protein (S935A) that cannot be phosphorylated at Ser-935 and investigated the localization of the phosphorylation-dead mutant, by performing immunofluorescence experiments in N2a neuronal lines. Epifluorescence microscopy revealed a diffuse localization of the WT protein in the cytosol. In contrast, the *LRRK2* S935A mutant was still detected in the cytoplasm but clustered in aggregates (Fig. 2.6). Next, we asked whether Ser-935 phosphorylation controls the membrane expression of LRRK2. Since LRRK2 is abundantly present at the cytosolic level, in order to appreciate the localization of LRRK2 at the plasma membrane or associated to intracellular organelles, cells were treated with saponin before fixation. Used at low concentrations and for short periods, saponin allows the permeabilization of plasma membranes and facilitates the clearance of cytosolic proteins, so that the fraction of LRRK2 associated to intracellular organelles can be more easily detected. By TIRFM we were able to reveal that a fraction of the WT protein was recruited to the cell membrane, enriched in discrete spots or clusters, whereas the S935A mutant, despite being expressed by the cell at a similar level was almost undetectable at the plasma membrane (Fig. 2.6). This finding supports literature data regarding the impact of Ser-935 on LRRK2 subcellular localization and reveals that the basal LRRK2 phosphorylation is probably required to allow LRRK2 to cycle between a cytosolic form and a membrane-bound form.

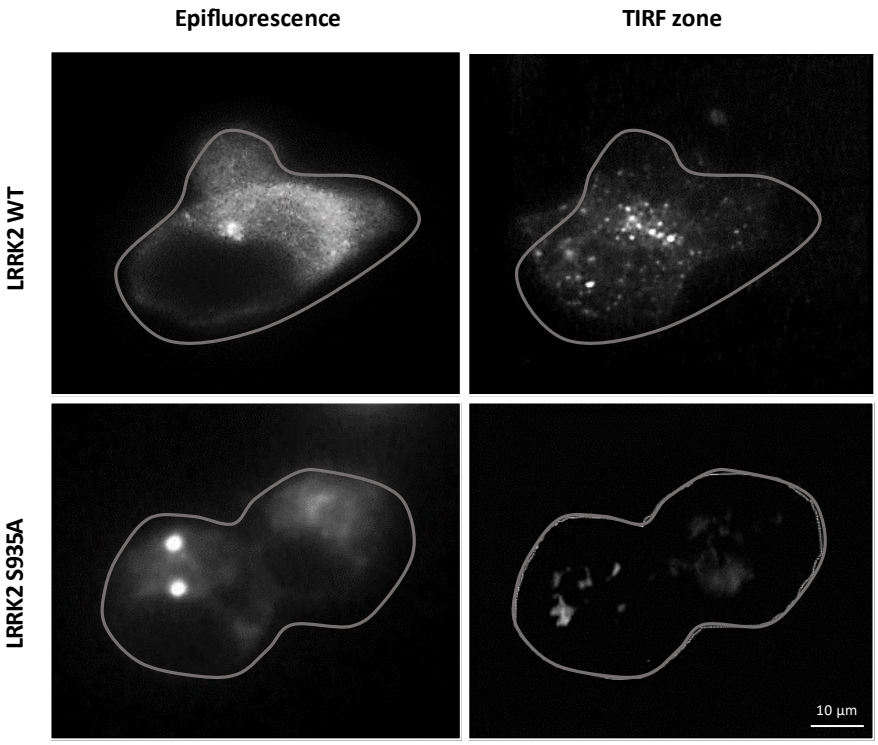

Figure 2.6. LRRK2 S935A phopho-dead mutant affect protein localization. *Representative images of N2a cells transfected with LRRK2 WT or LRRK2 S935A and incubated with 0.01% saponin for 1 minute. Then, cells were fixed and imaged by epifluorescence or TIRFM (100) to visualize LRRK2 localization to the plasma membrane. Scale bar: 10 µm.*

Since the localization of LRRK2 impacts its activation and controls the specificity of protein kinase activity on target substrates, we wondered whether this relocation may abolish the interaction of LRRK2 with the previously identified protein (synapsin I, actin and tubulin) and influence the intracellular distribution of SV. For this purpose, we manifested the total pool of sypHy vesicles through basification with NH_4Cl. Epifluorescence microscopy revealed no gross differences in the total number of vesicles between cells expressing wild-type or *S935A* LRRK2. In contrast, when we targeted our analysis to the TIRF zone, we found significantly more sypHy clusters in cells expressing the *LRRK2* S935A variant (Fig. 2.7A,B). These results further sustain the involvement of LRRK2 in SV trafficking and suggests that the reversable LRRK2 phosphorylation may control the number of SV in the readily releasable pool.

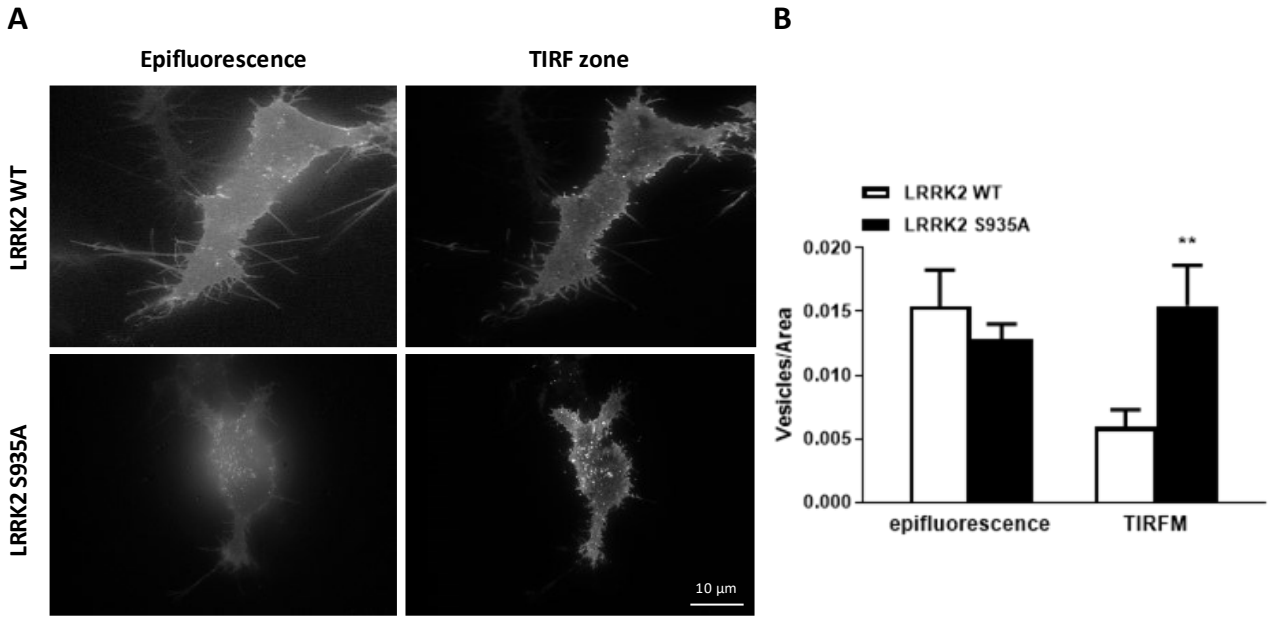

Figure 2.7. S935A mutation affects the SV number in the TIRF zone. *(**A**) Vesicle density in the TIRFM zone after NH_4Cl treatment. The cells were incubated with the membrane permeant NH_4Cl solution for 5 minutes, to label all sypHy positive clusters. Then, cells were fixed and imaged by epifluorescence or TIRFM to visualize vesicles docked to the plasma membrane. Each spot corresponds to a sypHy positive cluster. Scale bar = 10 µm. (**B**) The graph reports the number of sypHy positive clusters visualized in the same cell under epifluorescence or TIRFM. Data are normalized for the cell area and are expressed as mean ± SE; n = 15 cells for construct. **p < 0.01, Student's T-test.*

To verify whether the relocation of SV induced by the S935A construct also affect vesicle fusion, we overexpressed in N2a neuronal lines the sypHy reporter (green) together with RFP-LRRK2 full-length or RFP-*LRRK2* S935A variant (red) (Fig. 2.8A and B) and 48 hrs post-transfection, we monitored vesicle dynamics by TIRFM. As reported in figures 2.8C-E, upon overexpression, the S935A variant significantly increased the number of spontaneous fusion events and the total fluorescence elicited. A similar phenotype was detected also in cells transfected with the N-terminal mutants tested previously, thus indicating that *LRRK2* S935A mutations behaves like a loss of function mutation and that phosphorylation control LRRK2 activation.

Of note, single event amplitude was greater in cells expressing the *LRRK2* S935A mutant (Fig 2.8F). Peak amplitude represents the time required for vesicle fusion, attachment, and endocytosis prior to reacidification and recycling and is normally indicative of the vesicle mode of fusion (complete fusion vs transient fusion) (Daniele et al., 2015). The observed increase peak width in the S935A variant is indicative of complete vesicle fusion events at the plasma membrane, suggesting that phosphorylation not only controls the kinetics but also the fusion mechanism of SV.

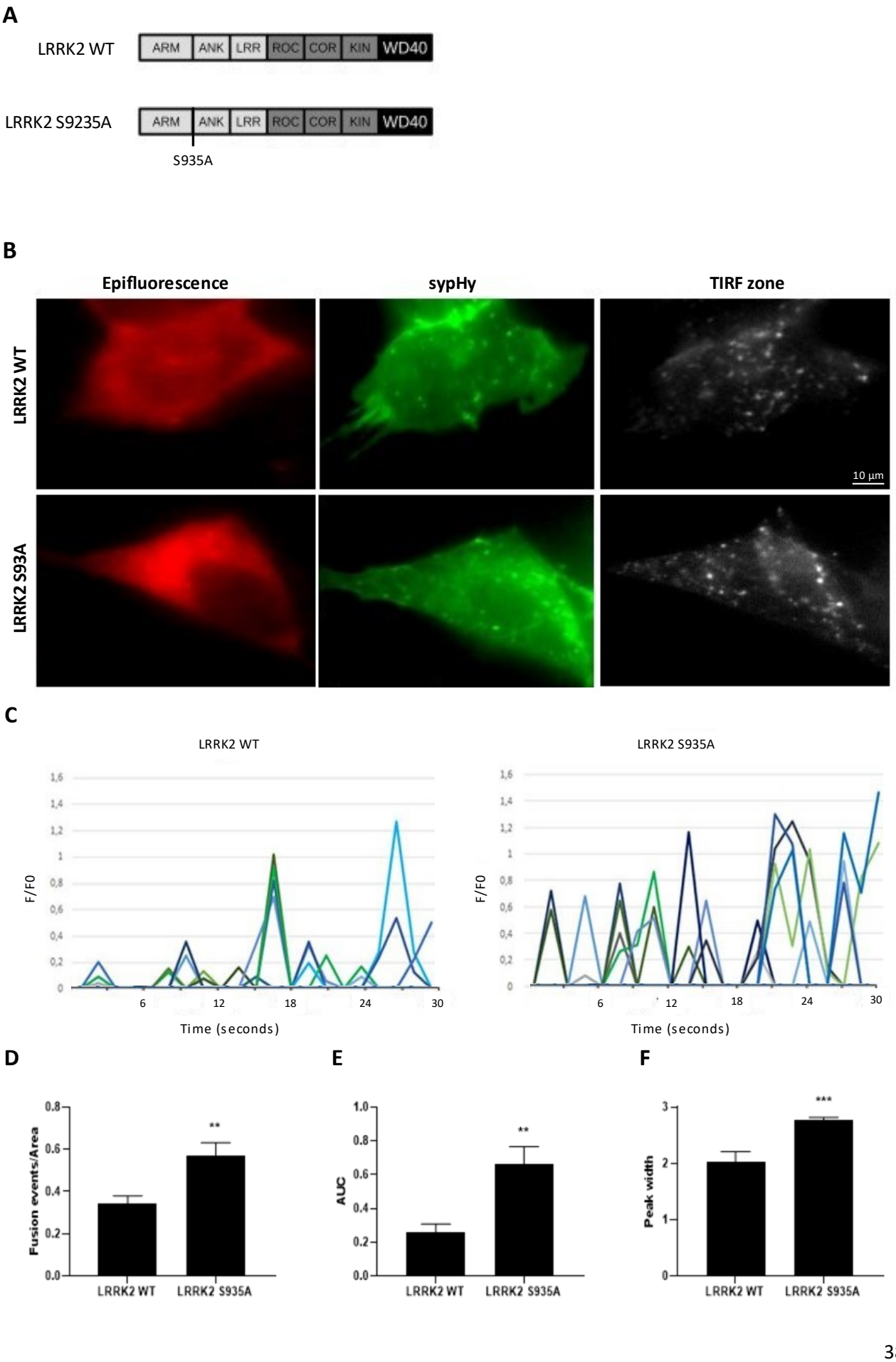
A
LRRK2 WT
ARM
ANK
LRR
ROC
COR
KIN
WD40
LRRK2 S9235A
S935A
B
Epifluorescence
sypHy
TIRF zone
LRRK2 WT
LRRK2 S93A
10 µm
C
LRRK2 WT
LRRK2 S935A
F/F0
Time (seconds)
D
Fusion events/Area
E
AUC
F
Peak width
LRRK2 WT
LRRK2 S935A

Figure 2.8. The LRRK2 S935A mutant increases the rate of synaptic vesicle exocytosis. *(**A**) Schematic representation of LRRK2 wild type and S935A variant. The distinct LRRK2 domains are indicated.(**B**) Representative epifluorescence and TIRFM (100 nm) images in N2a cells transfected with sypHy reporter (green) and the indicated RFP-LRRK2 (red) derived constructs. Scale bar: 10 µm. (**C**) Time course analysis of fusion events occurring in N2a cells transfected with the different LRRK2 derived constructs. N2a cells were co-transfected with sypHy reporter and the indicated RFP-LRRK2 derived constructs. TIRFM imaging was performed 48 h after transfection. Peaks of fluorescence intensity correspond to single fusion events. Fluorescence data are expressed as F/F0. The graphs show the total number of fusion events (**D**) and the resulting fluorescence changes (**E**) expressed as Area Under Curve (AUC) for each construct. Data are normalized for the cell area and are expressed as mean ± SE; n = 16 cells per construct, in three independent experiments. **p < 0.01, ANOVA. (**F**) The graph shows the average peak height of the synaptic events for the different constructs. Data are expressed as mean ± SE of up to 15 cells per construct. **p < 0.01, ANOVA.*

In conclusion, these findings highlight a critical role of N-terminal heterophosphorylation site at serine 935 in the control of LRRK2 membrane targeting and SV dynamics. Indeed, the S935A *LRRK2* mutant precipitates in intracellular aggregates and cannot be recruited to the plasma membrane. At the same time, the S935A substitution increases the frequency and amplitude of spontaneous synaptic events, as observed with other loss-of-function LRRK2 mutants (Carrion et al., 2017).

2.3.1 Future perspectives

The phosphorylation is a fundamental regulatory mechanism governing protein function. The Ser-935 residue is a phosphorylation site, however, unlike other serines found in the LRRK2 protein, its phosphorylation is potentially carried out by distinct upstream kinases. Possible candidates are members of the casein kinase (CK) family, protein kinase C (PKC), and kappa B kinase (IKK) inhibitor. In particular, PKC family of enzymes is a known regulator of synaptic function, including release of neurotransmitter (Sun and Alkon, 2012), where LRRK2 is known to play an important role. Since PKC-mediated phosphorylation modulates several proteins involved in vesicular trafficking (Leenders and Sheng, 2005), we have started to investigate if the serine 935 residue of LRRK2 might be a potential PKC target. Clarifying which players are engaged in tuning the phosphorylation balance of LRRK2 will be pivotal to further elucidate the molecular mechanisms underlying modulation of neurotransmitter release and how LRRK2 is (de)-regulated and impacts downstream signaling pathways.

3. Conclusions – Chapter I

Previous observations provide evidence that LRRK2 performs a critical role at the presynaptic site. As an integrated component of the presynaptic protein network, LRRK2 may act as a molecular hub that coordinates both storage and mobilization of SV (Piccoli et al., 2014, 2011). Our results further support such a role of LRRK2. We demonstrated that the N-terminal domain is crucial for interaction of LRRK2 with proteins implicated in SV mobilization and for the protein localization in intracellular compartments and suggest that mutations in this domain or modulation of its phosphorylation may affect LRRK2 function *via* perturbation of its localization and its physiological network of interactors (Fig 3.1).

LRRK2 influences SV dynamics, in part by binding to proteins involved in the mobilization of SV such as α-tubulin, β-actin, and synapsin I *via* its N-terminal domain. Synapsin I is known to control SV trafficking and availability at the plasma membrane, by reversibly cross-linking SV to each other and to the actin cytoskeletal network. This action is believed to be important for the formation and maintenance of a reserve pool (RP) of SV, as well as for the fine regulation of the balance between this RP and the ready releasable pool (RRP) (Cesca et al., 2010). Since the binding of synapsin I to SV and actin filaments participates in the formation of SV clusters and their anchorage to the actin cytoskeleton, we speculate that LRRK2, through its N-terminal domain, may take part to this event and control the transition of SV from the RP to the readily releasable pool. Accordingly, upon ΔN-*LRRK2* overexpression, we found that the density of sypHy-positive vesicles in the TIRF zone and the number of SV fusion events are increased.

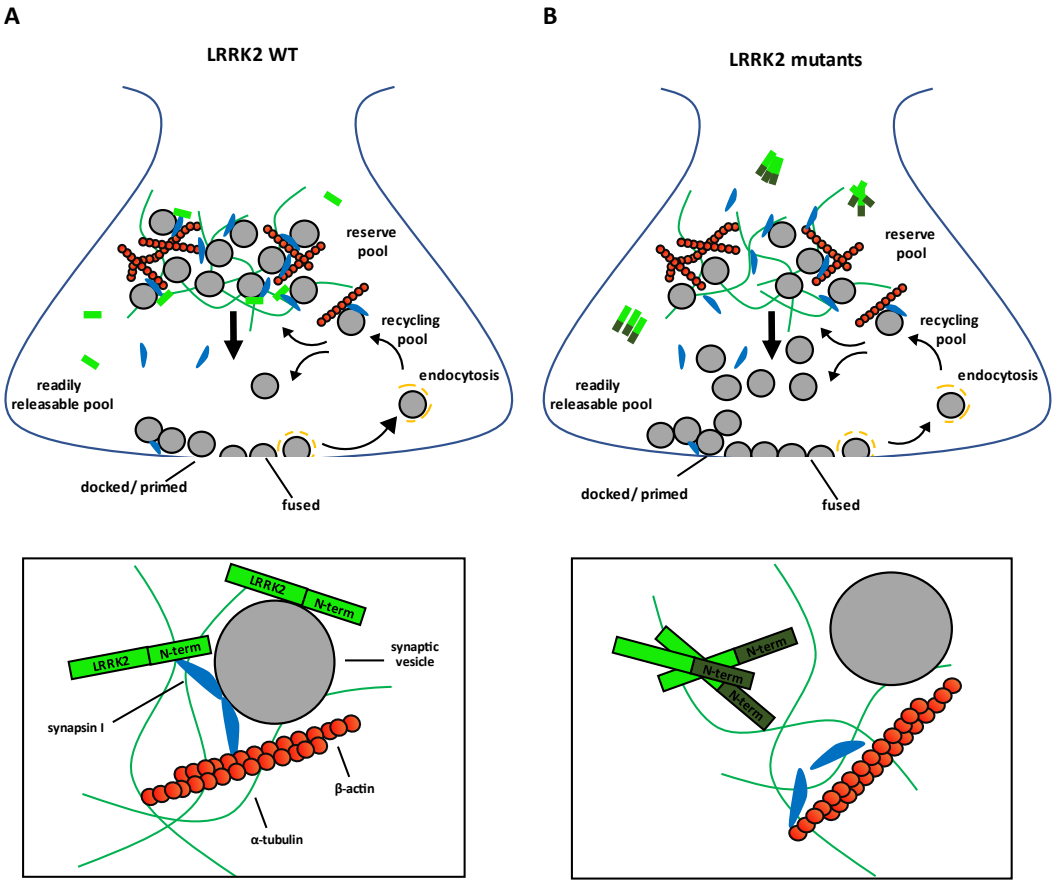

Figure 3.1. LRRK2 N-terminal domain controls molecular complexes at the synaptic site. *(**A**) LRRK2 WT binds SVs via its N-terminal domain and regulates their trafficking via interaction with a panel of synaptic proteins, including synapsin I, β-actin, and α-tubulin. (**B**) Removal of the N-terminal domain or the E193K mutation decreases the LRRK2 affinity for these proteins and for SVs themself. As a result, more SVs are recruited in the readily releasable pool and fused with the plasma membrane.*

A similar impact on SV trafficking occurs after expression of *LRRK2* E193K construct, which carries a mutation within the N-terminal domain. The substitution of the negative residue with a positive one, probably impacts on the N-terminal domain folding and modifies its interactome. In line with this possibility, we detected decreased interactions with β-actin, α-tubulin and synapsin I and increased vesicles fusion events. All together, these findings suggested that the Parkinson-linked E193K variant reduces the physiological function of the LRRK2 N-terminal domain and behaves as a partial loss-of-function mutation. Together with previous reports on the G2385R mutation, a mutation associated to the WD40 protein-protein motif (Carrion et al., 2017; Rudenko et al., 2012), this finding suggests that the pathophysiology underlying PD-associated LRRK2 mutations may be more complex than a simple gain-of-function of kinase activity.

An additional important aspect emerging from the S935A mutant, is that the LRRK2 subcellular localization is a key regulator of its kinase activity. Indeed, while the WT LRRK2, which can be phosphorylated, is located in the cytosol but also associated to membrane structures (both plasma membrane and vesicles), the S935A mutant, which cannot be phosphorylated, forms cytosolic aggregates and was hardly detected in membranes. These results are in line with literature data, indicating that phosphorylation of the serine 935 residue controls the LRRK2 interaction with 14-3-3 proteins, which, in turn, modulate the localization of the kinase to the plasma membrane where it can be activated (Nichols et al., 2010). Interestingly, increased of both SV fusion events and sypHy-positive clusters in the TIRF zone in cells expressing the S935A mutant were detected in these cells, suggesting that membrane targeting of LRRK2 is required for a proper SV trafficking.

In conclusion, these data suggest that the N-terminal domain plays a key role in the control of LRRK2 interactome and function. Perturbation of this region (through phosphorylation or missense mutations) may profoundly modify LRRK2 impact on SV dynamics. Interestingly, alteration of Ser-935 phosphorylation has been found in patients affected by PD, and our data indicate a possible mechanism by which altered phosphorylation may be implicated in the pathophysiology of PD. To further confirm these data, it would be important to characterize the functional impact of both variants, E193K and S935A, in primary culture and animal models of disease.

Disruption of vesicular trafficking pathways are emerging as important pathological events in PD, suggesting that alteration of this process might be an important aspect of disease neurodegenerative cascade. Our results confirm the physiological and pathological relevance of the nature of the LRRK2-associated macro-molecular complex solidifying the idea that different pathological mutations critically alter the scaffolding function of LRRK2 resulting in a perturbation of the vesicular trafficking. Finally, it is critical to understand how phosphorylation affects LRRK2 function and gain insight into its relevance in Parkinson's disease. Our increased understanding of the molecular mechanisms among LRRK2-associated PD pathways may provide a framework for uncovering additional knowledge that will expand our ability to stratify patients with PD for future disease-modifying therapies.

4. Introduction – Chapter II

4.1 The association between Type 2 Diabetes and Parkinson's disease

An extensive comorbidity spectrum has been closely associated with PD in a longitudinal study, where hypertension and diabetes were found being the most frequent comorbidities in PD patients (Santos García et al., 2017). Diabetes is an emerging public health concern that is estimated to afflict over 400 million people globally (Javeed and Matveyenko, 2018) with the number expected, by 2040, to increase to 642 million (Zheng et al., 2018). There are four distinct types of diabetes based on their etiopathogenesis: type 1 and type 2 diabetes, maturity onset diabetes of the young (MODY) and gestational diabetes (American Diabetes Association, 2014). By far the most common form of diabetes is type 2 diabetes mellitus (T2DM), featuring disrupted feedback loops between insulin action in insulin-sensitive tissues and insulin secretion by pancreatic β-cells by resulting in insulin resistance, altered glucose tolerance, and abnormal blood glucose levels. As a matter of fact, a potential association between T2DM and PD, both age-related chronic diseases, started in the early 1960s and confirmed by multiple recent reports.

Epidemiological studies regarding the connection between the 2 disorders are rather ambiguous. Previously, early reports affirmed a wide concordance regarding the association between T2DM and PD, since PD patients showed abnormal glucose tolerance when tested, disclosing a significantly high prevalence (50% to 80%) of T2DM in PD patients (Sandyk, 1993). This same study showed that the occurrence of diabetes indicated a greater severity of symptoms in PD patients (Sandyk, 1993). However, it is suggested in a more recently published study that abnormal glucose metabolism occurs in only about 20% of PD patients (Marques et al., 2018). Over the past few years, evidence has emerged for a higher risk of PD occurrence in people with T2DM. Several case-control and cohort studies across different ethnic groups have pointed to T2DM as a risk factor for the development of PD (De Pablo-Fernandez et al., 2018; Schernhammer et al., 2011; Sun et al., 2012; Yang et al., 2017; Yue et al., 2016). While the majority of studies claim such association, nevertheless, it is important to note that some of the studies sustained an inverse association (D'Amelio et al., 2009; Lu et al., 2014), or the absence of association between them (Palacios et al., 2011; Savica et al., 2012). These discrepant results may be attributed to both differences in methodology and study design, as well as remaining confounding factors, including methods for reaching a diagnosis of PD, dishomogeneity of parkinsonisms and lack of control of drug effects on patients.

Although epidemiological studies on the connection between the 2 disorders have been equivocal, several recent findings have shown that the pathological mechanisms of these diseases are similar. Environmental factor exposure and genetic susceptibility play a role in the aetiology and contributes significantly to the pathogenesis of both diseases (Figure 4.1). In this regard, the neurotoxin MPTP is widely employed in inducing parkinsonism through the production of oxidative stress in dopaminergic neurons, leading to mitochondrial dysfunction and cell death. By inhibiting complex I of the respiratory chain, this drug reduces ATP production as well as trigger free radical production (McKnight and Hack, 2020) which can, in turn, precipitate insulin resistance progression by increased reactive oxidative species (ROS) production (Szendroedi et al., 2012). Besides, mice treated with MPTP exhibited a concomitant upregulation of pro-inflammatory cytokine and α-synuclein levels in the pancreas and midbrain, strongly suggesting that PD and T2DM may be linked in an organ-specific manner (Wang et al., 2014). Between 5 and 10% of all cases with PD and T2DM are accounted by genetic alterations (Santiago and Potashkin, 2013). In fact, the genetic association among the two diseases is supported by genetic mapping of genes for both diseases. A genome-wide association study (GWAS) and microarrays identified a cluster of 478 genes closely associated with confirmed PD and T2DM genes (Santiago and Potashkin, 2013). Consistently, 84 PD and T2DM-associated genes were identified in another study employing GWAS alone (Santiago et al., 2014). However, a separate study found an absence of direct genetic evidence for an association between genome-wide meaningful

T2DM and PD loci (Chung et al., 2015). There is involvement of both T2DM and PD in accumulating misfolded proteins to create amyloid aggregates. Among diabetic patients, the specifically misfolded protein is amyloid polypeptide (APP) and within pancreatic cells can lead to cellular dysfunction (Obasse et al., 2017). The human α-synuclein is the misfolding protein associated with the development of PD and it eventually aggregates into LBs. The latter is encoded by the *SNCA* gene which is expressed in neurological as well as peripheral tissues comprising the pancreas (Emamzadeh, 2016). There is an association between the *SNCA* gene and the regulation of both glucose and insulin levels by the modulation of K^+ channels in the pancreatic β-cell (Rodriguez-Araujo et al., 2015). Furthermore, APP and α-synuclein interaction apparently occur across the two diseases (Horvath and Wittung-Stafshede, 2016) suggesting that they may affect each other *in vivo*, leading to T2DM and PD (Martinez-Valbuena et al., 2018; Mucibabic et al., 2020). In addition to α-synuclein, the expression of DJ-1, an antioxidant protein encoded by the PD gene *PARK7*, was found to be significantly upregulated during *in vitro* and *in vivo* hyperglycaemic conditions (Eberhard and Lammert, 2017; Inberg and Linial, 2010; Waanders et al., 2009). Consistently, *DJ-1*-deficient mice exhibited impaired glucose tolerance and decreased β-cell mass, prompting the suggestion that DJ-1 plays a key role in the glucose homeostasis (Jain et al., 2012). Likewise, reduced transcription of the *PARK6* gene, encoding the *PTEN-induced putative kinase 1* (PINK1) mitochondrial kinase, previously associated with PD, has been reported in T2DM patients (Scheele et al., 2007). A further study demonstrated that loss of *PINK1* function is coupled with increased insulin release and disruption of glucose sensing, implicating PINK1 in β-cell function (Deas et al., 2014). Additionally, the comorbidity between LRRK2-associated Parkinson and T2DM is about 9% (30 of 342 patients) (Healy et al., 2008). In a recent cohort study, higher triglyceride levels and higher rates of prediabetes were found to be more frequent among LRRK2 carriers, although these metabolic alterations did not affect the LRRK2-PD phenotype (Thaler et al., 2020). Furthermore, LRRK2 deficiency in rodents impairs insulin-dependent glucose transporter type 4 (GLUT4) translocation suggesting a key role for LRRK2 in insulin-dependent signal transduction (Funk et al., 2019). These findings provide support for the possibility of using genes associated with T2D to identify genes associated with PD and *vice versa*.

In parallel, experimental evidence point toward a possible underlying overlapping of T2DM and PD disease's dysregulated mechanisms and pathways (Santiago et al., 2017). In this context, a rather curious hypothesis has developed suggesting that mitochondrial dysfunction, endoplasmic reticulum stress, inflammation, and metabolic abnormalities may lead to insulin resistance and finally diabetes and/or neurodegeneration. (Santiago and Potashkin, 2013). There are clinical symptoms in either case principally involving a decline and subsequent lack of biological substances (insulin and dopamine respectively) resulting in significant or almost total loss of cells within the specialized tissue producing this compound (Das and Unger, 2018). In T2DM, the rate of insulin response is reduced, and systemic insulin resistance has long been a crucial hallmark of the disease. Recently, studies emphasized that such insulin resistance similarly can occur in the brains of patients with PD, also among those without diabetes, soliciting the suggestion that impaired insulin signaling is involved in the development of the pathological features of PD (Morris et al., 2014). Interestingly, the areas of the brain most affected in patients with PD, such as the basal ganglia and substantia nigra, are relatively abundant in insulin receptors. Mounting evidence suggests an essential regulatory role for insulin in regulating neuronal survival and growth, as well as dopaminergic transmission (D. Athauda and Foltynie, 2016a; Cheong et al., 2020). Moreover, it is noted that insulin modulates both dopamine synthesis and uptake in the substantia nigra. Hence, streptozotocin-induced hypoinsulinemia suppresses the transcript levels of both the dopamine transporter and tyrosine hydroxylase (TH) in the substantia nigra pars compacta. Accordingly, deficiency of dopamine in the striatum is capable of lowering insulin signaling in the basal ganglia, formulating the hypothesis that PD should be considered a risk factor for T2DM (Lima et al., 2014).

Considering these potential shared disease mechanisms, unsurprisingly is the fact that established diabetes drugs are considered among the most promising treatments being investigated to target insulin resistance in the management of PD (discussed below).

Both T2DM and PD are common disorders that negatively impact patients' quality of life. It is therefore extremely essential to investigate these diseases not only separately, but also to study their associations and interactions.

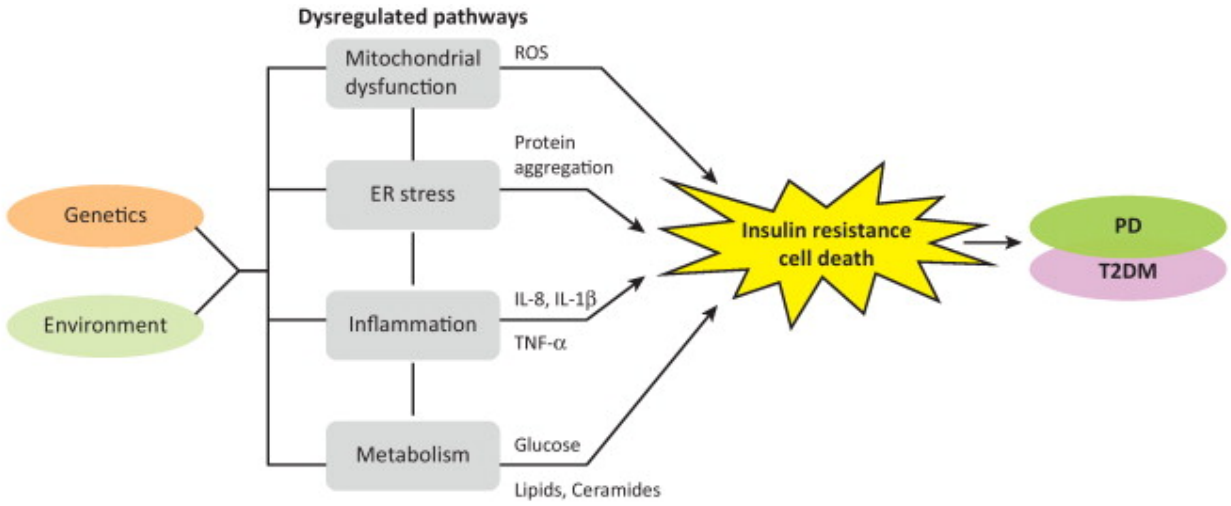

Shared pathways	Parkinson's disease	Diabetes
Mitochondrial dysfunction	Increased ROS production – damage to lipids, protein, and DNA. Endoplasmic reticulum stress.	Increased ROS production, lipid accumulation. Insulin resistance. Endoplasmic reticulum stress.
Autophagy	α-Synuclein aggregation. Lipid accumulation.	Inclusion bodies in the liver and pancreas.
Inflammatory response	Increased production of cytokines IL-1β and TNF-α. Anti-inflammatory treatments are neuroprotective.	Chronic inflammation increases risk of diabetes. Anti-inflammatory treatments improve insulin resistance.
Impaired glucose tolerance/ Insulin resistance	60–80% of PD patients exhibit impaired glucose tolerance. Loss of insulin-receptor immunoreactivity in the substantia nigra. Dopamine release is glucose-sensitive.	Peripheral insulin resistance leads to ischemic cerebro-vascular disease. Insulin resistance is associated with cognitive decline. Hyperglycemia is associated with neurodegeneration.

Figure 4.1. Environmental and genetic factors cause dysregulation in common pathways leading to neurodegeneration and diabetes. *Some examples of these shared pathways are described in the table in the lower panel (Adapted from Santiago and Potashkin, 2013).*

4.2 Insulin

4.2.1 Peripheral insulin

Insulin polypeptide hormone is a relatively small protein possessing native helical structure with molecular weight of approximately 6 kDa. It is synthesized as an inactive prohormone and is activated prior to secretion. The principal site for the regulated manufacture and secretion of insulin is the β-cell of the pancreas. Insulin synthesis begins in the ER of β-cells where preproinsulin is synthesized as an inactive single-chain precursor with a signal sequence. After the signal sequence is cleaved into the ER by proteolysis, preproinsulin

transforms to proinsulin. The correctly folded proinsulin then gets delivered to the Golgi apparatus and packaged within secretory granules pending its release. The active insulin is composed of two polypeptide chains, joined together with disulfide bonds (Hou et al., 2009; Omar-Hmeadi and Idevall-Hagren, 2021). This hormone is normally secreted in a regulated manner by β-cells in response to different secretagogue stimuli, with glucose being the most important physiological driver. Indeed, when blood glucose concentrations exceed 100 mg/dL, β-cells internalise glucose through the GLUT 1 (in humans) or GLUT 2 (in rodents) transporter. The resulting metabolism *via* glycolysis and the Krebs cycle, increases intracellular ATP/ADP concentration, closes K^+ channels, and activates voltage-gated calcium channels (VGCCs). The subsequent increase in intracellular Ca^{2+} provides the triggering signal for insulin granule fusion with the plasma membrane, a process controlled by the SNARE complex (Rorsman and Braun, 2013; Rorsman and Renström, 2003). Insulin is a peptide hormone essential for carbohydrate, protein, and fat metabolism. The effect of insulin is accomplished by binding to insulin receptors (IRs) on target cell membranes. Across many tissues, insulin receptors are found in different concentrations and provide an extensible multi-organ signaling pathway mechanism that is coupled with the intracellular tyrosine phosphorylation: the insulin signaling system (ISS). ISS's primary target are the liver, the adipose tissue, and the skeletal muscle (Bilotta et al., 2017). The regulation of a broad spectrum of physiological processes by insulin makes its synthesis and levels critical in the onset and progression of several chronic diseases.

4.2.2 Insulin in the brain

Besides the peripheral targets, insulin also exerts a neuroregulatory function (Bilotta et al., 2017; Grote and Wright, 2016). In the past few years, accumulating evidence has emerged about the human brain being an insulin-sensitive organ. In particular, three distinct sources of insulin are proposed to exist in the brain (D. Athauda and Foltynie, 2016). Most notably, insulin may be delivered to the CNS by the insulin receptor-mediated saturable pathway. On the other hand, the insulin can flow directly into the CSF without passing through the BBB as the circumventricular regions feature an absence of the typical BBB structure as well as have porous capillaries that allow the plasma to diffuse unimpeded. Ultimately, it was suggested by experimental studies, using animal models, that insulin could be produced in the brain (Baranowska-Bik and Bik, 2017). Throughout the brain, insulin receptors are widely expressed and dispersed and are primarily the insulin receptor A (IR-A) isoform instead of the more prominent IR-B isoform located across the rest of the body. Once insulin binds to IR-A, in turn, the receptor is subject to autophosphorylation and gets activated. The activation of the receptor results in phosphorylation of the downstream insulin receptor substrate (IRS) proteins found to be involved in a broad range of cellular signaling pathways. It is worthy to note that IRS proteins are triggered and activated also upon binding of Insulin-like Growth Factor 1 (IGF-1) ligand to its receptor. Thereby, IRS proteins couple the signaling cascades of both insulin and IGF-1 (Akintola and van Heemst, 2015). An important role in brain metabolism, neuronal growth, and neurogenesis is attributed to insulin. Furthermore, it may have a positive impact on the emotions and higher cognitive processes including attention, executive functioning, learning, and memory. On the other hand, insulin exerts its effects on the peripheral metabolism by acting through the hypothalamic-pituitary-adrenal axis. Specifically, central insulin is actually involved in the maintenance of energy homeostasis, body weight, as well as peripheral metabolism of lipids and glucose (Baranowska-Bik and Bik, 2017; Hughes and Craft, 2016). There is therefore a potential risk that disruption of brain insulin signaling may potentially prompt changes in brain (and whole body) energy metabolism and, simultaneously, can be a major contributor to late-stage expression of neurodegenerative disease (D. Athauda and Foltynie, 2016).

4.2.2.1 Overview in insulin signaling pathways

Across the brain, insulin receptors have a broad spectrum of distribution (including hypothalamus, hippocampus, olfactory bulb, cerebellum, amygdala, cerebral cortex, the striatum, midbrain, and brainstem) pointing to multiple functions of insulin (Duarte et al., 2012; Kleinridders et al., 2014). Insulin binds to the α-subunit of the receptor and triggers its tyrosine kinase activity, leading to tyrosine phosphorylation of the β-subunit of the receptor. Upon activation, the IR phosphorylates IRS proteins. As previously cited, IRS proteins also became activated upon binding of IGF-1 ligand to its cognate receptor. As a result, insulin binding to the IR/IRS is able to induce phosphorylation of a variety of downstream effectors (summarized in Figure 4.2). In turn, these activate downstream secondary messengers via three principal pathways (D. Athauda and Foltynie, 2016; Cheong et al., 2020).

A principal downstream effector of IRS proteins is the activation of phosphatidylinositol 3-kinase pathway, which, through cyclic nucleotide phosphodiesterase 3B (cPD3B), impacts neurotransmission in a direct way and consequently affects cognitive function, information processing and memory (Cheong et al., 2020). An additional signal transduction cascade comprises activation of the PI3K/(protein kinase B) Akt pathway. This, in turn, can regulate multiple downstream pathways shown to have fundamental roles in normal brain function, including mammalian-targeted rapamycin (mTOR), glycogen synthase kinase-3B (GSK-3B), forkhead box O1 (FOXO1) transcription factor, and nuclear factor kappa-light-chain-enhancer of activated B cells (NFκB). The protein synthesis mediated by mTORC1 plays an important role in synaptic plasticity and regulation of autophagy, a key mechanism involved in misfolded proteins and damaged organelles in neurons degradation. When the mTOR kinase is activated by AKT, it suppresses excessive autophagy, thereby promoting cell growth and survival. Indeed, disruption of mTORC1-dependent autophagy within neurons leads to neuronal cell death and the onset of neurodegenerative diseases (Kleinridders et al., 2014). A key downstream target of the IR/PI3K/Akt is the inhibition of the GSK3β, which governs multiple aspects of neuronal functioning, and so plays an important role in brain pathology. Specifically, it is involved in neural progenitor cell proliferation, neuronal polarity, and neuroplasticity (D. Athauda and Foltynie, 2016; Salcedo-Tello et al., 2011). Important roles in CNS, including control of energy homeostasis and leptin sensitivity, as well as locomotor activity, have been reported for FOXO1 (Kleinridders et al., 2014). Moreover, FOXOs phosphorylation results in their translocation from the nucleus, leading to changes in the transcription of several important factors implicated in metabolism, cell cycle regulation, apoptosis, and resistance to oxidative stress. An additional important effector of the IR/PI3 K/Akt cascade is NFκB, mediating the microglia proinflammatory response. Since it represents a master regulator of inflammatory gene expression, NFκB regulation has been involved in the pathogenesis of neuroinflammation in PD (D. Athauda and Foltynie, 2016).

IR signal transduction is further mediated through the parallel signaling pathway of mitogen-activated protein kinase (MAPK), which mediates synaptic plasticity modulation, density and neurotransmission, and perhaps even neurogenesis. Accordingly, activation of this pathway appears to modulate the effects of insulin on learning and memory (Cheong et al., 2020).

More recently, insulin has been reported to mediate neurotransmission through direct modulation of N-methyl-D-aspartate (NMDA) glutamate receptors to increase Ca^{2+} channel influx and, thus, promote NMDA-mediated neurotransmission, thereby modulating neuronal functions involved in learning and memory. The latter was further supported by the cell surface insulin-mediated control of the density of glutamate and

GABA receptors, by modulating targeting of the receptor to the membrane as well as endocytic internalization, and thus influencing synaptic plasticity (Cheong et al., 2020; Duarte et al., 2012).

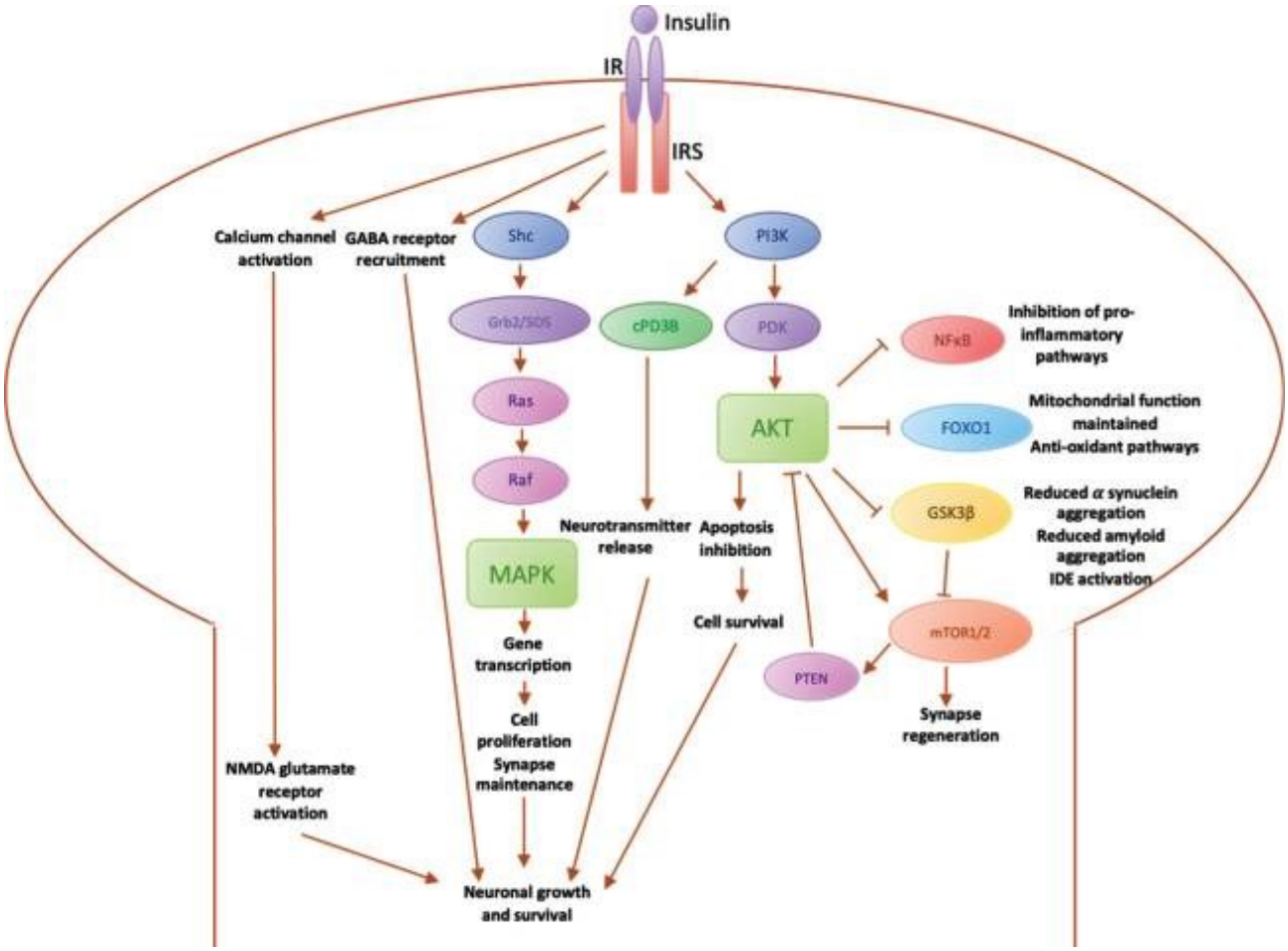

Figure 4.2. Schematic summary of main signal transduction pathways involved in insulin signalling in the brain *(Adapted from Cheong et al., 2020).*

4.3 Common therapeutic approaches to Type 2 Diabetes and Parkinson's disease

An additional suggesting point of correlation between PD and T2DM has been illustrated by the interaction of hypoglycaemic and antiparkinsonian drugs. Consistent with this, the effects of several drugs used to treat PD, such as levodopa, have been accounted, as they are able to induce both hyperglycaemia and hyperinsulinemia. On the other hand, there are others that can raise insulin sensitivity (Camargo Maluf et al., 2019). More importantly, it has been suggested that modulating the insulin signaling pathway and restoring sensitivity to insulin, potentially represents a novel target for PD disease modification. Indeed, hypoglycaemic drugs, especially biguanides (Lu et al., 2020; Paudel et al., 2020), thiazolidinediones (Zhu et al., 2019), and incretin mimetic agents (D. S. Kim et al., 2017), are increasingly being used in the management of patients with PD.

4.3.1 Antidiabetic drugs

Metformin is a synthetic biguanide of herbal origin widely used in the T2D treatment as a first-line drug due to its outstanding safeness and efficacy. The anti-hyperglycemic activity is believed to be caused by the inhibition of hepatic gluconeogenesis *via* alteration of the complex I mitochondrial respiratory chain (Rena et al., 2013; Sanchez-Rangel and Inzucchi, 2017). Moreover, metformin has also been shown to be an insulin sensitizer in skeletal muscle (Hostalek et al., 2015). However, the full understanding of its mechanism of action still remains unclarified. Over time, different uses of metformin were discovered and its benefits, including immunoregulatory properties (Podhorecka et al., 2017), have been verified in several diseases including cancer, cardiovascular, and neurodegenerative diseases (Foretz et al., 2014; Morales and Morris, 2015). Interestingly, in the investigation of neuroprotective/alternative strategies against PD, very recent evidence highlights the potential role of metformin as a novel neuroprotective agent (Paudel et al., 2020; Rotermund et al., 2018). Specifically, newly studies performed on MPTP-induced PD animals have demonstrated that metformin reduces the destructive effect of MPTP on dopaminergic neurons (Rotermund et al., 2018). Further pre-clinical data also suggest that metformin appears to improve motor and cognitive dysfunction by reducing oxidative stress, modulating autophagy through AMPK activation, and preventing mitochondrial dysfunction (Lu et al., 2016; Patil et al., 2014). Finally, metformin seems also to promote neurogenesis by activating the Protein kinase C-CREB-binding protein (PKC-CBP) pathway (Wang et al., 2012), which plays a central role in neurodevelopment, synaptic plasticity, and neuroprotection. Taken together, all these findings suggest that the greatest value of metformin at present may be in its potential contribution to the understanding of these mechanisms frequently involved in neurodegeneration.

Thiazolidinediones (TZDs), comprising pioglitazone and rosiglitazone, are a class of peroxisome proliferator-activated receptor-gamma (PPAR-γ) agonists. They act by potentiating the action of insulin and can improve insulin sensitivity and lower the blood glucose level of patients with type 2 diabetes (Davidson et al., 2018; Hevener et al., 2007). However, these receptors are noted for expression in insulin-sensitive organs such as the pancreas, as well as in regions of the brain including the substantia nigra and putamen (Swanson and Emborg, 2014). TDZs are another class of oral anti-hyperglycaemic agents widely investigated in the treatment of PD. Several recent studies performed across a variety of PD animal models have suggested that TZDs may exert anti-inflammatory and neuroprotective effects (Barbiero et al., 2014; Martinez et al., 2015; Pinto et al., 2016). TZDs, by interacting with a protein of the external mitochondrial membrane, called MitoNEET, have shown positive effects on the activity of complex I of the respiratory chain in neuronal cells. As well, it is believed that they inhibit microglial activation and lower oxidative stress in neurons, enhancing mitochondrial function and effectively preventing neurodegeneration (Cheong et al., 2020). Furthermore, these drugs, by decreasing nitric oxide synthase (NOS) activity, oxidative stress, and free radical release, exhibited protective action against neurodegeneration and neuroinflammation in MPTP-treated mice (Camargo Maluf et al., 2019). The evidence from human studies about the effectiveness of TZDs in PD is inconclusive. In fact, a few studies have found a significant decrease in PD risk with the use of TZDs in patients with T2DM (Brakedal et al., 2017; Brauer et al., 2015). However, no significant decrease in PD risk with TZD use was found in a retrospective cohort study in the United States (Connolly et al., 2015). As such, the difficulty in obtaining meaningful data in neurological disorders as parkinsonism may likely be related to the limited capacity of TZDs to pass through the BBB (Chang et al., 2015). To date, several trials from human studies have evaluated the interaction between the use of TZDs and the incidence of PD in diabetic patients, yet with controversial and inconclusive results.

Glucagon-like peptide-1 (GLP-1) is a growth factor released from gut enteroendocrine cells (Drucker, 2018). GLP-1 receptor agonists such as exenatide, lixisenatide, and liraglutide, are licensed drugs for the management of T2D (Nauck et al., 2021). They work primarily by stimulating pancreatic GLP-1 receptors, which trigger insulin release from pancreatic β-cells in a glucose-dependent manner and inhibit glucagon secretion from α-cells, resulting in a lowering blood-glucose action (Cornell, 2020; Mulvaney et al., 2020). Besides their role in glucose homeostasis, growing evidence suggests that GLP-1 mimetics exercise several extrapancreatic effects due to their ability to cross BBB, affecting several pathways in the CNS including neuroinflammation, neuroprotection, and mitochondrial function (Dilan Athauda and Foltynie, 2016). Thus, talking about neurodegenerative disorders, mice models of MPTP-induced Parkinson's disease promisingly support liraglutide and lixisenatide good neuroprotective effect (Hölscher, 2018). More so, in the same models, these GLP-1 analogues appear to reduce pro-apoptotic mitochondrial cell signaling and enhance growth factor kinase activity, playing a neurotrophic role (Liu et al., 2015). Furthermore, their involvement in neuroinflammation, widely involved in neurodegeneration, have been demonstrated to be related to the inhibition of the pro-inflammatory cytokine interleukin-1β (IL-1β) synthesis (Iwai et al., 2006). At present, clinical trials of the effects of GLP-1 agonists in neurodegenerative disorders are on their way (Athauda et al., 2017), including besides PD also AD (Hunter and Hölscher, 2012).

4.4 Aims

Over the past 30 years, several epidemiological studies have forged links between metabolic syndromes, in particular diabetes, and PD, but a complete understanding of the mechanisms linking the two diseases is still missing. Dysregulated pathways, such as inflammation and mitochondrial dysfunction, may be common underlying mechanisms (Camargo Maluf et al., 2019). In light of these potential shared disease mechanisms, T2D drugs have been proposed for the treatment of PD and recent clinical studies have shown promising results (D. S. Kim et al., 2017; Lu et al., 2020; Paudel et al., 2020; Zhu et al., 2019).

Genetic susceptibility plays a role in the aetiology and contributes significantly to the pathogenesis of both diseases. Of note, the genetic forms of PD reveal some mutations in genes which are expressed also in the endocrine pancreas (Deas et al., 2014; Jain et al., 2012; Rodriguez-Araujo et al., 2015), suggesting a possible co-dysfunction. Considering the comorbidity between PD and T2DM, we decided to investigate whether genetic alterations in PD could eventually explain the association of the two diseases. Specifically, we focused on LRRK2, the most common genetic cause of both familial and sporadic PD (4% of hereditary PD and 1% of patients with idiopathic PD) (Healy et al., 2008) and on its possible contribution to the control of β-cell function. Although neurons and pancreatic β-cells are very different structurally and embryologically, these two cell types are involved in similar release processes: endocrine cells, as well as neuronal cells, need to store hormones or neurotransmitters in vesicular structures, and to secrete them in a regulated manner. As discussed in the first part of the thesis, LRRK2 play a key role in the control of SV trafficking (Carrion et al., 2017; Matta et al., 2012; Piccoli et al., 2011; Shin et al., 2008), and the mechanism that regulates neurotransmitter secretion is similar to that employed by endocrine cells to control hormone release, sharing common molecular mechanisms and effector proteins.
Based on these considerations, we decided to investigate whether LRRK2 may be expressed in the pancreas and verify if its activity is required for its function. The study was performed in the insulin-secreting murine βTC3 cell line. After having demonstrated LRRK2 expression in the endocrine pancreas and in β-cells, we aimed to evaluate its physiological impact on insulin granule trafficking and insulin secretion by modulating LRRK2 expression through pharmacological and molecular approaches. We attempted to identify LRRK2 interactors and mechanisms of regulation of LRRK2 activation. A further objective for the proposed study

was to investigate the possible impact of LRRK2 on glucose homeostasis in animal models. To this aim, in collaboration with Dr. Giovanni Piccoli from University of Trento, we characterized bacterial artificial chromosome (BAC) transgenic mice expressing the PD-associated mutant G2019S *LRRK2*.

In the last decades, PD and T2DM incidence has dramatically increased in the population, probably for both the sedentary lifestyle and the increasing population aging. Therefore, a more extensive understanding of the molecular mechanisms underlying the correlation between these disorders may open opportunities for the development of new strategies to prevent or modify PD and T2DM progression.

5. Results and Discussion – Chapter II

As previously anticipated, the aim of this second part of the project was to characterize the role of LRRK2 protein and its structural domains in the endocrine pancreas using pharmacological, molecular, and functional approaches, and to assess its involvement in insulin release and glucose homeostasis. Specifically, we aimed (i) to verify LRRK2 expression in pancreatic beta cells and to characterize the role of LRRK2 in insulin secretion in murine βTC3 cell line, in primary mouse islets and in human isolated islets of Langerhans, (ii) to identify LRRK2 interactors in β-cells and regulatory mechanisms of LRRK2 activation, and (iii) to verify the involvement of LRRK2 in glucose homeostasis in animal model.

5.1 LRRK2 is expressed in the endocrine pancreas

LRRK2 have been reported to be widely expressed in the brain and in peripheral tissues (Westerlund et al., 2008; Zimprich et al., 2004). We first confirmed LRRK2 expression in the pancreas taking advantage of the Protein Atlas (Fig. 5.1A). As shown in figure 5.1A, LRRK2 is reported to be present in both humans and rodent pancreas, and particularly is enriched in the endocrine pancreas. We confirmed the results reported in the Protein Atlas, by western blotting analysis and demonstrate the expression of LRRK2 in lysates from the P2 brain fraction (positive control), whole mouse pancreas, and mouse primary islets of Langerhans, wherein it was enriched (Fig. 5.1B). To have a model to interfere with LRRK2 function pharmacologically and molecularly, we focused on the murine βTC3 cell line, which is widely used and retain glucose-stimulated insulin secretion *in vitro.* The expression of LRRK2 in βTC3 cells was confirmed at the mRNA level by RT-PCR (Fig 5.1C) and at the protein level, by western blotting analysis (Fig 5.1D). To detect the localization of LRRK2 in β-cells, we performed double immunofluorescence studies on βTC3 cells and revealed that LRRK2 is abundant in the mouse β-cell and localized to vesicular structures partially positive for insulin, as illustrated in figure 5.1E.

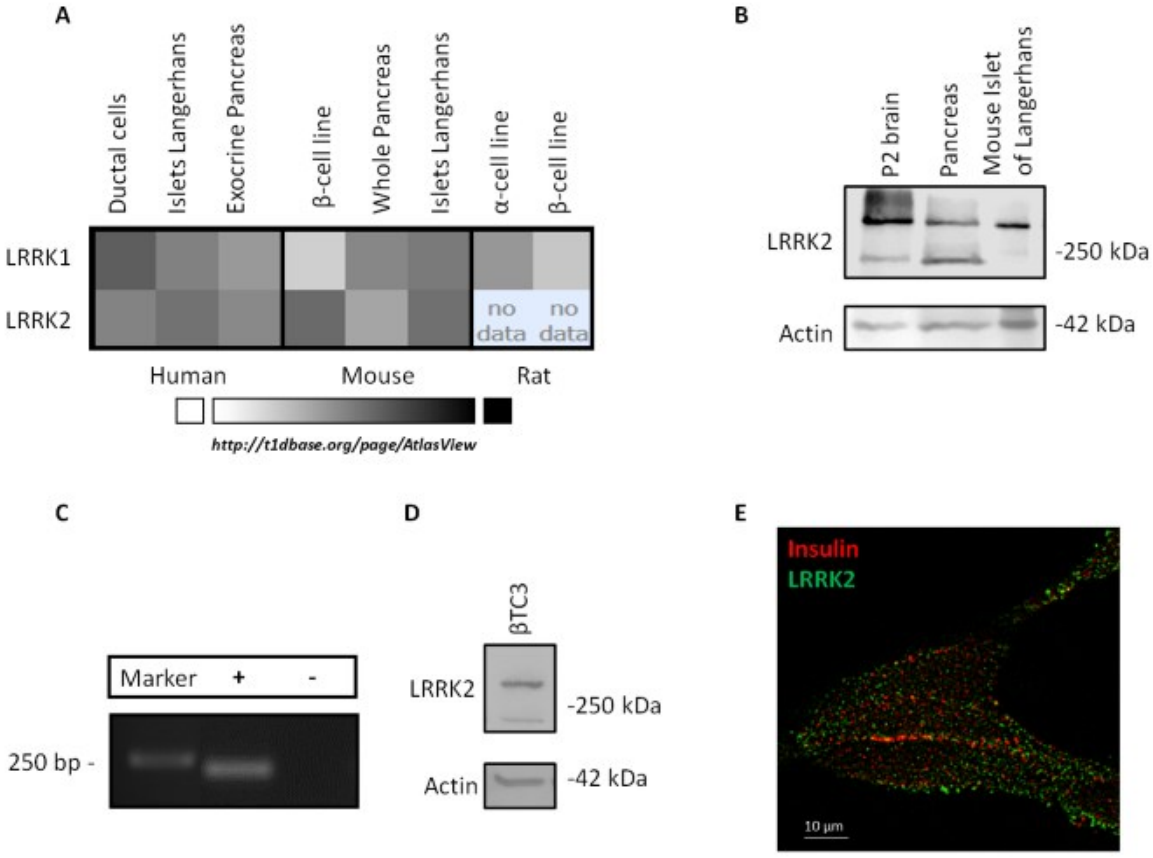

Figure 5.1.Expression of LRRK2 in the endocrine pancreas. *(**A**) LRRK2 gene expression in human, mouse, and rat pancreas according Protein Atlas database are shown. (**B**) Western blotting analysis of LRRK2 expression in murine pancreas and isolated islets. P2 brain fraction is used as positive control. (**C**) Determination of LRRK2 expression in βTC3 by means of RT-PCR. -, negative controls without enzymes. (**D**) Western blotting analysis of LRRK2 expression in βTC3 cell line. (**E**) Representative immunofluorescence images of βTC3 cells double stained with anti-LRRK2 (green) and anti-insulin (red) antibodies. The colocalization between LRRK2 and insulin is shown in yellow. Scale bar: 10 µm.*

5.2 LRRK2 silencing alter insulin granules trafficking and release in βTC3 cells

Mounting evidence suggest an important role of LRRK2 in the control of vesicle trafficking (Carrion et al., 2017; Piccoli et al., 2011). Therefore, we investigated the possibility that LRRK2 may impact secretory vesicles dynamics also in the β-cell. To assess the function of endogenous LRRK2 in insulin secretion, we employed the small RNA interference (siRNA) strategy to acutely downregulate LRRK2 levels. A scrambled siRNA was used as a control, siControl (Fig. 5.2A). Western blotting analysis confirmed that the siLRRK2 strategy depleted endogenous LRRK2 levels (Fig. 5.2B,C) in βTC3 cells. In order to visualise the spatio-temporal dynamics of the secretory vesicles in βTC3 cells, we monitor exocytosis of secretory vesicles tagged with the aforementioned sypHy reporter by time-lapse TIRF microscopy. In pancreatic cells two types of vesicles coexist: large dense-core vesicles, which store hormones (insulin), and small synaptic-like vesicles, which contain neurotransmitters (Reetz et al., 1991); both of them express synaptobrevin, the engineered protein used in our assay. Hence, we expect that sypHy labels both vesicle types, in βTC3 cell lines. Interestingly, assessment of fusion events over time, under resting conditions, showed a significantly increased number of spontaneous fusion events without changing single peak intensities in LRRK2-silent β-cells compared with control β-cells (Fig. 5.2D-F). Most intriguingly, the same phenotype was reported in the SH-SY5Y neuronal cells upon silencing of endogenous LRRK2 (Perez Carrion et al., 2018). Collectively, this evidence suggests that LRRK2 protein control vesicle trafficking probably by preventing vesicle exocytosis.

To further elucidate the physiological impact of LRRK2 silencing on β-cell function, the insulin secretion under basal (KRH, 1 mM glucose) and stimulated (KRH, 20 mM glucose) conditions was measured by means of ELISA assay in cells transfected with the LRRK2 and Control-siRNA (Fig. 5.2G). As expected, cells transfected with the Control siRNA significantly increased insulin secretion upon glucose stimulation. Conversely, the LRRK2 silencing caused alterations in insulin secretion insulin in response to both basal and high glucose concentrations. Curiously, in accordance with the previously reported data on vesicular trafficking by TIRFM analysis, the amount of insulin released in the medium by 45 minutes static incubation under basal glucose concentrations, was significantly increased in LRRK2-silent cells compared with control cells. A reduced glucose-stimulated insulin secretion response was also observed, as a result the stimulated/basal insulin secretion ratio was significantly decreased in LRRK2-deficient cells (Fig. 5.2H). All together, these findings indicate that LRRK2 is a critical effector of secretory vesicles dynamics and insulin secretion in βTC3 cells.

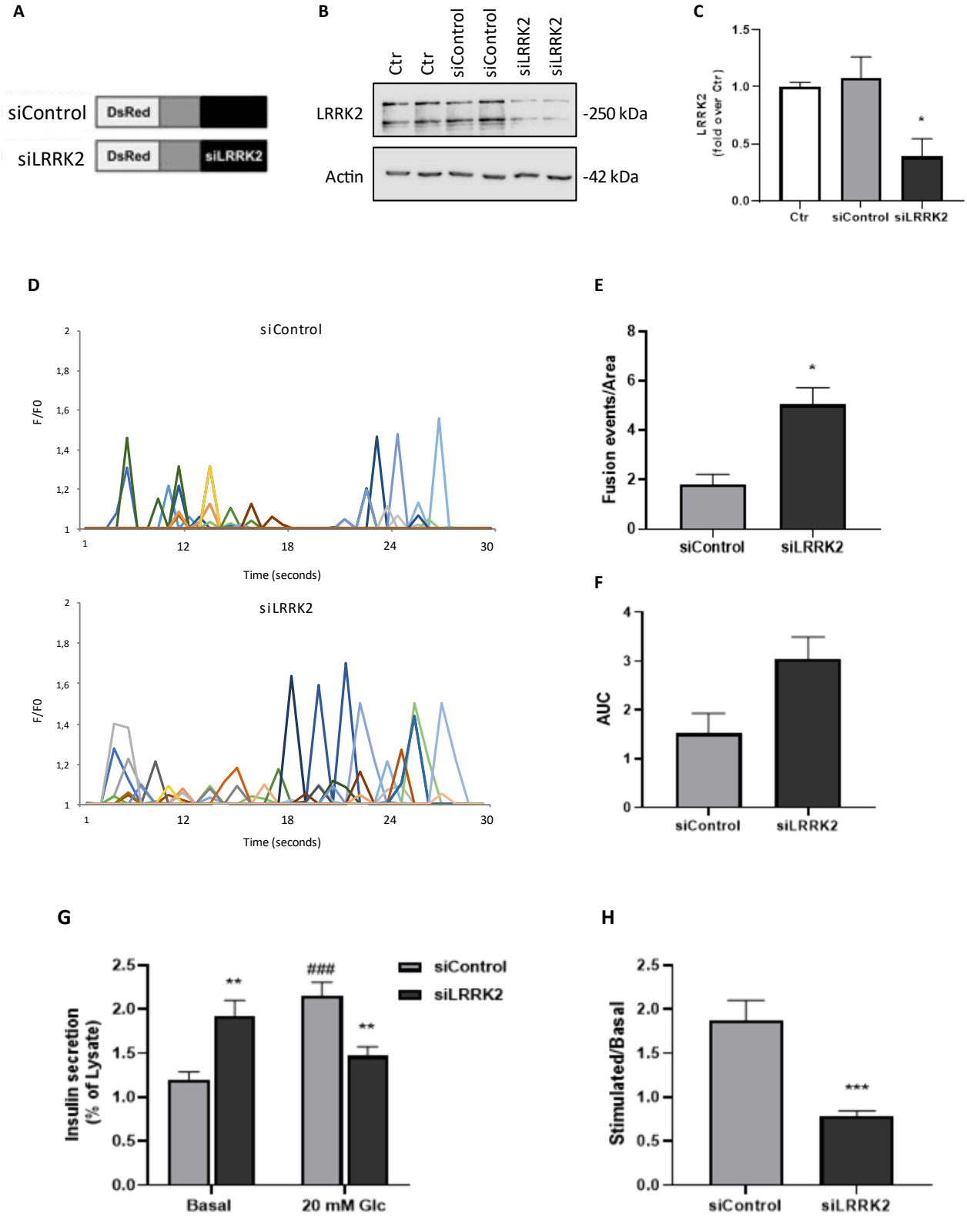
A
siControl
DsRed
siLRRK2
DsRed
siLRRK2
B
Ctr
Ctr
siControl
siControl
siLRRK2
siLRRK2
LRRK2
-250 kDa
Actin
-42 kDa
C
LRRK2 (fold over Ctr)
Ctr
siControl
siLRRK2
D
siControl
F/F0
Time (seconds)
siLRRK2
F/F0
Time (seconds)
E
Fusion events/Area
siControl
siLRRK2
F
AUC
siControl
siLRRK2
G
Insulin secretion (% of Lysate)
siControl
siLRRK2
Basal
20 mM Glc
H
Stimulated/Basal
siControl
siLRRK2

Figure 5.2. LRRK2 controls insulin granule trafficking and secretion in βTC3 cells. *(**A**) Schematic representation of siControl and siLRRK2 constructs. (**B**) Western blotting analysis of LRRK2 in βTC3 cells expressing siControl and siLRRK2 constructs and (**C**) relative quantitative analysis. Data (mean values ± SE) are expressed as fold change over Ctr. *p<0.05, ANOVA. (**D**) Time course analysis of synaptic events occurring in βTC3 cells transfected with siControl or siLRRK2 under resting conditions. βTC3 cells were co-transfected with ANP-GFP and the indicated constructs and imaged by TIRFM 48 hours later. Peaks of variable fluorescence intensity correspond to single fusion events. Fluorescence data are expressed as F/F0. The graphs show the total number of fusion events (**E**) and the resulting fluorescence changes (**F**) expressed as Area Under Curve (AUC). *p<0.05, Student's T-test. (**G**) The insulin secretion measured by static incubation under basal (1 mM glucose) and stimulated (20 mM glucose) conditions. Insulin was evaluated by means of ELISA assay in BTC3 cells. Data (mean ± SD) are normalized on the insulin content and expressed as percentual of insulin content (n = 3, in triplicate). **p < 0.01 vs siControl; ###p < 0.001 stimulated vs relative basal, ANOVA. (**H**) Stimulatory index was evaluated, and data (mean ± SD) are expressed as stimulated over basal release. ***p<0.001, Student's T-test.*

5.3 LRRK2 controls the glucose-stimulated insulin secretion through its kinase activity

In neurons, it has been reported that inhibition of LRRK2 kinase activity causes impairment in SV dynamics, indicating a role for LRRK2 catalytic activity in SV fusion cycle (Cirnaru et al., 2014). Thus, we investigated the functional impact of LRRK2 kinase activity on insulin granules trafficking upon LRRK2 pharmacological inhibition. We modulated LRRK2 kinase activity taking advantage of two potent LRRK2 inhibitors, GSK-2578215A (Reith et al., 2012) (hereinafter GSK) and MLi-2 (Fell et al., 2015). Firstly, as there are no data on LRRK2 GSK and MLi-2 inhibitors effect on β-cells, we performed MTT test to evaluate its possible toxicity. As shown in figure 5.3A, after an acute pre-treatment with both LRRK2 inhibitors, 200 nM (GSK) and 10 nM (MLi-2), no change in β-cell survival was observed. There is evidence that chronic LRRK2 kinase inhibitor treatment leads to degradation of LRRK2, thus reducing endogenous levels of the protein (De Wit et al., 2019). Since our studies are performed under acute conditions (45 minutes), we assessed the effect of LRRK2 inhibitors on the protein's endogenous levels during this same time window. Of interest, both GSK and MLi-2 did not cause alterations in the stability of LRRK2 as similar levels of proteins were detected after treatment with both inhibitors (Fig. 5.3B,C).

Next, we investigated whether altered LRRK2 kinase activity may lead to defects in vesicles trafficking. To this aim, the pH-sensitive dye acridine orange was used as a tool to monitor the basal and regulated vesicle trafficking. The fluorescent dye accumulates in acidic vesicular compartments and is released in the medium when vesicles fuse with the plasma membrane. As expected, the fluorescent signal in the medium was increased when regulated exocytosis was induced by incubating the cells with 20 mM glucose (the physiological stimulus) or with the depolarizing agent 40 mM KCl. Intriguingly, pre-incubation of cells with 200 nM GSK or 10 nM MLi-2, the specific inhibitors of LRRK2 kinase activity, completely prevented the stimulated exocytosis, thus confirming the involvement of LRRK2 in the control of vesicle trafficking and indicating a critical role of LRRK2 kinase activity in the phenomenon (Fig. 5.3D).

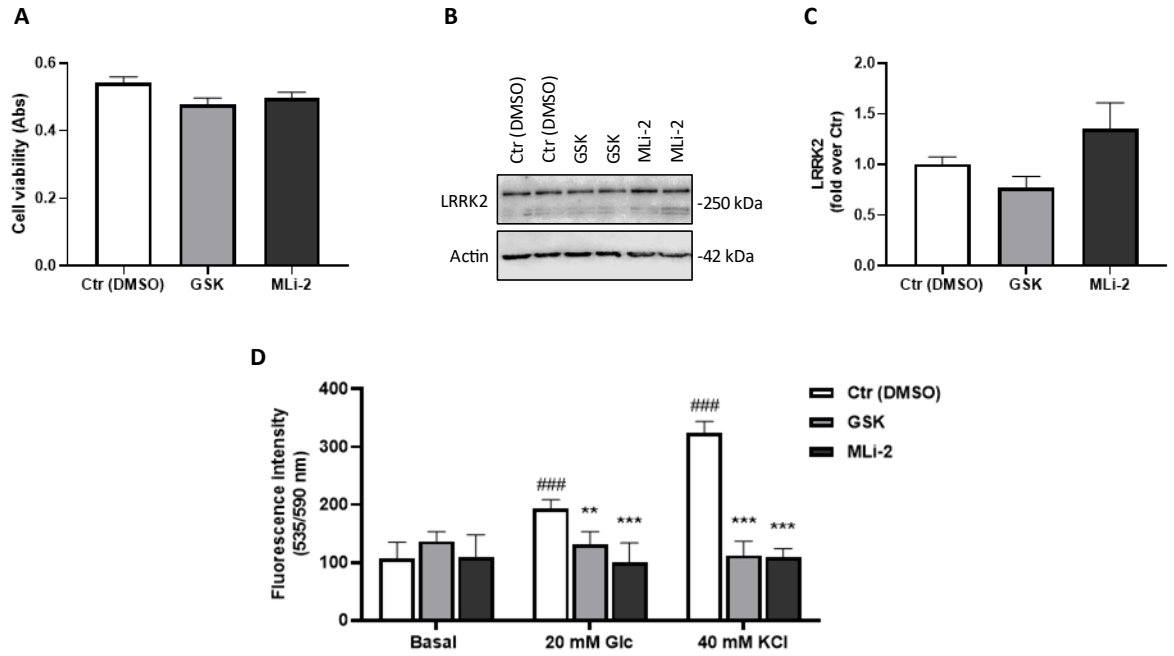

Figure 5.3. LRRK2 kinase activity inhibition impairs the regulated vesicular trafficking. *(**A**) MTT test. Mouse βTC3 cells were treated with 200 nM GSK or 10 nM MLi-2 for 45 minutes and DMSO treated cells were used as controls. Data of three independent experiments are expressed as ± SD. (**B**) Western blotting analysis of LRRK2 in βTC3 cells treated with DMSO (Ctr), 200 nM GSK or 10 nM MLi-2 for 45 minutes and (**C**) relative quantitative analysis. Data (mean values ± SE) are expressed as fold change over Ctr. (**D**) The vesicle trafficking in basal (1 mM glucose) and stimulated (20 mM glucose or 40 mM KCl) conditions was evaluated in βTC3 cells in the absence (Control) or presence of the specifics LRRK2 inhibitors (200 nM GSK and 10 nM MLi-2) by using an acridine orange assay. Data of three independent experiments are expressed as ± SD. **p < 0.01; ***p<0.001 vs Control stimulated; ###p < 0.001 stimulated vs relative basal, ANOVA.*

As the major vesicular compartment in mature β-cells are insulin secretory granules, we further explored the effect of LRRK2 kinase activity by monitoring insulin release by ELISA assay. To this aim, we measured insulin release in the murine βTC3 cell line in the presence or absence of two specific's inhibitors of the kinase activity of LRRK2, GSK and MLi-2, in either basal or stimulated condition. As expected, 20 mM glucose incubation induced a significant increase of insulin secretion. Contrariwise, the pre-incubation of cells with 200 nM GSK or 10 nM MLi-2 did not affect the basal insulin release, but completely prevented the increase of insulin secretion expected after glucose stimulation, suggesting that the kinase activity of LRRK2 is essential to control the regulated secretion of insulin in β-pancreatic cells (Fig. 5.4A).

The impact of LRRK2 kinase activity on glucose-stimulated insulin secretion was further confirmed by TIRF microscopy. Control cells or cells pre-incubated for 45 minutes with 10 nM MLi-2 were maintained in a basal KRH solution or stimulated for 10 minutes with a 20 mM glucose KRH solution. After staining with insulin, we assessed the distribution of insulin granules by TIRFM and quantified their number in the TIRF zone by means of a semi-automatic analysis (Fig. 5.4B,C). Unsurprisingly, the density of insulin granules in the TIRF zone significantly increased under glucose stimulation. Pre-treatment with the LRRK2 kinase inhibitor, did not change the insulin granule density under basal conditions. On the contrary, when pharmacological inhibition of LRRK2 was combined with glucose stimulation, the granules density at the plasma membrane increased, but remained significantly lower than what was observed under glucose stimulation, in the absence of MLi-2 (Fig. 5.4B,C).

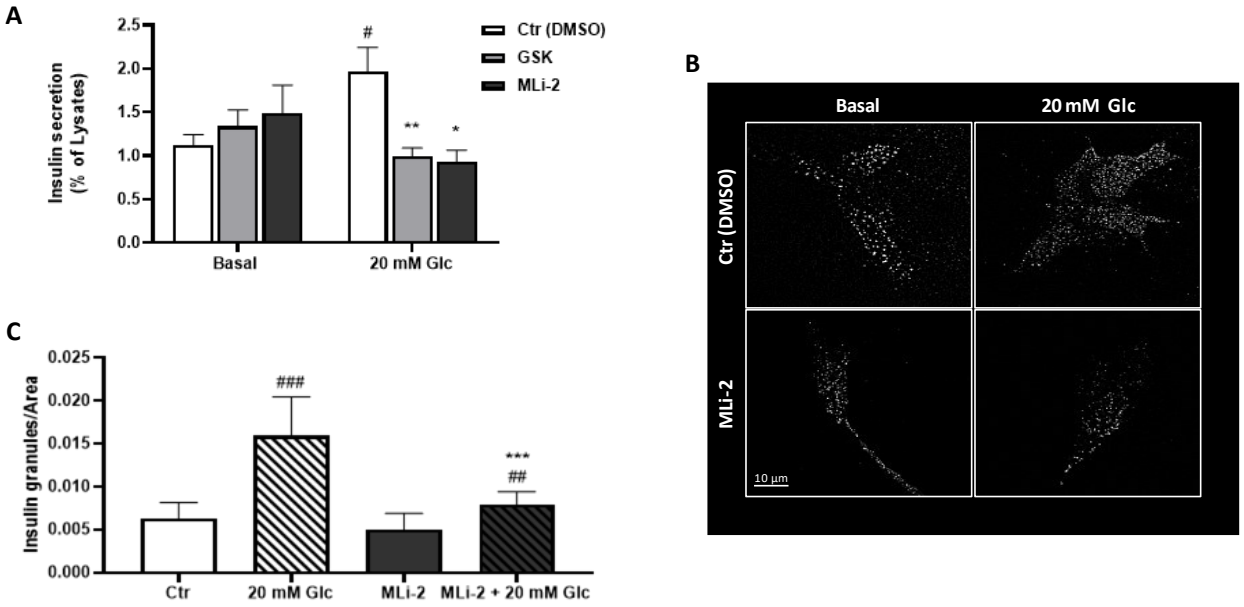

Figure 5.4. LRRK2 controls the glucose-stimulated insulin secretion through its kinase activity. *(**A**) The insulin secretion measured by static incubation under basal (1 mM glucose) and stimulated (20 mM glucose) conditions in the absence (Control) or presence of the LRRK2 inhibitors (200 nM GSK and 10 nM MLi-2). Insulin was evaluated by means of ELISA assay in BTC3 cells. Data (mean ± SD) are normalized on the insulin content and expressed as percentual of insulin content (n = 3, in triplicate). *p<0.05; **p < 0.01 vs Control stimulated; #p < 0.05 stimulated vs relative basal, ANOVA. (**B**) Representative images of vesicle density in the TIRF zone (100 nm). Βtc3 cells were incubated with DMSO (Control) or treated with 10 nM MLi-2 for 45 minutes and maintained in a basal (1 mM glucose) or stimulated (20 mM glucose) KRH solution for 10 minutes. Then, cells were fixed, stained with anti-insulin antibody, and imaged by TIRFM to visualise SGs docked to the plasma membrane. Scale bar: 10 µm. (**C**) The graph reports the quantitative analysis of insulin positive granules under the TIRF zone in control and treated cells under basal (1 mM glucose) stimulated (20 mM glucose) conditions. Data are normalized for the cell area and expressed as mean ± SE; n= 16 cells per condition. ***p<0.001 vs Control stimulated; ##p<0.01; ###p < 0.001 stimulated vs relative basal, ANOVA.*

These results further sustain the involvement of LRRK2 kinase activity on glucose-stimulated insulin secretion and suggest that LRRK2 may play a role in tuning the number of granules in the readily releasable pool.

In neurons, it has been shown that LRRK2 controls the storage and mobilization of SV within the recycling pool, which is constituted by vesicles of the readily releasable pool and reserve pool. Coherently with this role, the fraction of recycling synapses was enhanced in siLRRK2 neurons under baseline conditions. However, similar to our data, an inability to further increase the ratio of recycling synapses after long-lasting depolarization in siLRRK2-silenced neurons was observed. This lack of response may indicate the exhaustion of the readily releasable pool because of a perturbation of the recycling mechanism (Piccoli et al., 2011). Indeed, sustained repetitive activity beyond the first presynaptic release requires not only the readily releasable pool but also the mobilization of SV from the reserve pool to overcome the rapid depletion of the readily releasable pool (Dobrunz and Stevens, 1997; Murthy and Stevens, 1998).

A similar mechanism has been described for the dynamics of insulin granules in pancreatic beta cells (Rorsman and Renström, 2003). Our findings are consistent with such data, where LRRK2 may act as a molecular hub controlling both the storage and the activity-driven SV mobilization. Under basal conditions, LRRK2 protein may act as a brake and control the number of secretory vesicles available for the release. LRRK2 deficiency, therefore, is expected to confer on granules a greater ability for membrane contact and fusion, but in doing so it might also affect the organization of the exocytosis machinery in β-cells, thereby impairing the mobilization of insulin granules required during high activity. On the other hand, activation of

its kinase activity is required to release the brake and allow vesicles to reach the surface and release their cargo.

5.4 RAB8 protein is LRRK2 target also in β-cells and their phosphorylation promotes the insulin release

Since our results demonstrated the involvement of LRRK2 kinase activity in the control of insulin granule trafficking, we addressed our studies to Rab proteins, which are key players in vesicle trafficking in neuronal and endocrine cells and have been shown to be phosphorylated by LRRK2. Indeed, phosphoproteomic studies have identified a subset of Rab proteins as *in vivo* LRRK2 kinase substrates, with Rab8 being one of the most prominent (Steger et al., 2017). In this regard, we decided to focus on Rab8, a small G protein expressed also in β-cells and involved in the control of post-Golgi exocytic membrane trafficking, retromer-mediated trafficking, and endocytic recycling steps (Hattula et al., 2006; M. J. Kim et al., 2017; Peränen, 2011; Zhu et al., 2018).

To confirm Rab8 as LRRK2 effector in the control of insulin secretion, we interfered functionally on the LRRK2-Rab8 assay. Phosphoproteomic studies have shown that LRRK2-mediated phosphorylation occurs at the threonine-72 residue, which is located in a region of Rab8 interaction with its effectors. We generated and transfected in βTC3 cells the LRRK2-specific Rab8 phospho-death mutant, T72A, which cannot be phosphorylated. We measured insulin release, by means of ELISA assay, under resting (KRH, 1 mM glucose) and stimulated (KRH, 20 mM glucose) conditions in mock-transfected cells and βTC3 cells overexpressing Rab8 WT or Rab8 T72A (Fig. 5.5). As expected, incubation with 20 mM glucose induced a significant increase of insulin secretion on mock and Rab8 WT overexpressing cells. Upon overexpression of the Rab8 T72A mutant, the basal insulin secretion was not affected, indicating that the phosphorylation of Rab8 is not required for the basal trafficking of insulin granules. However, the glucose stimulated secretion, was severely inhibited. This effect appears to be the result of the T72A substitution because the overexpressing Rab8 WT protein did not change the insulin secretion. These findings suggest that Rab8 may represent the LRRK2 effector and further indicate that LRRK2 kinase activity is necessary to allow the stimulated insulin secretion.

To confirm that Rab8 and its phosphorylation play a role in the control of vesicular trafficking, we also generated phospho-mimic mutants, T72E/T72D the alanine substitution with a negatively charged amino acid, mimics a state of hyper-activation of LRRK2 kinase activity (Fig. 5.5). If LRRK2-mediated Rab8 phosphorylation is required to allow secretory vesicles to enter in the recycling pool and fuse with the plasma membrane, we expect increased insulin secretion already under basal conditions in cells overexpressing the Rab8 T72E/T72D mutants. Accordingly, the expression of both phosphomimic mutants increased the basal insulin secretion compared with mock and Rab8 WT overexpressing cells (statistically significant difference only in the Rab8 T72D mutant). In contrast, despite high basal insulin release, the amount of insulin release was not further increased after incubation with 20 mM glucose.

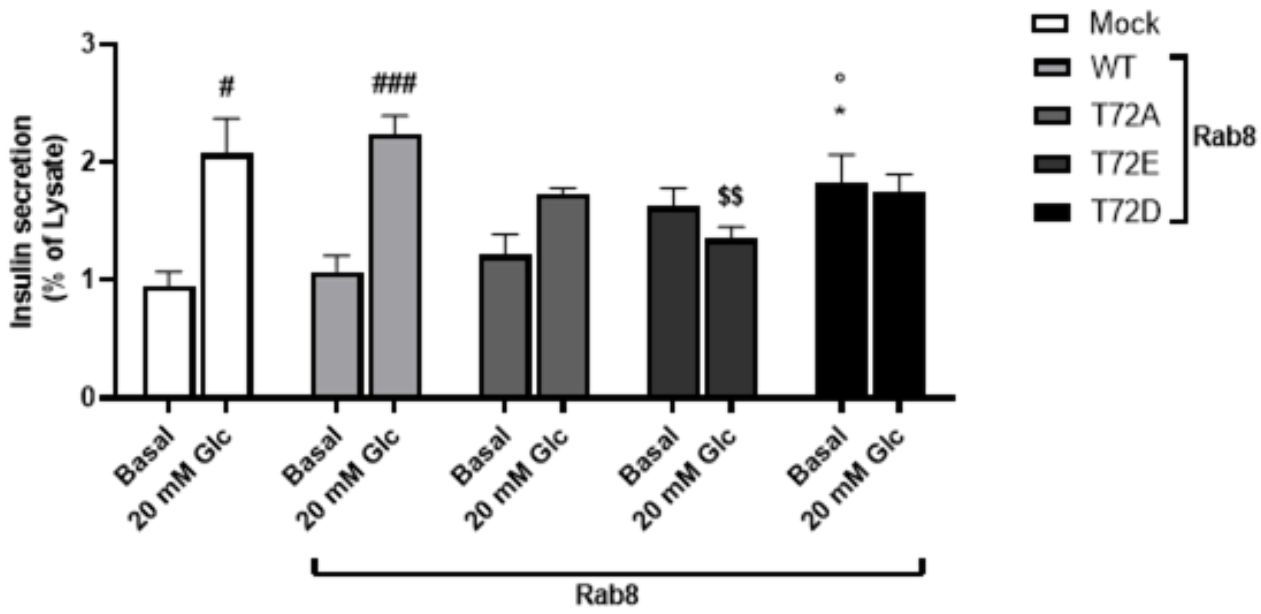

Figure 5.5. RAB8 protein is LRRK2 target also in β-cells and their phosphorylation promotes the insulin release. *βTC3 cells were transfected with empty vector (Mock), Rab8 WT, and Rab8 T72A/E/D mutants. After 48 h from transfection the insulin secretion was measured by static incubation under basal (1 mM glucose) and stimulated (20 mM glucose) conditions. Insulin was evaluated by means of ELISA assay in BTC3 cells. Data (mean ± SD) are normalized on the insulin content and expressed as percentual of insulin content (n = 3, in triplicate). *p < 0.5 vs basal Mock cells; °p < 0.5 vs basal Rab8 WT; $$p<0.01 vs stimulated Rab8 WT; #p<0.05; ###p < 0.001 stimulated vs relative basal, ANOVA.*

Taken together, our data suggest that Rab8 protein is a functional interactor of LRRK2 also in β-cells. LRRK2 action on Rab8 is required to promote glucose-stimulated insulin secretion as demonstrated by the altered response in termed of insulin secretion, detected under stimulated conditions in the phospho-dead mutant Rab8 T72A. Nevertheless, the fact that the Rab8 T72A mutant only partially prevents glucose-stimulated insulin secretion suggests that Rab8 is not the only target. Besides Rab8, LRRK2 was found to phosphorylate other Rab proteins, among them the Rab3 (Steger et al., 2017). The Rab3 is particularly interesting since it is known to be expressed in pancreatic beta cells and implicated in glucose-stimulated insulin exocytosis (Cazares et al., 2014; Iezzi et al., 2000; Yaekura et al., 2003), thereby suggesting that other Rabs may be implicated in the phenomenon as well.

How LRRK2-mediated phosphorylation control the Rabs activity is unclear. Since the T72 residue of Rab8 is in the region of Rab8 binding to its effectors, a hypothesis is that LRRK2-mediated Rab phosphorylation modifies the Rab binding to its interactors (Taylor and Alessi, 2020), thus inducing cell-specific effects.

Another important aspect emerging from these results is that the kinase activity of LRRK2 have to be switched on to promote insulin granule fusion; however, this activation must be transient to allow the regular granule trafficking. This is suggested by data obtained with phospho-mimetic Rab8 mutants that exhibited higher basal insulin release compared to Rab8 WT protein but failed to afford a further increase under stimulation conditions. Therefore, indicating that LRRK2 probably acts by controlling the granule movement in the recycling pool.

5.5 LRRK2 phosphorylation on the serine 935 is a critical player in LRRK2 signaling

Since the LRRK2 kinase is required for the regulated insulin secretion, we hypothesize that LRRK2 activation may occurs as a consequence of glucose-mediated stimulation.

LRRK2 kinase activity is tightly regulated by the balance between auto- and hetero-phosphorylation of the LRRK2 protein (Reynolds et al., 2014). As reported in the first chapters, in neurons phosphorylation of the serines 910/935, located between the ANK and LRR domains, is an important modulator of LRRK2 kinase activity (Marchand et al., 2020).

Firstly, *via* western blotting analysis with a specific anti-LRRK2-P-Ser-935 antibody, we confirmed the phosphorylation of LRRK2 at this site in βTC3 cells expressing the WT protein. As expected, no signal was detected in βTC3 cells transfected with the *LRRK2* S935A mutant, characterized by the replacement of the serine residue with alanine residue in position 935, and therefore not phosphorylable, thus confirming the specificity of the antibody (Fig. 5.6A). Given the tight functional correlation we observed between LRRK2 kinase activity and the stimulated insulin secretion, we exploited the possibility of a glucose-dependent phosphorylation of LRRK2. To this aim, *via* immunoblotting, we evaluated LRRK2 expression and its phosphorylation levels in βTC3 cells stimulated with 20 mM glucose in different time frames (5, 15 and 30 minutes). Surprisingly, while LRRK2 total expression was unaltered in the different experimental groups, LRRK2 phosphorylation at Ser-935 showed a time-dependent change (Fig. 5.6B,C). In particular, the fraction of LRRK2 P-935 abruptly increased after 5 minutes, and then gradually decreased at 15 and 30 minutes after stimulation, indicating that LRRK2 is transiently phosphorylated at the Ser-935 under glucose stimulation.

Several pieces of evidence indicate that the Ser-935 LRRK2's phosphorylation site appear to exert a key regulatory role on the subcellular distribution of LRRK2 (Berwick et al., 2019; Marchand et al., 2020; Nichols et al., 2010). Since LRRK2 localization impacts on its activation and controls the specificity of the protein kinase activity on target substrates (Marchand et al., 2020), we hypothesized that the control of subcellular localization may represent a mechanism for regulating LRRK2 function. In this regard, the localization of the phosphorylated form of LRRK2, LRRK2 P-935, was estimated by TIRFM experiments using the anti-Phospho ser-935 antibody. TIRFM studies revealed that 5 minutes after 20 mM glucose-stimulation - same time window of the transient increase in the phosphorylation observed *via* western blotting - the protein was enriched at the plasma membrane and on vesicular structures, partially overlapping with insulin granules (Fig. 5.6D,E), thus leading to the hypothesis of a role of Ser-935 heterophosphorylation in membrane targeting also in endocrine cells.

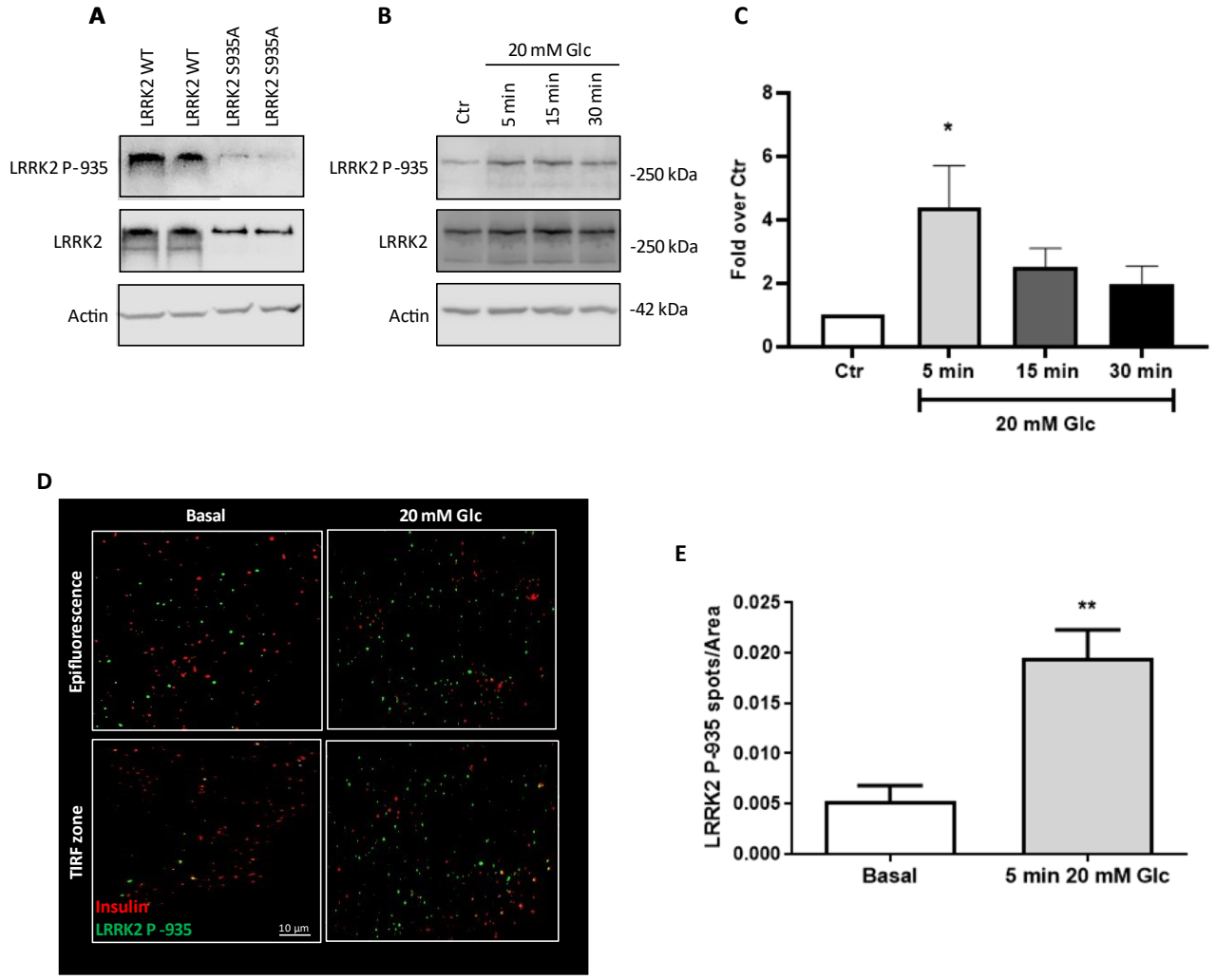

Figure 5.6. Time course analysis of LRRK2 P-935 phosphorylation pattern upon glucose stimulation. *(**A**) Western blotting analysis of LRRK2 P-935 fraction in βTC3 cells expressing LRRK2 WT and LRRK2 S935A constructs. (**B**) Western blotting analysis of LRRK2 P-935 fraction in βTC3 cells incubated with 1 mM (Control) or 20 mM (Stimulated) glucose for 5, 15 and 30 minutes and (**C**) relative quantitative analysis. Data (mean values ± SE) are expressed as fold change over Ctr. *p<0.05 vs Control, ANOVA. (**D**) Representative epifluorescence and TIRFM (100 nm) images in βTC3 cells incubated with 1 mM (Basal) or 20 mM glucose for 5 minutes. Then, cells were fixed and stained with of anti-LRRK2 P-935 (green) and anti-insulin (red) antibody. Scale bar: 10 µm. (**E**) The graph reports the quantitative analysis of LRRK2 P-935 positive spots under the TIRF zone under basal and after 5 minutes stimulation with 20 mM glucose. Data are normalized for the cell area and expressed as mean ± SE; n= 12 cells per condition. **p<0.05, Student's T-test.*

To confirm this hypothesis, we also investigated the localization of the phosphorylation-death mutant, *LRRK2* S935A (Fig. 5.7A,B). Under basal conditions, the WT *LRRK2* protein prevalently localized in the cytosol, some expression was also detected at the plasma membrane by TIRFM. 5 min after glucose stimulation, as previously observed, the WT protein accumulated to the plasma membrane. Of note, the *LRRK2* S935A protein aggregated in clusters within the cytoplasm; no expression was observed by TIRFM under either basal or stimulated conditions. Taken together, these results confirm that Ser-935 residue, and most likely its phosphorylation, promotes the LRRK2 shuttling to the plasma membrane.

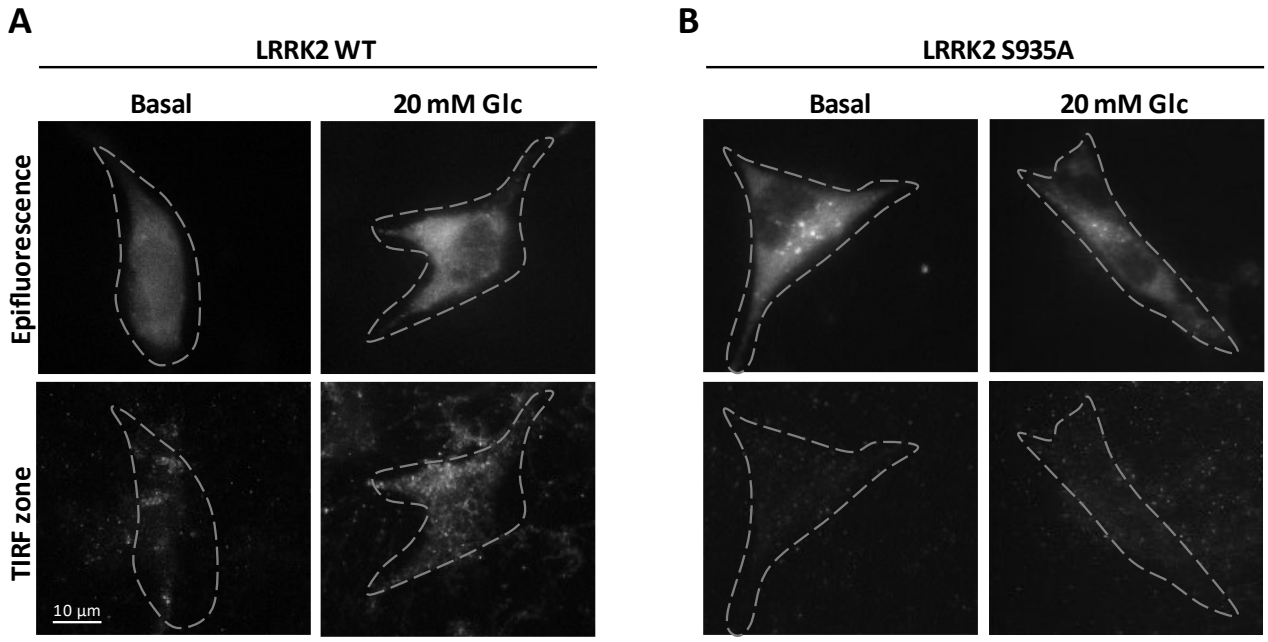

Figure 5.7. LRRK2 S935A phopho-dead mutant affect protein localization. *(**A**) Representative images of LRRK2 localization by epifluorescence and TIRM (100 nm) of βTC3 cells transfected with LRRK2 WT incubated with 1 mM (Basal) or 20 mM glucose for 5 minutes. (**B**) Representative images of LRRK2 localization by epifluorescence and TIRM (100 nm) of βTC3 cells transfected with LRRK2 S935A incubated with 1 mM (Basal) or 20 mM glucose for 5 minutes. Scale bar: 10 µm.*

Next, we exploit whether this re-localization is essential to promote the glucose-stimulated insulin release. To this purpose, we measured insulin release, by means of ELISA assay, under resting (KRH, 1 mM glucose) and stimulated (KRH, 20 mM glucose) conditions in mock-transfected cells and βTC3 cells overexpressing *LRRK2* WT or *LRRK2* S935A (Fig. 5.8A). As expected, a significant increase in insulin secretion upon glucose stimulation in mock and LRRK2 WT overexpressing cells was revealed by Elisa assays. No modification in the basal insulin release was observed in cells transfected with the *LRRK2* S935A mutant, indicating that the phosphorylation of LRRK2 is not required for the basal trafficking of insulin granules. Conversely, the glucose-stimulated insulin secretion was completed lost in cells expressing the S935A mutant compared with both mock cells and cells transfected with *LRRK2* WT. Consequently, the stimulation ratio (stimulated/basal insulin secretion) was significantly lower in βTC3 cells transfected with *LRRK2* S935A than in those transfected with the empty vector or the WT protein (Fig. 5.8B). Taken together, these results suggest that phosphorylation at Ser-935 appears to be a critical player to control LRRK2 translocation to the plasma membrane and to promote glucose-stimulated insulin secretion.

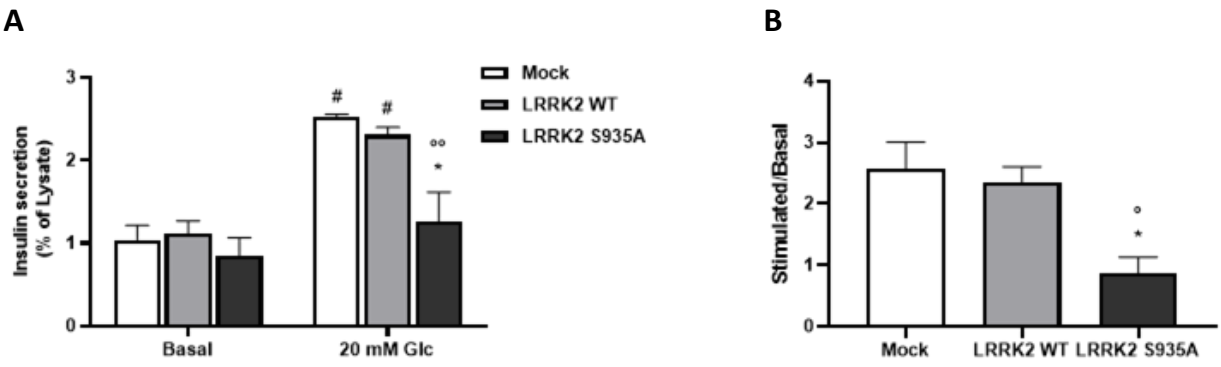

Figure 5.8. LRRK2 S935A phospho-dead mutant impacts on glucose-stimulated insulin secretion. *(**A**) βTC3 cells were transfected with empty vector (Mock), LRRK2 WT and LRRK2 S935A mutants. After 48 h from transfection the insulin secretion was measured by static incubation under basal (1 mM glucose) and stimulated (20 mM glucose) conditions. Insulin was evaluated by means of ELISA assay in BTC3 cells. Data (mean ± SD) are normalized on the insulin content and expressed as percentual of insulin content (n = 3, in triplicate). *p < 0.05 vs stimulated LRRK2 WT; °°p<0.01 vs stimulated Mock cells; #p<0.05; #p < 0.05 stimulated vs relative basal, ANOVA. (**B**) Stimulatory index was evaluated, and data (mean ± SD) are expressed as stimulated over basal release. *p < 0.05 vs LRRK2 WT; °p<0.05 vs Mock cells; ANOVA.*

LRRK2 has been suggested to form a dimer structure, and dimerization is relevant to its kinase activity and localization to cellular membranes (Berger et al., 2010; Deng et al., 2008; Greggio et al., 2008; Sen et al., 2009). In particular, the dimeric forms of LRRK2 are enriched on membranous structures and possess enhanced kinase activity, while the monomeric LRRK2 is predominantly cytosolic and is characterized by lower kinase activity (Berwick et al., 2019). The LRRK2 recruitment to the plasma membrane and activation are controlled by its interaction with 14-3-3 proteins, which in turn is modulated by LRRK2 heterophosphorylation at residue Ser-910 and Ser-935 (Doggett et al., 2012; Dzamko et al., 2017; Lobbestael et al., 2013; Mamais and Cookson, 2014; Nichols et al., 2010; Perera et al., 2016). Interestingly, several cellular processes affected by LRRK2 activity occur at the membrane, i.e., vesicle trafficking. The findings that LRRK2 displays greater membrane-associated kinase activity prompts us to speculate that the membrane compartment is probably the site where LRRK2 exerts its physiological function within the cell i.e. phosphorylate effector proteins, thus fine tuning their activation. Consistent with this scenario, we found that LRRK2 undergoes a phosphorylation peak at Ser-935 after 5 minutes of treatment with 20 mM glucose, the physiological stimulus for insulin secretion. Furthermore, within the same temporal window, the protein was observed to exhibit an enrichment on vesicular structures where it can phosphorylate effectors, such as Rab8, thus promoting insulin secretion.

5.6 LRRK2 is also expressed in human β-cells, and they are vulnerable to inhibition of its kinase activity

Given the possible clinical implication of these data, we confirmed the physiological relevance of LRRK2 in isolated human islets of Langerhans. RT-PCR and western blotting experiments both validated the expression of LRRK2 in human isolated islets (Fig. 5.9A,B). A specific anti-LRRK2 antibody confirmed the localization of LRRK2 to vesicular compartments (Fig. 5.9C). Noteworthy, LRRK2 staining was not limited to insulin-positive cells, thus suggesting its expression throughout endocrine cell populations, and supporting the possibility that LRRK2 may control hormone release, other than insulin.

We confirm the relevance of LRRK2 on insulin release by ELISA assay after inhibition of LRRK2 kinase by the specific LRRK2 inhibitor. As observed in βTC3 cells, we found that incubation of human islets with 200 nM

GSK or 10 nM MLi-2, that specifically targeted LRRK2 kinase activity, elicited a decrease in insulin secretion only upon high glucose stimulation (Fig. 5.9D). Thus, indicating that alteration of LRRK2 kinase activity impacts on β-cell function also in human islets of Langerhans and supporting the possibility of altered insulin release in PD patients carrying LRRK2 mutations characterized by altered kinase activity.

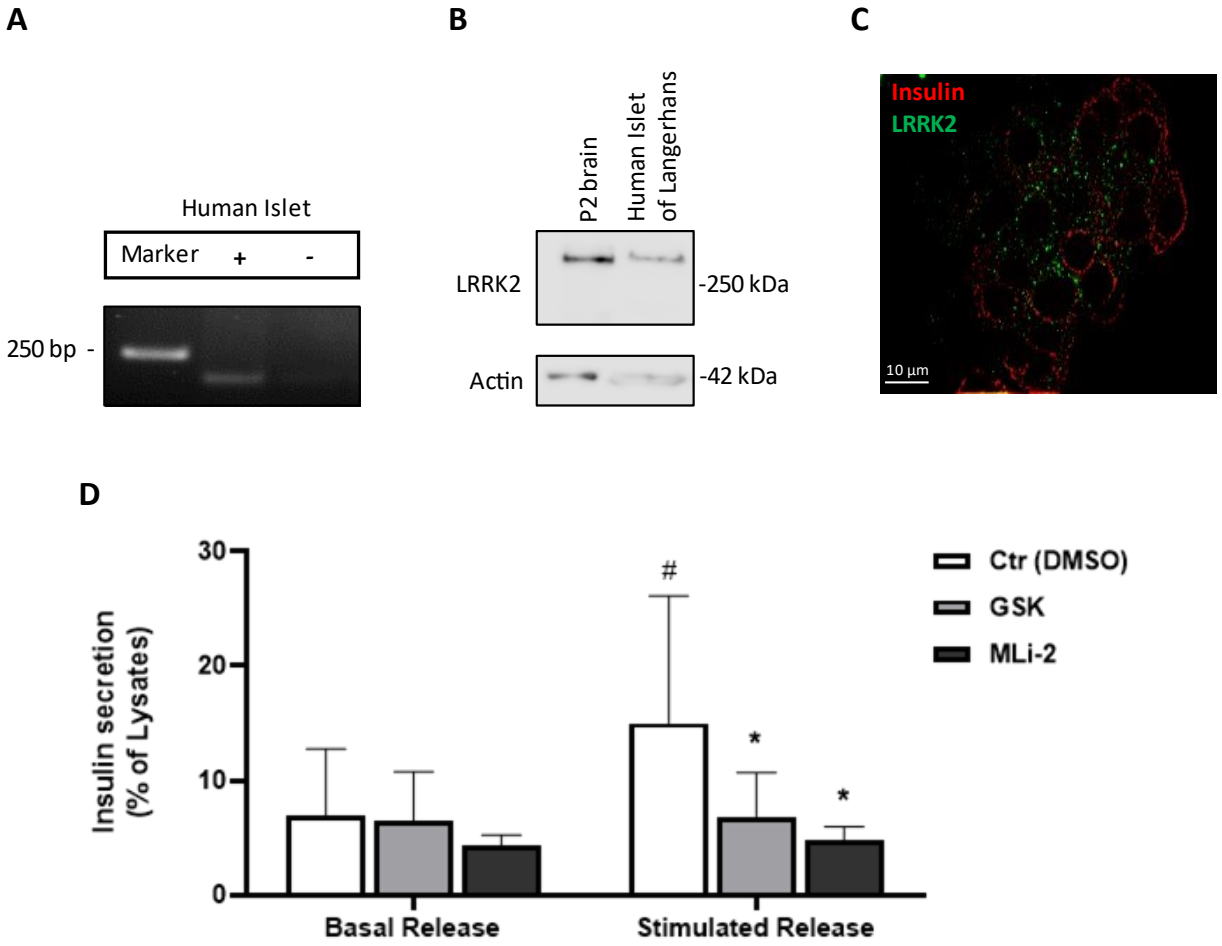

Figure 5.9. LRRK2 is also expressed in human β-cells and its kinase activity controls the regulated insulin secretion in human islets of Langerhans. A*) Determination of LRRK2 expression in human islets of Langerhans by means of RT-PCR. -, negative controls without enzymes. (**B**) Western blotting analysis of LRRK2 expression human isolated islets. P2 brain fraction is used as positive control. (**C**) Representative immunofluorescence images of isolated human islets double stained with anti-LRRK2 (green) and anti-insulin (red) antibodies. Scale bar: 10 µm. (**D**) The insulin secretion measured by static incubation under basal (3.3 mM glucose) and stimulated (16.7 mM glucose) conditions in the absence (Control) or presence of the LRRK2 inhibitors (200 nM GSK and 10 nM MLi-2). Insulin was evaluated by means of ELISA assay in isolated human islets. Data (mean ± SD) are normalized on the insulin content and expressed as percentual of insulin content (n = 3, in triplicate). *p<0.05; **p < 0.01 vs Control stimulated; #p < 0.05 stimulated vs relative basal, ANOVA.*

5.7 A possible link to metabolic dysfunction in Parkinson's disease

Our data strongly suggest an important role of LRRK2 kinase activity in promoting glucose-stimulated insulin secretion. Interestingly, the majority of pathological PD mutants are characterized by increased kinase activity. Besides the peripheral targets, insulin also exerts a neuroregulatory function (Grote and Wright, 2016). Growing evidence suggests an essential role for insulin in regulating neuronal survival and growth, as well as dopaminergic transmission (D. Athauda and Foltynie, 2016; Cheong et al., 2020). Therefore, we asked

whether kinase activity may also influence stimulated insulin secretion among LRRK2 carriers, which in turn may impact central nervous system function, disease progression, and the onset of metabolic syndrome.

We focused on the *LRRK2* G2019S PD-related pathological mutant, which is the most common disease-causing mutation, and investigated its possible impact on insulin secretion. We measured insulin release, by means of ELISA assay, under resting (KRH, 1 mM glucose) and stimulated (KRH, 20 mM glucose) conditions in mock-transfected cells and βTC3 cells overexpressing *LRRK2* WT or *LRRK2* G2019S. As predicted, incubation with 20 mM glucose induced a significant increase of insulin secretion on mock and LRRK2 WT overexpressing cells. Intriguingly, expression of *LRRK2* G2019S mutant significantly increased the basal insulin secretion compared with mock and LRRK2 WT overexpressing cells. On the other hand, although insulin release at baseline was enhanced, the amount of insulin release was not further increased after incubation with 20 mM glucose. In fact, a disrupted glucose-stimulated insulin release response was observed (Fig. 5.10A). Consequently, the stimulated ratio (stimulated/basal insulin secretion) was significantly lower in βTC3 cells transfected with *LRRK2* G2019S than in those transfected with the empty vector or the WT protein (Fig. 5.10B). These data are in line with previous results obtained with phospho-mimic mutants of Rab8, suggesting once again that the kinase activity of LRRK2 acts by facilitating granule movement toward the plasma membrane and/or fusion of insulin-containing granules. Indeed, when the kinase activity is enhanced, most probably the β-cell exhausts the reserves of insulin granules, leading to impaired insulin secretion.

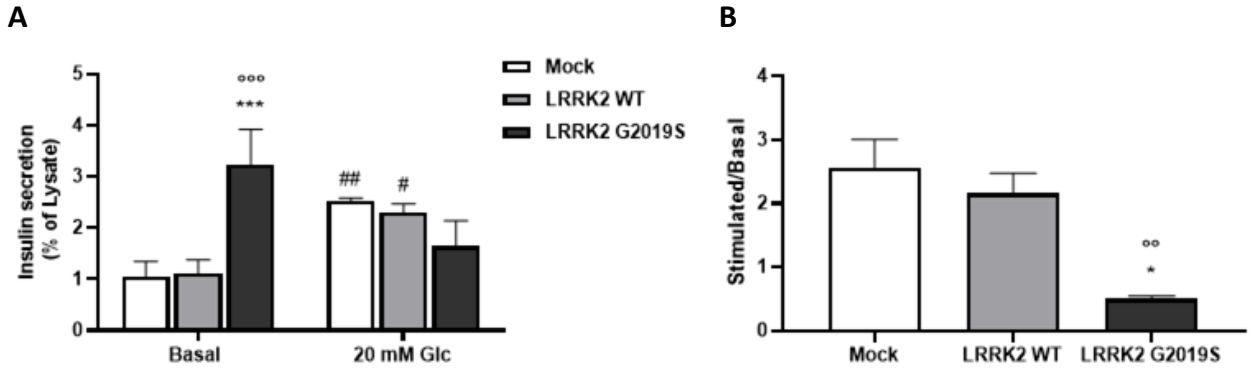

Figure 5.10. LRRK2 G2019S mutant impacts on glucose-stimulated insulin secretion. *(**A**) βTC3 cells were transfected with empty vector (Mock), LRRK2 WT and LRRK2 G2019S mutants. After 48 h from transfection the insulin secretion was measured by static incubation under basal (1 mM glucose) and stimulated (20 mM glucose) conditions. Insulin was evaluated by means of ELISA assay in BTC3 cells. Data (mean ± SD) are normalized on the insulin content and expressed fold over basal release (n = 3, in triplicate). ***p < 0.001 vs stimulated LRRK2 WT; °°°p<0.001 vs stimulated Mock cells; #p<0.05; ##p<0.01 stimulated vs relative basal, ANOVA. (**B**) Stimulatory index was evaluated, and data (mean ± SD) are expressed as stimulated over basal release. *p < 0.01 vs LRRK2 WT; °°p<0.01 vs Mock cells; ANOVA.*

Considering these promising results obtained on pancreatic β-cells in cellular model, we aimed, in collaboration with Dr. Giovanni Piccoli of the University of Trento, to translate our results in an animal model and analyze a possible implication of LRRK2 in the link between PD and metabolic disorder. For this purpose, we decided to focus on the BAC transgenic mouse models expressing the kinase active *LRRK2* hG2019S mutant, commonly used in the field of PD research. The mice develop an age-related decrease in striatal dopamine content, without loss of dopaminergic neurons, behavioral motor deficits or brain abnormalities at least out to the age of 12 months. For this reason, the animals were studied starting from this temporal window (from the age of 12 months) and we investigated if beside the dopamine decrease and the motor symptoms onset, the animals also presented glucose homeostasis alterations.

We first looked at animal weight. Interestingly, a significant increase in body weight was observed in *LRRK2* hG2019S mice compared with WT mice, suggestive of a metabolic disorder in these mice (Fig. 5.11A). Indeed, in line with this possibility we detected lower glycaemia in *LRRK2* hG2019S mice compared to WT littermates (Fig. 5.11B). Given our results on β-cells, we next assessed if the hypoglycaemia observed in the *LRRK2* hG2019S mice may result from altered insulin secretion. After overnight fasting, *LRRK2* hG2019S mice exhibited significantly higher plasma insulin levels than WT mice (Fig. 5.11C). To have a statistical numerosity, we pooled data from the different courts of animals (12-18 months of age). However, we also analysed the various courts separately and metabolic defects were clearly evident already at 12 months (significant for body weight and fasting blood glucose). The animal models clearly showed a metabolic defect, characterized by hypoglycaemia probably as a result of hyperinsulinemia.
Nevertheless, in order to have a complete metabolic profile of the animals we aim, in the future, to collect data from the 6 months aged animals and evaluate whether the metabolic problem is already existing at an early age.

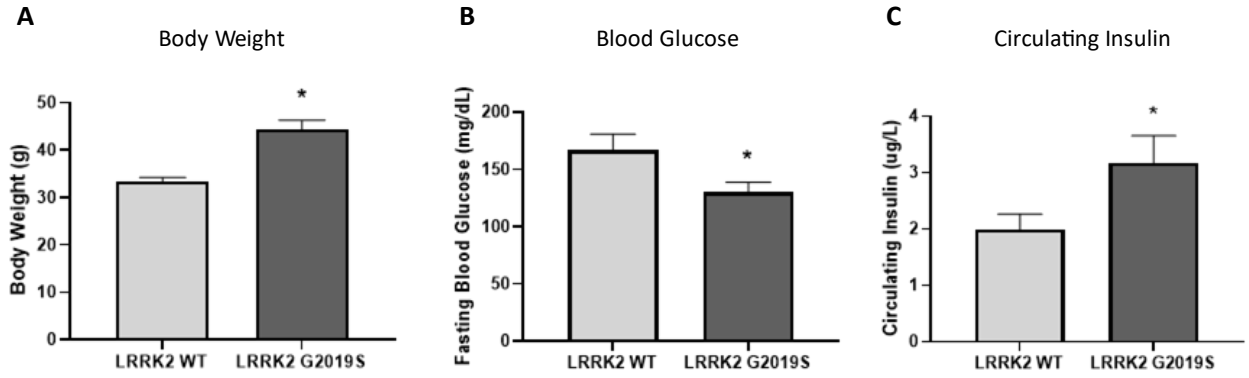

Figure 5.11. BAC hG2019S mice presents an altered metabolic profile. *Quantitative analysis of (**A**) body weight (g), (**B**) fasting blood glucose levels (mg/dL) and (**C**) circulating insulin (ug/dL) in LRRK2 G2019S and WT mice. Data are expressed as ± SD (n=12 mice per each group). *p<0.05, Student's T-test.*

The hyperinsulinemia observed may result from alterations in islet size and/or insulin secretion mechanism. In this regard, we studied the morphology of pancreatic islets in *LRRK2* G2019S and WT mice (12 month of age). A detailed analysis of pancreatic sections revealed larger islets (8088±680 μm^2) coupled with a significant increase in the major and minor axis of islets in the pancreas of BAC hG2019S mice compared with WT mice (3195±328 μm^2) (Fig. 5.12A-D). These results correlated with a different frequency of islet size distribution between the two experimental groups (Fig. 5.12H). WT mice are more frequently characterized by the presence of small and medium sized islets, usually characterized by an optimal stimulus-secretion coupling. Conversely, in G2019S mice, enlarged size islets were prevalently observed (rarely detected in WT mice). Morphological analysis of islet-cell composition did not reveal any significant difference in the percentage of α-, β- or δ-cells or in the cytoarchitecture of Langerhans islets: β-cells were found in the islet core and more abundant, whereas α- and δ-cells were located at the periphery of the islets.

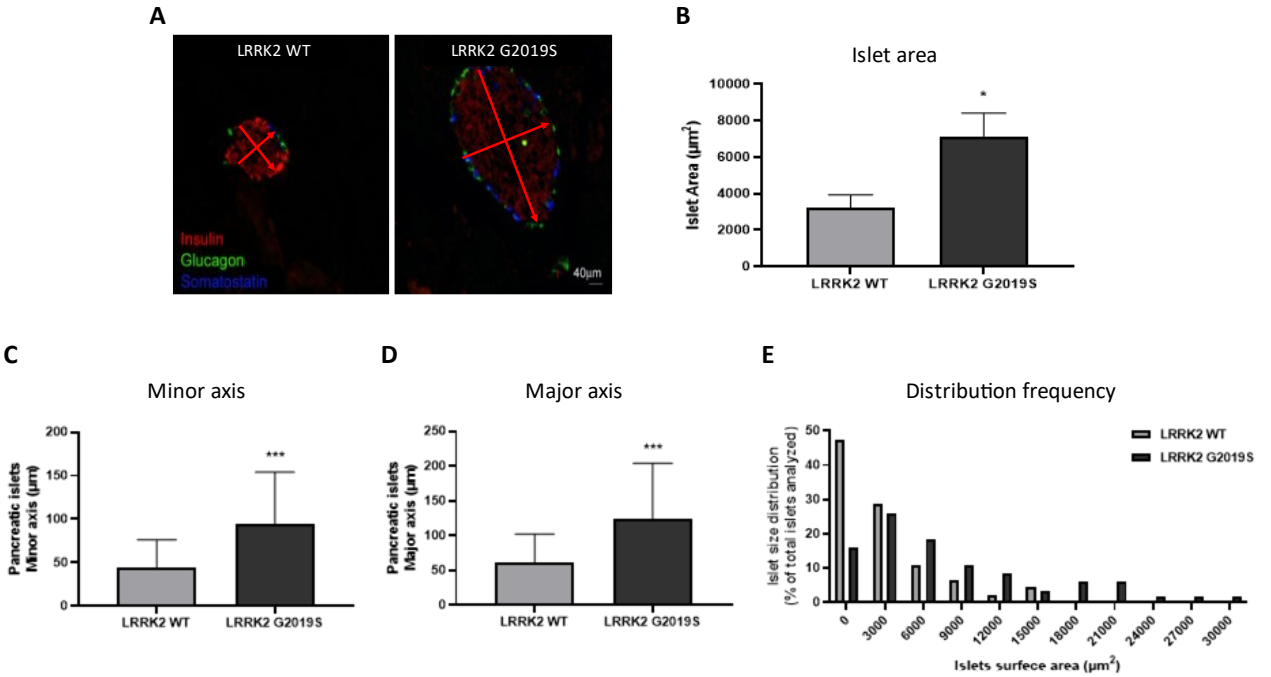

Figure 5.12. BAC hG2019S mice results in altered pancreatic morphology. *(**A**) Representative immunofluorescence images of mouse islet of Langerhans stained with anti-insulin (red), anti-glucagon (blue) and anti-somatostatin (green) antibodies. Scale bar: 40 µm. (**B**) Quantitative analysis of the islets size. Data are shown as mean ± SD (n=7 mice per each group). * p<0.05, Student's T-test. Quantitative analysis of (**D**) minor and (**C**) major axis of each islet analysed. Data are shown as mean ± SD (n=7 mice per each group). ***p<0.001, Student's T-test. (**E**) Islet size distribution, as percentage of total islets analysed, is shown. Islets were categorized according to the surface area (eleven categories: from <3 000 µm² to >30 000 µm²).*

Therefore, the observed hyperinsulinemia in G2019S mice may be related to the increased islets area of mutant mice. We also assessed whether the phenotype may arise from compromised insulin release. We isolated islets of Langerhans from mice and insulin secretion was performed under basal (KRH, 3 mM glucose) and stimulated conditions (KRH, 28 mM glucose) (Fig. 5.13A). As expected, the 28 mM glucose incubation induced a significant increase of insulin secretion in LRRK2 WT mice. In contrast, we observed a significant increase in the basal insulin secretion of G2019S mice, suggesting that the observed hyperinsulinemia in these animals is due to both a defective insulin production and release.

Similar to our findings in βTC3 cells, we failed to detect an additional increase in insulin secretion after stimulation with 28 mM glucose. Therefore, the stimulated ratio (stimulated/basal insulin secretion) was significantly lower in mice expressing the *LRRK2* G2019S compared to WT littermates (Fig. 5.13B).

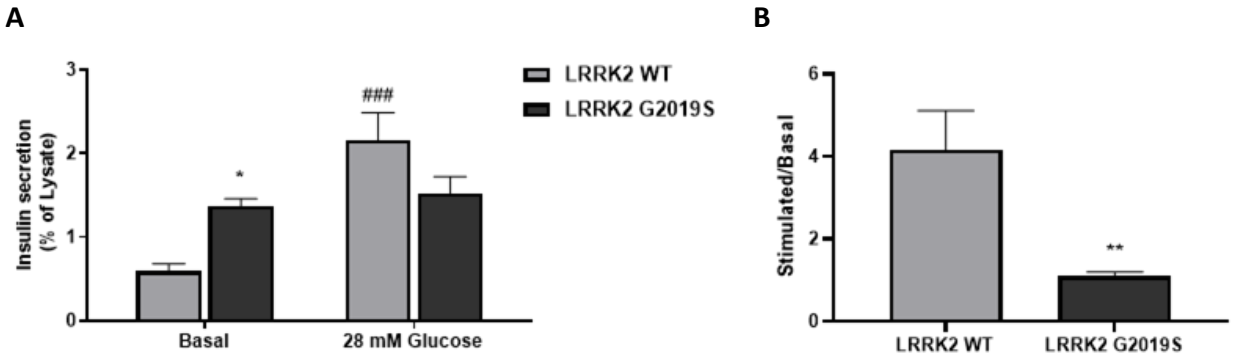

Figure 5.13. BAC hG2019S mice results in impaired insulin secretion. *(**A**) Islets isolated from LRRK2 WT and LRRK2 G2019S mice were incubated in 3 mM glucose (basal), or 28 mM glucose and insulin secretion was measured by ELISA assays. Data (mean ± SD) are normalized on the insulin content and expressed as percentual of insulin content (n = 3, in triplicate). *p<0.05; vs Control basal; ###p < 0.05 stimulated vs relative basal, ANOVA. (**B**) Stimulatory index was evaluated, and data (mean ± SD) are expressed as stimulated over basal release. **p < 0.01, Student's T-test.*

All together, these findings confirmed the relevance of LRRK2 on pancreatic β-cell function also *in vivo*. The animal model clearly showed a metabolic defect, characterized by alteration of both basal and stimulated insulin secretion. These findings strongly support the idea that there is a causal link between PD and metabolic dysfunctions, among them T2D. Not surprisingly, the drugs used in T2D are among the most promising treatments currently being considered as a possible new therapy for PD.

6. Conclusions – Chapter II

Our data demonstrate for the first time a role of LRRK2 and its kinase activity in the control of the glucose-stimulated insulin secretion and suggest a possible molecular mechanism of action of LRRK2 in the pancreas (Fig. 6.1).

LRRK2, as a scaffold protein, restrains secretory granules (SG) in a reserve pool, thus preventing their recruitment to the plasma membrane. Indeed, assessment of fusion events over time in LRRK2 deficient cells, under resting conditions, showed a significantly increased number of spontaneous fusion events. In accordance with this data, the amount of insulin released under basal glucose concentrations, was significantly increased in these cells.

On the other hand, LRRK2 kinase activity is required for an appropriate glucose-stimulated insulin secretion. Indeed, LRRK2 kinase activity inhibition impairs the regulated vesicular trafficking and prevents the increase of insulin secretion expected after glucose stimulation. TIRFM experiments clearly show a significant lower density of insulin granules in the TIRF zone in conditions of kinase activity inhibition and glucose stimulation, thus suggesting that LRRK2 kinase activity tunes the number of granules available for the regulated secretion, probably by phosphorylating proteins necessary for granules mobilization like synapsin I (which also anchors SG to actin, thus preventing their entry in the recycling pool) or Rab8 (which promotes the Golgi-plasma membrane trafficking of SG).

In line with this possibility, we found decreased stimulated insulin release in cells transfected with the Rab8 T72A mutant, which cannot be phosphorylated by LRRK2 and increased basal insulin release in cells transfected with the active Rab8 T72E/D phopho-mimetic mutants. Based on these data, we can hypothesise that LRRK2 function is to control the number of SG available for the release. Under basal condition LRRK2 kinase activity is low and the vesicles remain in the reserve pool, under stimulated conditions LRRK2 kinase activity is switched on, and phosphorylating key effectors, allow the vesicles to reach the plasma membrane and release their burden. This model predicts that excessive LRRK2 activation (as detected in the active Rab8 T72E/D phopho-mimetic mutants) probably increases the pool of constitutive recycling vesicles, thus increasing the basal release, but also depleted the reserve pool of vesicles necessary to sustain the stimulated insulin secretion.

Our data on *LRRK2* S935A mutant, also suggest the mechanism by which LRRK2 kinase activity is switched-on during glucose stimulation. We found that after 5 minutes of treatment with 20 mM glucose, LRRK2 becomes transiently phosphorylated at Ser-935 and this phosphorylation is required to recruit the kinase at membrane domains (we found enrichment of phospho-ser 935 LRRK2 protein at both plasma membrane and vesicles compartments) where it can phosphorylate specific effectors and promote insulin secretion. In line with this possibility, cells transfected with the phospho-dead S935A LRRK2 mutant, which fails to be recruited to the plasma membrane under stimulated conditions, shows a secretory phenotype similar to that observed with the pharmacological inhibition of LRRK2 kinase activity (no modification in the basal insulin release; impaired glucose-stimulated insulin secretion). In agreement with our data, in neurons it has been demonstrated that LRRK2 phosphorylation at residue Ser-935 promotes its interaction with 14-3-3 proteins, which is required to recruit LRRK2 at the plasma membrane where the protein can dimerize and become activated (Berger et al., 2010; Berwick et al., 2019; Nichols et al., 2010).

Our results are characterized by functional assays; further biochemical studies of *in vitro* kinases and binding assays would be necessary to definitively confirm our hypotheses.

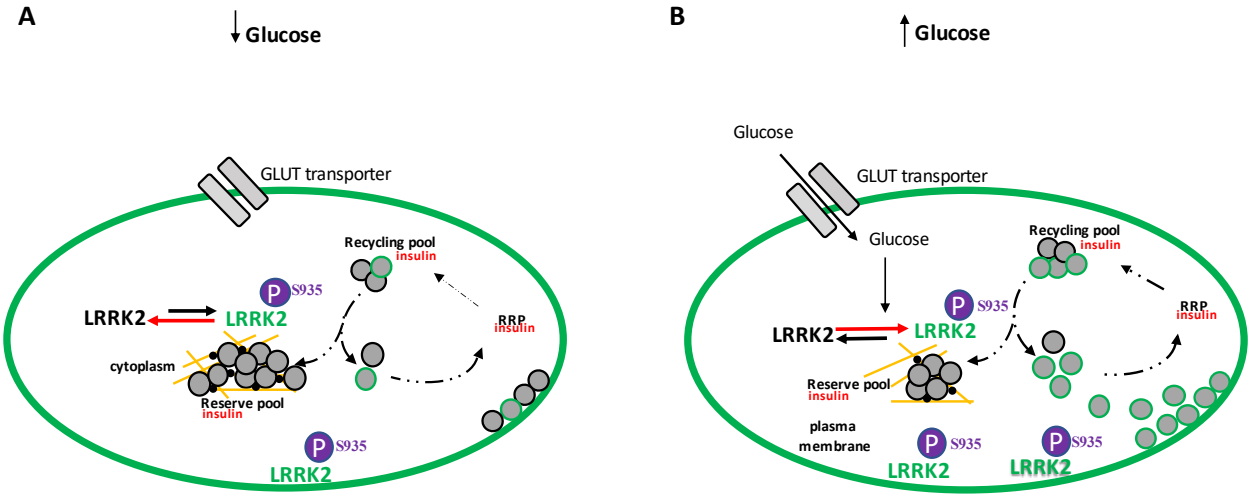

Figure 6.1. Model for LRRK2 action in the pancreatic β-cell. *(**A**) Under basal conditions (low glucose), LRRK2 is uniformly distributed at the cytosolic level, acting as a brake, and controlling the number of secretory vesicles available for release. (**B**) Under stimulated conditions (hight glucose), LRRK2 is transiently phosphorylated on Ser-935. This heterophosphorylation is required for LRRK2 recruitment to membrane compartments and its activation, where LRRK2 exerts its physiological function within the cell i.e., phosphorylate effector proteins (Rab8), thus promoting the glucose-stimulated insulin secretion.*

Our data on the BAC mouse model expressing the kinase active *LRRK2* hG2019S mutant, confirmed the relevance of LRRK2 on pancreatic β-cell function also *in vivo*.

The animal models clearly show a metabolic defect, characterized by hypoglycaemia as a result, at least in part, of hyperinsulinemia. As LRRK2 seems to be expressed in other cells of the endocrine pancreas, the secretion of additional hormones involved in glucose homeostasis should be assessed i.e., glucagon.
The altered blood insulin levels appeared to be linked to a direct effect of LRRK2 and its kinase activity on the pancreas. Indeed, we observed larger islets area in the pancreas of BAC hG2019S mice compared to WT mice and dysregulated insulin secretion in islets isolated from the animals.
The increase in islet dimensions observed in mice carrying the hG2019S mutation may be the result of enhanced islet cell proliferation due to dysregulated LRRK2 kinase activity (Ballian et al., 2007). From previous data on β-cell lines, we know that pharmacological inhibition of LRRK2 kinase activity affects neither cell viability nor cell proliferation. However, whether the G2019S mutant may play a direct role in cell proliferation remains to be established.
Alternatively, islets enlargement may be the consequence of adaptation to increased insulin resistance (Mezza et al., 2019; Wang and Jin, 2009). In line with this hypothesis, a possible role of LRRK2 in insulin-resistance has been recently described (Funk et al., 2019; Imai et al., 2020). LRRK2 deficiency in rodent fibroblasts affects insulin-dependent translocation of glucose transporter type 4 (GLUT4). Similar molecular alterations in fibroblasts from Parkinson's patients with the pathogenic G2019S LRRK2 mutation are also reported (Funk et al., 2019).
Although we cannot exclude a compensatory effect due to insulin resistance, we favour the idea that defective insulin release may be an early effect, since G2019S overexpression directly modulates the baseline insulin release. A possibility is that altered insulin signalling occurs early in these mice, as kinase-active LRRK2 mutations directly affect insulin release and insulin action in these animals.

Interestingly, insulin receptors are abundant in the basal ganglia and substantia nigra, the brain areas mostly affected in PD, and alteration of insulin action have been reported in PD patients (Morris et al., 2014). An essential regulatory role has been suggested for insulin in neuronal survival and growth, as well as in dopaminergic transmission (D. Athauda and Foltynie, 2016; Cheong et al., 2020). Indeed, insulin modulates both dopamine synthesis and uptake in the substantia nigra. Therefore, altered insulin release and signaling may explain the dopamine deficiency observed in the striatum and basal ganglia of PD (Lima et al., 2014).

In conclusion, our findings on animal models strongly support the idea that there is a causal link between PD and metabolic disorders such as T2D, and they suggest that LRRK2 might be directly involved in the abnormalities of insulin signaling observed in PD. The use of established T2D drugs targeting insulin resistance in the management of PD reinforces this association (Camargo Maluf et al., 2019; M. J. Kim et al., 2017; Paudel et al., 2020; Zhu et al., 2019). Both T2DM and PD are common disorders that negatively impact patients' quality of life. It is therefore extremely essential to investigate these diseases not only separately, but also to study their associations and interactions.

7. Materials and Methods

7.1 Cells culture conditions and processing

Isolated human islets of Langerhans, isolated mouse islets of Langerhans, mouse βTC3 cells, and mouse N2a cells were used for the experiments.

Isolated human islets of Langerhans. Human islets of Langerhans were isolated in Niguarda Ca' Granda Hospital (Milan, Italy) according to the procedure described by Ricordi et al. (Ricordi et al., 1988) in conformity to the ethical requirements approved by the Niguarda Cà Granda Ethics Board. The isolated islets were provided by cadaveric multiorgan donors with no medical history of diabetes or other metabolic disorders. In this study, at least 3 different islets preparations were used. Human islets (80 ± 10% purity) were cultured in RPMI-1640 culture medium (ECB900, *EuroClon*e) containing 5.5 mM glucose, 10% (v/v) heat-inactivated fetal bovine serum (ECS0180L, *EuroClone*), 0.7 mM glutamine (ECB300, *EuroClone*), 50 units/mL penicillin-streptomycin (ECB3001D, *EuroClone*). Islets were maintained in culture for 3 days in humidified atmosphere containing 5% of CO_2 at 37 °C prior to the arrival in the laboratory.

Isolated mouse islets of Langherhans. Mouse islets of Langerhans were isolated by cannulating the bile duct and clamping the duodenal end of the pancreas. Islets were isolated from WT/G2019S mice pancreas by collagenase digestion followed by Histopaque density gradient and handpicking. Pancreata were perfused with 2 mL of collagenase from Clostridium histolyticum (2 mg/mL; C9263, *Sigma Aldrich*) and digested at 37 °C in a water bath for 17,5 min. Undigested tissue was removed by filtration through a nylon mesh. After centrifugation of the digested tissue, the islets were isolated on a gradient of Histopaque 1119 (11191, *Sigma Aldrich*), Histopaque 1077 (10771, *Sigma Aldrich*), and Hanks' Balanced Salt 1x solution (HBSS) containing 0.4% BSA. Islets were collected, passed through a 40 µm strainer, and washed with HBSS. At the end of the isolation, islets were handpicked into fresh media, and cultured overnight in RPMI supplemented with 10% heat-inactivated fetal bovine serum, 1% L-glutamine, and 1% penicillin-streptomycin in humidified atmosphere containing 5% of CO_2 at 37 °C.

Cell lines. βTC3 cells were kindly provided by Prof. Douglas Hanahan of Department of Biochemistry and Biophysics, University of California, San Francisco. These are beta tumour cells obtained from transgenic mice constitutively expressing the SV40 T Antigen (*Tag*) (Efrat et al., 1988). The *Tag* expression is controlled by the insulin promoter and is responsible for the immortalization of these cells with a maintenance of a differentiated phenotype for 50 passages in culture. Differentiated βTC3 cells produce both proinsulin I and II, and efficiently process them into mature insulin, even if with a lower threshold for maximal stimulation when compared to primary β-cells (Skelin, 2010). βTC3 cells were cultured in RPMI 1640 medium (ECB900, *EuroClone*) supplemented with 10% (v/v) heat-inactivated fetal bovine serum (ECS0180L, *EuroClone*), 50 units/mL penicillin-streptomycin (ECB3001D, *EuroClone*), and 1 mM L-glutamine (ECB300, *EuroClone*).

N2a cells (Neuro2a, ATCC CCL-131) were kindly provided by Prof. Giovanni Piccoli, Department of Cellular, Computational, and Integrative Biology, Università degli Studi di Trento, Italy. Cloned Neuro-2a cells, generated from a spontaneous tumour of an albino mouse strain A, are a widely used *in vitro* model to investigate neuronal differentiation, axonal growth, and to characterize different pathways involved in signal transduction. This cell line is easily amplified and has a high transfection efficiency. N2a cells were cultured in DMEM HG (Dulbecco's Modified Eagle Medium High Glucose; ECM0101L, *Euroclone*) supplemented with 10% fetal bovine serum (ECS0180L, *EuroClone*), 1% penicillin/streptomicin (ECB3001D, *EuroClone*), and 1% L-glutamine (ECB300, *EuroClone*). Cells, both βtc3 and N2a, were cultured under sterile conditions in humidified atmosphere containing 5% of CO_2 at 37 °C using tissue-culture treated supports.

Reached the 80% confluence, cells were trypsinizated for 5 minutes with trypsin-EDTA (trypsin 0.5 g/L + EDTA 0.221 g/L - ECM0920D, *EuroClone*). The resulting cells were counted and plated on tissue-culture treated supports or cover slips, according to the desired density.

7.2 Pharmacological Treatments

The pharmacological treatments performed include:

- *rel*-3-[6-[(2*R*,6*S*)-2,6-Dimethyl-4-morpholinyl]-4-pyrimidyl]-5-[(1-methylcyclopropyl)oxy]-1*H*-indazole (MLi-2; 10 nM, 45 min; HY-100411/CS-634 *TOCRIS*). Selective LRRK2 kinase inhibitor.
- 5-(2-Fluoro-4-pyridinyl)-2-(phenylmethoxy)-*N*-3-pyridinylbenzamide (GSK2578215A; 200 nM, 45 min; SML0660 *Sigma Aldrich*). Selective LRRK2 kinase inhibitor.
- Saponin (S-1252, *Sigma-Aldrich*). A 2% w/v stock solution in water was used and diluted in Phosphate-buffered saline Low-Salts (PBS LS) to obtain a final 0.01% solution. The stock solution was prepared by weighing 2 g of powder and by subsequently dissolving it in 100 mL of distilled H_2O. Used at low concentrations and for short periods, saponin allows permeabilization of plasma membranes and enables cytosol clearance, making the proteins associated with intracellular organelles easier to be detected.

7.3 Hormone immunoassay

For *ex vivo* glucose-stimulated insulin secretion (GSIS) on isolated human islets of Langerhans, 20 islets per well were plated in a 96-multiwell and pre-incubated with Krebs-Ringer-HEPES (KRH) buffer containing 0.2% BSA (A7030, *Sigma-Aldrich*) with 3.3 mM (basal release) or 16.7 mM (stimulated release) glucose concentrations.

For mouse isolated islets of Langerhans, 10 islets per well were plated in a 96-multiwell and pre-incubated in KRH-0.2% BSA solution for 1 hour at 37 °C in a 5% CO_2 incubator. The islets were then transferred for 45 minutes to low-glucose (3 mM, basal secretion) or high-glucose (28 mM, stimulated secretion) KRH- 0.2% BSA buffer.

For βTC3 cells, 3×10^4 cells per well were plated in a 96-well and pre-incubated for 1 hour at 37 °C in 1 mM glucose KRH buffer plus 0.2% BSA. Then cells were incubated for 45 minutes in fresh 1 mM glucose KRH-0.2% BSA buffer to assess the basal release. Afterward, stimulated release was evaluated in 20 mM glucose KRH-0.2% BSA buffer for 45 minutes.

For all the GSIS experiments, the culture supernatants were collected after 45 minutes of static incubation and stored at -20 °C. The basal insulin secretion, stimulated insulin secretion, and the total insulin content were measured by means of a mouse or human insulin ELISA kit (*Mercodia*. 10-1247-01 for βTC3 and mice islets; 10-1113-01 for human islets). Insulin secretion was expressed as a percentage of insulin content or as fold over the basal release; values for released insulin in the supernatants were normalized to total βTC3 cells, mice or human islets insulin content.

For the detection of insulin in serum, blood samples were collected and centrifuged for 14 min at 4000 g at 4 °C. The serum insulin concentration was detected by mouse ELISA assay as described above.

7.4 Mice

Non-transgenic wild-type and BAC *LRRK2* G2019S mice were used. The G2019S mutation, characterized by an increased kinase activity of LRRK2 (Smith et al., 2006), is among the most common causes of familial PD (Arbez et al., 2020). Therefore, *LRRK2* G2019S mice models are commonly used in the field of PD research. Specifically, the *LRRK2* G2019S mouse BAC Tg is a transgenic animal overexpressing the G2019S *LRRK2*-mutated protein in the brain, obtained by taking advantage of a bacterial artificial chromosome (Li et al., 2010). Hemizygous mice develop an age-associated decrease in striatal dopamine, without loss of dopaminergic neurons, behavioral motor deficits or brain abnormalities at least out to the age of 18 months. The animal samples used in this work were kindly supplied by Prof. Giovanni Piccoli, Department of Cellular, Computational, and Integrative Biology, University of Trento, Italy.

7.5 Vectors: amplification, purification, and transfection

The plasmids used in this work were kindly supplied by Prof. Giovanni Piccoli, Department of Cellular, Computational, and Integrative Biology, University of Trento, Italy. Human LRRK2 full-length, *LRRK2* 914-end (hereinafter termed as LRRK2ΔN-terminus), *LRRK2* 1–983 (hereinafter termed as LRRK2 N-terminus), *LRRK2* S935A variant, and *LRRK2* G2019S variant were inserted into the pDEST57 vector (N-terminal red fluorescent protein-RFP tag, *Invitrogen*). hLRRK2 full-length and LRRK2ΔN-terminus were inserted in N-terminal Strep-FLAG (SF-TAP) plasmid (Gloeckner et al., 2007) using the Gateway system (*Invitrogen*). Instead, full-length RFP and Strep-FLAG E193K variants were created *via* site-directed mutagenesis using the QuikChange mutagenesis kit (*Stratagene*). LRRK2-target sequences were identified using Ambion-web-based Oligo-search Software; one sequence (AAGTTGATAGTCAGGCTGAAT, AY792512: 58–79) was selected, synthesized, and subcloned. Transduced cultures were included as controls for unspecific dsRNA-mediated off-target effects (Bauer et al., 2009). SynaptopHluorin was obtained from rat synaptophysin1 cDNA and amplified by PCR. The product was then inserted into the synaptopHluorin vector, thereby connecting it to pHluorin and replacing the synaptobrevin region of synaptopHluorin (Granseth et al., 2006). The Rab8a-WT, Rab8a-T72A, Rab8a-T72D, and Rab8a-T72E constructs were realized by Dr. Sabine Hilfiker, Institute of Parasitology and Biomedicine "López-Neyra," Consejo Superior de Investigaciones Científicas, Granada, Spain. Rab8a constructs were generated using Gibson Assembly Master Mix (*New England Biolabs*). Rab8a-T72A, Rab8a-T72D, and Rab8a-T72E mutant constructs were generated by site-directed mutagenesis (*QuikChange, Stratagene*). Identity of all constructs was verified by sequencing of the entire coding region (Madero-Pérez et al., 2018).

The amplification of DNA vectors was performed in JM109 bacteria (genotype: endA1 glnV44 thi-1 relA1 gyrA96 recA1 mcrB+ Δ(lac-proAB) e14- [F' traD36 proAB+ lacIq lacZΔM15] hsdR17(rK -mK +), an *Escherichia Coli* strain.

Preparation of competent JM109 bacteria. Original JM109 bacteria were cultured in 3 mL of lysogeny broth (LB) overnight under constant agitation (125 g) at 37 °C. The day after, the bacterial culture was transferred into a sterile plastic Erlenmeyer flask containing 100 mL of LB and were grown under agitation (220 rpm) at 37 °C. Since bacteria can be made competent only during the exponential growth, an aliquot of the bacterial culture was taken every 30 minutes and their growth was analysed by spectrophotometry (600 nm). When the measured optical density (OD) was around 0.6, bacteria reached the exponential growth phase and were processed as follow:

- 10 minutes centrifugation at 1700 g at 4 °C.
- Resuspension of the pellet in cold Transformation Buffer Japanese (TB JAP) solution and incubation in ice for 10 minutes.
- 10 minutes centrifugation at 1400 g at room temperature (RT).
- Resuspension of the pellet in TB JAP supplemented with 7% (v/v) DMSO and incubation in ice for 10 minutes.

JM109 transformation, DNA extraction, and purification. DNA vectors were inserted into competent JM109 bacteria through a heat shock consisting in 30 minutes ice incubation, 1 minute at 42 °C, and 1 minute in ice again. JM109 were then incubated at 37 °C for 60 minutes under constant agitation (220 rpm). Ampicillin (50 µg/mL) or kanamycin (30 µg/mL) were used for bacteria selection and added to the bacterial culture, which was incubated overnight at 37 °C (for LRRK2 constructs the incubation was performed at RT to avoid recombination phenomena). Transformed bacteria were then incubated at 37 °C (for LRRK2 constructs at RT) overnight under agitation (220 rpm) for amplification. Finally, DNA vectors were extracted and purified using the EuroGold Plasmid Miniprep kit (EMR500050, *EuroClone*), following the manufacturer's protocol. The concentration of the extracted cDNAs was quantified by gel electrophoresis.

Cell transfection N2a cells were transfected with the different constructs using Lipofectamine™ 3000 Reagent (*Invitrogen*) according to manufacturer's instructions, meanwhile βTC3 cells were transfected by electroporation, which was accomplished using a *Bio-Rad* Gene Pulser II under optimized conditions (950 F and 180 V).

7.6 Western Blotting

Cells were collected and lysed in RIPA buffer added with 0.01% SDS (only for human islets) supplemented with 0.5 µg/mL aprotinin, 0.5 mg/mL PMSF, and 1x Roche inhibitors for 15 minutes at 4 °C followed by a 10-minute centrifugation at 7400 g. After lysis, protein concentration was determined by Bradford assay using Bradford Reagent (B6916, *Sigma Aldrich*). Samples were prepared by adding to the calculated volume of lysates the β-mix 2x solution, containing the reducing agent β-mercaptoethanol, and the tracking marker bromophenol blue. Samples were boiled on a dry plate at 100 °C for 45 seconds to unfold the 3D protein structure and kept on ice until use. Polyacrylamide Gel Electrophoresis (PAGE) (9% gel) was used for protein separation. The polyacrylamide gel was mounted vertically between two buffer chambers, then filled with the running buffer. Samples and a prestained protein marker (EPS025500, *EuroClone*) were loaded and an electric field of 100 V was applied to allow samples entering the running gel. Separation was performed at 60 V for about 3 hours. Separated proteins, according to their electrophoretic mobility, were electrotransferred from the gel to a 0.45 µm pore size PDVF membrane (Immobilon®- P, IPVH00010, *Millipore*). Briefly, PVDF membranes were activated by incubating them in methanol (15 seconds) and deionized water (2 minutes), and then equilibrated for 5 minutes in the blotting buffer. The sandwich was mounted into the transfer chamber filled with the blotting buffer. The electrotransfer was performed overnight at 90 mA at 4 °C. The evaluation of protein transfer was performed by labelling the membranes with a solution of 0.1% (w/v) Ponceau S in 5% acetic acid (P-7170, *Sigma Aldrich*).

Immunodetection. For proteins detection, a chemiluminescent (ECL) assay was performed by using antibodies conjugated to the horseradish peroxidase (HRP), a chemiluminescent substrate (luminol), and an oxidizing agent (hydrogen peroxide). Immunodetection was performed according to the following protocol:

- *Blocking phase*: incubation of the membrane with the blocking buffer for 1 hour at RT to prevent non-specific binding of the antibodies; the blocking buffer composition is strictly dependent on the antibody used.
- *Primary antibody staining*: incubation of the membrane with the primary antibody diluted in the incubation buffer on a plate-shaker; the timing and the buffer used for the labelling are strictly dependent on the antibody.
- *Secondary antibody staining*: incubation of the membrane with the HRP-conjugated antibody diluted in the blocking buffer for 1 hour at RT on a plate-shaker.

The ETA C 2.0 WESTAR kit (XLS075, *Cyanagen*) was used as HRP-substrate. The luminol and the peroxide solutions were mixed 1:1, then the membrane was incubated in the ECL solution for 5 minutes in the dark at RT. The signal of the ECL-based reaction was detected with the Odyssey Fc. Imaging system (Li-Cor, *Biosciences*). The optical density of the bands was quantified by using the Image Studio™ Lite software (version 3.1, Li-Cor, *Biosciences*). Band intensity was quantified with the ImageJ software.

Primary antibodies included:

- rabbit anti-LRRK2 1:500 (MJFF2, c41-2, abB1334A4, *Abcam*)
- rabbit anti-LRRK2-PS935 1:500 (VDD10(12), ab133450, *Abcam*)
- rabbit anti-RFP 1:250 (ab62341, *Abcam*)
- rabbit anti-GFP 1:500 (PA1-9533, *Thermo Fisher*)
- mouse anti-β-Actin 1: 10000 (NB600-501, *Novus Biologicals*)
- mouse anti-α-tubulin 1:2000 (T4026, *Sigma-Aldrich*)
- rabbit anti-Synapsin I 1:10000 (5297, *Cell signaling*)
- rabbit anti-S6 ribosomal protein 1:1000 (2217, *Cell Signaling*)

Secondary antibodies HRP-conjugated included:

- polyclonal anti-mouse IgG 1:1000 (7076, *Cell Signaling*)
- polyclonal anti-rabbit IgG 1:1000 (7074, *Cell Signaling*)
- polyclonal anti-mouse IgG 1:5000 (P0447, *Dako*)
- polyclonal anti-rabbit IgG 1:5000 (P0448, *Dako*)

7.7 Co-immunoprecipitation.

The affinity pull-down assay was performed on N2a cells. 48 h after transfection, N2a cellular proteins were extracted in RIPA lysis buffer supplemented with protease and phosphatase inhibitors (*Calbiochem*) for 1 hour at 4 °C. Samples were incubated on Strep-Tactin Superflow resin (*Iba-Lifesciences*) for 2 hours at 4 °C. Resin was then incubated with a washing buffer. Interacting proteins were eluted in 2X Laemmli buffer at 55 °C for 10 minutes. Samples were analysed by western blotting performed on 10% SDS-PAGE gels. To evaluate co-immunoprecipitation efficiency, the intensity of the co-immunoprecipitated protein was normalized to the amount of LRRK2 variants immunoprecipitated.

7.8 Immunochemistry

βTC3 cells, differently treated, were fixed with 4% paraformaldehyde for 20 minutes at RT. All antibodies used for cells staining were diluted in a GDB 1x solution (50% GDB 2x + 50% deionized water). βTC3 cells cultured on glass coverslips were labelled with guinea pig anti-insulin polyclonal antibody (1:250, A0564, *Dako*), rabbit anti-LRRK2 antibody (1:50, MJFF2 c41-2, abB1334A4, *Abcam*) or rabbit anti-LRRK2-PS935 antibody (1:50, VDD10(12), ab133450, *Abcam*) for 2 hours. Cells were then incubated with rhodamine-conjugated anti-guinea pig IgG (1:150, *Abcam*), FITC-conjugated anti-rabbit IgG (ab6717, *Abcam*) or biotinylated-conjugated anti-rabbit IgG (1:150, *Jackson ImmunoResearch Laboratories*) for 1 hour at RT. Slides were mounted with Fluoroshield with DAPI (4',6-diamidin-2-phenylindole - F6057, *Sigma* Aldrich). Samples were placed in an imaging chamber, and random fields were captured by epifluorescence and TIRF (Total Internal Reflection Fluorescence) microscopy using an Axio Observer Z1 microscope, fitted with a 100 × 1.45 numerical aperture (NA) oil immersion objective and an Argon laser as a source of illumination. The ImageJ particle analysis plug-in was employed to quantify the number of fluorescent objects. For improving the image quality prior to analysis, the background was subtracted, and the image were pre-processed using the "unsharp mask" filter. The cell area (μm^2) and the number of sypHy-positive cluster, insulin-positive granules or LRRK2 P-395-positive spots per cell were measured in a software-assisted manner. For each experimental condition, up to ten cells were imaged in not less of three independent experiments and the collected data were normalized to the cell area.

Human islets were dispersed into small clusters by disaggregating them with 1 mg/mL trypsin-EDTA (ECM0920D, *EuroClone*) + 0.25 mg/mL DNAse I (18068015, *Thermo Fisher*) solution: the digestion was carried out by pipetting up and down the cell suspension at 22 °C for 3 minutes. Once obtained a single cell suspension, cells were seeded on glass coverslips, fixed, and labelled as above reported.

For morphological studies, animals were sacrificed by cervical dislocation, and pancreases from wild type and transgenic mice were fixed in 4% (w/v) neutral-buffered formalin, processed, and embedded in paraffin blocks. After microwave antigen retrieval (2x5 min in 10 mM citrate buffer, pH 6.0), 5-µm-thick sections were incubated for two hours with primary antibodies against hormones. The following antibodies were used: guinea pig anti-insulin polyclonal (1:350, A0564, *Dako*), mouse anti-glucagon polyclonal (1:50, MAB1249, *Biotechn*e), and rat anti-somatostatin monoclonal (1:75, ab30788, *Abcam*). Staining with primary antibody was followed by incubation for one hour with rhodamine-conjugated anti-guinea pig IgG, FITC-conjugated anti-rat IgG, and Cy5-conjugated anti-mouse IgG (1:150, *Jackson ImmunoResearch Laboratories*). Samples were visualised using a Carl Zeiss Axiovert Z1 inverted fluorescence microscope equipped with a RetigaSRV Fast CCD camera. Single stain immunofluorescence images were acquired using a 40x objective, deblurred, and merged by using Image ProPlus Software (*Media Cybernetics*). Identical parameters (acquisition time and gain) were maintained to acquire images from all sections. To quantify the islet's area, the histological sections were stained with fluorophores-conjugated antibodies directed against hormones. For each islet, the area (μm^2), major axis (µm), and minor axis (µm) were measured in a software-assisted manner. For each mouse, up to 5 sections and 30 fields (correspondent to 20-30 different islets) were imaged and analysed. The analysis was performed in 1xBAC-LRRK2-G2019S and WT mice (n=7 per each group).

7.9 Reverse transcriptase PCR

Expression of LRRK2 protein in the endocrine pancreas was confirmed by reverse transcriptase-PCR using the MultiScribe Reverse Transcriptase (*Invitrogen*). Total RNA from 9×10^6 βTC3 or 1500 isolated human islets of Langerhans was extracted with Trizol (*Sigma Aldrich*). For cDNA synthesis, 2 µg of digested RNA was reverse transcribed using random oligonucleotides (final concentration, 12.5 ng/µL) as primers and 200 Moloney murine leukemia units. PFU Polymerase (*Promega*) was used as DNA polymerase. To confirm the absence of genomic contamination in the RNA samples, reverse transcriptase negative controls were introduced in each experiment (without Moloney murine leukemia virus reverse transcriptase). Cycling conditions were: 2 minutes at 95 °C; 30 seconds at 95 °C, 30 seconds at 60 °C, 1 minute at 72 °C, for 40 cycles; and a final elongation at 72 °C for 10 minutes.

Primer description. Each primer was used at the final concentration of 0.5 µM*:*

Couple 1 (for human). Forward primer: TGGGAAATACTGGGAGTGGT; Reverse primer: ACCTGCAAAATCCCACACAT

Couple 2 (for mouse). Forward primer: CGTCCTCGGATGTTGGTAAT; Reverse primer: TAGTCCGCAATCTTCGCAAT

7.10 Cell viability by MTT assay

βTC3 cells were plated with a density of 3×10^4 in 96 multi-well and treated with specific LRRK2 inhibitors for 45 minutes. After treatment, cells were incubated with fresh medium containing 0.5 mg/mL MTT (3-(4,5-dimethyltiazol-2-yl)-2,5-diphenyltetrazolium bromide) (M5655, *Sigma-Aldrich*) for 4 hours in a 37 °C-5% CO_2 incubator. After, a gently resuspension in 100 µL DMSO (276855, *Sigma-Aldrich*) was performed. Absorbance was detected at 540 nm with the microplate TECAN infinite® F500 reader. Mean values and standard deviations were based on three independent experiments.

7.11 Synaptic vesicle isolation and binding assay

Synaptic vesicles were isolated from rat brain using controlled-pore glass chromatography according to the protocol described by Huttner et al. (Huttner et al., 1983). This part of experiments was performed in collaboration with Prof. Franco Onofri, Department of Experimental Medicine, University of Genova, Italy. RFP-LRRK2 WT and E193K proteins were purified from N2a transfected cells using the RFP-Trap A kit according to manufacturer's protocol. To evaluate LRRK2 fusion proteins binding to SVs (synaptic vesicles), a high-speed sedimentation assay (Messa et al., 2010) was performed. SVs (5–10 µg total protein) were incubated with RFP-LRRK2 WT or RFP-LRRK2 E193K for 1 hour at 0 °C in dedicated buffer (220 mM glycine, 30 mM NaCl, 5 mM Tris/HCl, 4 mM Hepes, pH 7.4, 0.22 mM NaN_3, 0.2 mM PMSF, 2 µg/mL pepstatin, and 100 µg/mL of bovine serum albumin). Then, LRRK2 SV-bounded was isolated by high-speed centrifugation (400,000 × g for 45 min). Pellets were resuspended in Laemmli buffer 2x and analysed by Western blotting with RFP antibodies. The fraction of SVs binding LRRK2 in comparison to known number of fusion proteins was normalized on SV yield, determined by Western blotting with an anti-synaptophysin antibody (1:1000 - *Sigma-Aldrich*).

7.12 Vesicle trafficking by Acridine Orange assay

The pH-sensitive dye acridine orange (AO) was used as a tool to monitor the trafficking of acidic glucose insulin containing granules (GSs). βTC3 cells were loaded with 100 nM Acridine Orange (A-6014, *Sigma-Aldrich*) in KRH buffer supplemented with 1 mM glucose at 37 °C for 15 minutes. The fluorescence intensity

was detected after 30 minutes treatment with the specific LRRK2 inhibitors, both in basal and stimulated conditions, with the microplate TECAN infinite® F500 reader (535/590 nm Ex/Em). Mean values and standard deviations were based on three independent experiments

7.13 Time lapse microscopy by total internal reflection fluorescence microscopy (TIRFM) and image analysis

TIRF microscopy limits the fluorophore excitation to a thin field of about 100 nm by exploiting the total internal reflection phenomenon. The reflection generates a restricted electromagnetic field that extends for a few hundred nanometers into the lower-index phase medium and declines sharply with the increasing distance from the interface, leading to the visualization of a limited region in the proximity of the interface, as the plasma membrane. TIRF microscopy was performed 48 hours after the cell transfection. The microscope (Carl Zeiss Inc.) was equipped with an Argon laser and a 100× 1.45 numerical aperture (NA) oil immersion objective. Green fluorescence was excited with 488-nm laser line and imaged through a band-pass filter (Zeiss) onto a Retiga SRV CCD camera. Single-cell imaging under TIRF illumination was performed at 1Hz for a total of thirty seconds, in a standard KRH solution at room temperature (25 °C). On each coverslip, up to ten cells were imaged in not less than three independent experiments for each construct. Image-Pro Plus Analyser Image Software (Media Cybernetics) was used to analyse TIRF images. A set of automated image processing macro/subroutines based on existing algorithms of the Image-Pro Plus software (High Pass Gaussian filtering, nearest neighbouring deconvolution, photobleaching correction) have been employed for image processing. The corrected images were subsequently analysed by means of the Image-Pro Plus plug-in software (tracking object) that allows the selection and quantification of fluorescent spots based on their shapes, size, and intensity. We selected the following criteria to include individual structures in the analysis: (1) mean area 0.02–1 μm^2, (2) minimal pixel intensity six-fold over the average cell fluorescence intensity, (3) aspect (major/minor axis) 1–3, (4) velocity limit search radius 1 (micron/frame). Spots that showed up in the same position in at least 6 frames of the movie were automatically excluded from the analysis. Data were then exported in Microsoft Excel for further analysis. The fluorescence intensity (F) of each spot in the various frames was normalized to the minimal pixel intensity (F0, calculated as defined above) and plotted against time. A custom written macro has been used to automatically count the number of fusion events and the whole cell fluorescence changes. Data collected from at least 20 cells for each construct were normalized to the cell area. To quantify the vesicle density in the TIRF zone, the cells were incubated for 5 minutes with 50 mM NH_4Cl_2 KRH solution, to label all synapto-pHluorin positive vesicles. Then, cells were fixed in paraformaldehyde and imaged by TIRFM or epifluorescence. The number of vesicles was quantified as described above and normalized for the cell area.

For insulin granules count, the ImageJ particle analysis plug-in was employed to quantify the number of fluorescent objects. For improving the image quality prior to analysis, the background was subtracted, and the images were pre-processed using the "unsharp mask" filter. A 3.5 pixels radius and a 0.6 pixels *mask weight* 0.6 were used. The area (μm^2) of the cells and the number of insulin-positive granules per cell were measured in a software-assisted manner. For insulin granules size, we considered values between 0.015 and 0.5 µm. On each slide, up to ten cells were imaged in not less of three independent experiments and the collected data were normalized to the cell area.

7.14 Statistical analysis and guidelines

All statistical analyses were performed with GraphPad Prism 9.0 on independent biological replicates. Data are presented as means ± S.E. or S.D. of at least three independent experiments. The number of replicates for each experiment is reported. Statistical analyses between two groups were assessed using the two-tailed Student's *t*-test or among multiple groups using the analysis of variance (ANOVA). A P value <0.5 was considered statistically significant. All methods were performed in accordance with the relevant guidelines and national regulations. All procedures involving animals were approved by Institutional and National Agencies (authorization n. 793/2016-PR and 365 D.lgs 116/92-art.7, IRCCS San Martino-IST, PROT. n. 0005278/14).

7.15 Reagents and solutions

PFA 4% (Paraformaldehyde solution). Dissolve PFA powder in PO_4 pH 7.4 buffer (120 mM) at 50 °C in a water bath, then filter the solution. Store at -20 °C.

HBSS 4x (Hanks' balanced salt solution 4x). 0.74 g $CaCl_2$ * $2H_2O$, 1.45 g D-Glucose, 9.5 g Hepes, 1.6 g KCL, 0.24 g KH_2PO_4, 0.8 g $MgSO_4$ * $7H_2O$, 32 g NaCl, 1.4 g $NaHCO_3$, 0.24 g Na_2HPO_4* $2H_2O$. Up to 1 L with deionized water.

PBS LS (Phosphate buffer low salts). NaCl (150 mM), PO_4 buffer pH 7.4 (10 mM). Up to volume with deionized water.

1 mg/mL Aprotinin**.** Dissolve Aprotinin (A4529, *Sigma Aldrich*) in deionized water. Store at -20 °C. A 1:1000 dilution was used for the experiments.

200 mg/mL PMSF (PhenylMethaneSulfonyl Fluoride). Dissolve PMSF (10837091001, *Sigma Aldrich*) in Absolute Ethanol by heating. Store at -20 °C. A 1:200 dilution was used for the experiments.

25x Roche inhibitors. Dissolve one tablet of the cOmplete™ ULTRA Protease Inhibitor Cocktail (5892953001, *Sigma Aldrich*) in PO_4 pH 7.4 buffer (100 mM). Store at -20 °C. A 1:25 dilution was used for the experiments.

SDS 10%. Dissolve SDS (*Sigma.* Cat# L4509-100G) in deionized water. Store at room temperature.

RIPA buffer (RadioImmunoPrecipitation Assay). NaCl (150 mM), Tris-HCl pH 7.6 (50 mM), EDTA (1 mM), NP40 (1%), Deoxycholate (0.5%). Up to volume with deionized water.

2x β-mix. SDS-10% solution (50%), Glycerol (20%), Tris-HCl pH 8.9 (300 mM), β-mercaptoethanol (10%), Bromophenol blue (10%).

9% polyacrylamide running gel. Bis-Acrylamide (10%), Tris HCl pH 8.9 (375 mM), 10% SDS solution (0.1%), Tetramethylethylenediamine (TEMED) (0.05%), Ammonium persulfate (APS) (0.025%). Up to volume with deionized water.

10% polyacrylamide running gel. Bis-Acrylamide (10%), Tris HCl pH 8.9 (375 mM), SDS-10% solution (0.1%), Tetramethylethylenediamine (TEMED) (0.05%), Ammonium persulfate (APS) (0.025%). Up to volume with deionized water.

Polyacrylamide stacking gel. Bis-Acrylamide (4%), Tris HCl pH 6.8 (62.5 mM), 10% SDS solution (0.1%), Tetramethylethylenediamine (TEMED) (0.1%), Ammonium persulfate (APS) (0.05%). Up to volume with deionized water.

TBS pH 7.4 (Tris Buffer Saline). Dissolve Trizma® base (0.6%; T1503, *Sigma Aldrich*) and NaCl (1.20 %; S9888, *Sigma Aldrich)* in deionized water. Adjust the pH to 7.4 with 10 N HCl.

Running buffer. Tris-Glycine 10x (1x), 10% SDS solution (0.1%). Up to volume with deionized water.

Blotting buffer. Tris-Glycine 10x (1x), Methanol (10%). Up to volume with deionized water.

1x blocking buffer. Non-fat dried milk (3% or 5%), TBS (1x), Tween 20 (0.1%).

KRH (Krebs Ringer Buffer). NaCl (125 mM), KCL (5 mM), $MgSO_4$ (1.2 mM), KH_2PO_4 (1.2 mM), Hepes-NaOH pH 7.4 (25 mM), $CaCl_2$ (2 mM). Up to volume with deionized water.

GDB 2x. NaCl (4 M), PO_4 buffer pH 7.4 (240 mM), Triton X-100 (6%), gelatine (0.2%). Up to volume with deionized water. Store at -20°C.

LB (Lysogen broth). Dissolve Tryptone (1%; A1553, *BioChemica*), Yeast Extract (0.5%; A1552, *BioChemica*), and NaCl (0.5%; S9888, *Sigma Aldrich*) in deionized water. Sterilize by autoclaving.

TB JAP. Dissolve PIPES (0.3%; P6757, *Sigma Aldrich*), $CaCl_2$ (0.22 %; 223506, *Sigma Aldrich*), KCl (1.86%; P3911, *Sigma Aldrich*), and $MnCl_2$ (1.09%; 1375127, *Sigma Aldrich)* in deionized water; adjust the pH to 6.7 with NaOH 1 N. Filter the solution with 0.22 µm filter. Store at 4 °C.

8. Bibliography

Aarsland, D., Marsh, L., Schrag, A., 2009. Neuropsychiatric symptoms in Parkinson's disease. Mov. Disord. 24, 2175–2186. https://doi.org/10.1002/mds.22589

Akintola, A.A., van Heemst, D., 2015. Insulin, Aging, and the Brain: Mechanisms and Implications. Front. Endocrinol. 6. https://doi.org/10.3389/fendo.2015.00013

Alcalay, R.N., Mirelman, A., Saunders-Pullman, R., Tang, M.-X., Mejia Santana, H., Raymond, D., Roos, E., Orbe-Reilly, M., Gurevich, T., Bar Shira, A., Gana Weisz, M., Yasinovsky, K., Zalis, M., Thaler, A., Deik, A., Barrett, M.J., Cabassa, J., Groves, M., Hunt, A.L., Lubarr, N., San Luciano, M., Miravite, J., Palmese, C., Sachdev, R., Sarva, H., Severt, L., Shanker, V., Swan, M.C., Soto-Valencia, J., Johannes, B., Ortega, R., Fahn, S., Cote, L., Waters, C., Mazzoni, P., Ford, B., Louis, E., Levy, O., Rosado, L., Ruiz, D., Dorovski, T., Pauciulo, M., Nichols, W., Orr-Urtreger, A., Ozelius, L., Clark, L., Giladi, N., Bressman, S., Marder, K.S., 2013. Parkinson disease phenotype in Ashkenazi jews with and without *LRRK2* G2019S mutations: PD Phenotype and *LRRK2* Mutations. Mov. Disord. 28, 1966–1971. https://doi.org/10.1002/mds.25647

Amara, A.W., Memon, A.A., 2018. Effects of Exercise on Non-motor Symptoms in Parkinson's Disease. Clin. Ther. 40, 8–15. https://doi.org/10.1016/j.clinthera.2017.11.004

Andersen, M.A., Wegener, K.M., Larsen, S., Badolo, L., Smith, G.P., Jeggo, R., Jensen, P.H., Sotty, F., Christensen, K.V., Thougaard, A., 2018. PFE-360-induced LRRK2 inhibition induces reversible, non-adverse renal changes in rats. Toxicology 395, 15–22. https://doi.org/10.1016/j.tox.2018.01.003

Antoniou, N., Vlachakis, D., Memou, A., Leandrou, E., Valkimadi, P.-E., Melachroinou, K., Re, D.B., Przedborski, S., Dauer, W.T., Stefanis, L., Rideout, H.J., 2018. A motif within the armadillo repeat of Parkinson's-linked LRRK2 interacts with FADD to hijack the extrinsic death pathway. Sci. Rep. 8, 3455. https://doi.org/10.1038/s41598-018-21931-8

Arbez, N., He, X., Huang, Y., Ren, M., Liang, Y., Nucifora, F.C., Wang, X., Pei, Z., Tessarolo, L., Smith, W.W., Ross, C.A., 2020. G2019S-LRRK2 mutation enhances MPTP-linked Parkinsonism in mice. Hum. Mol. Genet. 29, 580–590. https://doi.org/10.1093/hmg/ddz271

Arranz, A.M., Delbroek, L., Van Kolen, K., Guimarães, M.R., Mandemakers, W., Daneels, G., Matta, S., Calafate, S., Shaban, H., Baatsen, P., De Bock, P.-J., Gevaert, K., Vanden Berghe, P., Verstreken, P., De Strooper, B., Moechars, D., 2014. LRRK2 functions in synaptic vesicle endocytosis through a kinase-dependent mechanism. J. Cell Sci. jcs.158196. https://doi.org/10.1242/jcs.158196

Athauda, D., Foltynie, T., 2016. Insulin resistance and Parkinson's disease: A new target for disease modification? Prog. Neurobiol. 145–146, 98–120. https://doi.org/10.1016/j.pneurobio.2016.10.001

Athauda, Dilan, Foltynie, T., 2016. The glucagon-like peptide 1 (GLP) receptor as a therapeutic target in Parkinson's disease: mechanisms of action. Drug Discov. Today 21, 802–818. https://doi.org/10.1016/j.drudis.2016.01.013

Athauda, D., Maclagan, K., Skene, S.S., Bajwa-Joseph, M., Letchford, D., Chowdhury, K., Hibbert, S., Budnik, N., Zampedri, L., Dickson, J., Li, Y., Aviles-Olmos, I., Warner, T.T., Limousin, P., Lees, A.J., Greig, N.H., Tebbs, S., Foltynie, T., 2017. Exenatide once weekly versus placebo in Parkinson's disease: a randomised, double-blind, placebo-controlled trial. The Lancet 390, 1664–1675. https://doi.org/10.1016/S0140-6736(17)31585-4

Ballian, N., Hu, M., Liu, S.-H., Brunicardi, F.C., 2007. Proliferation, Hyperplasia, Neogenesis, and Neoplasia in the Islets of Langerhans. Pancreas 35, 199–206. https://doi.org/10.1097/mpa.0b013e318074c6ed

Baranowska-Bik, A., Bik, W., 2017. Insulin and brain aging. Menopausal Rev. 2, 44–46. https://doi.org/10.5114/pm.2017.68590

Barbiero, J.K., Santiago, R.M., Persike, D.S., da Silva Fernandes, M.J., Tonin, F.S., da Cunha, C., Lucio Boschen, S., Lima, M.M.S., Vital, M.A.B.F., 2014. Neuroprotective effects of peroxisome proliferator-activated receptor alpha and gamma agonists in model of parkinsonism induced by intranigral 1-methyl-4-phenyl-1,2,3,6-tetrahyropyridine. Behav. Brain Res. 274, 390–399. https://doi.org/10.1016/j.bbr.2014.08.014

Bauer, M., Kinkl, N., Meixner, A., Kremmer, E., Riemenschneider, M., Förstl, H., Gasser, T., Ueffing, M., 2009. Prevention of interferon-stimulated gene expression using microRNA-designed hairpins. Gene Ther. 16, 142–147. https://doi.org/10.1038/gt.2008.123

Beilina, A., Rudenko, I.N., Kaganovich, A., Civiero, L., Chau, H., Kalia, S.K., Kalia, L.V., Lobbestael, E., Chia, R., Ndukwe, K., Ding, J., Nalls, M.A., International Parkinson's Disease Genomics Consortium, North American Brain Expression Consortium, Olszewski, M., Hauser, D.N., Kumaran, R., Lozano, A.M., Baekelandt, V., Greene, L.E., Taymans, J.-M., Greggio, E., Cookson, M.R., Nalls, M.A., Plagnol, V., Martinez, M., Hernandez, D.G., Sharma, M., Sheerin, U.-M., Saad, M., Simon-Sanchez, J., Schulte, C., Lesage, S., Sveinbjornsdottir, S., Arepalli, S., Barker, R., Ben-Shlomo, Y., Berendse, H.W., Berg, D., Bhatia, K., de Bie, R.M.A., Biffi, A., Bloem, B., Bochdanovits, Z., Bonin, M., Bras, J.M., Brockmann, K., Brooks, J., Burn, D.J., Charlesworth, G., Chen, H., Chong, S., Clarke, C.E., Cookson, M.R., Cooper, J.M., Corvol, J.C., Counsell, C., Damier, P., Dartigues, J.-F., Deloukas, P., Deuschl, G., Dexter, D.T., van Dijk, K.D., Dillman, A., Durif, F., Durr, A., Edkins, S., Evans, J.R., Foltynie, T., Gao, J., Gardner, M., Gibbs, J.R., Goate, A., Gray, E., Guerreiro, R., Gustafsson, O., Harris, C., van Hilten, J.J., Hofman, A., Hollenbeck, A., Holton, J., Hu, M., Huang, X., Huber, H., Hudson, G., Hunt, S.E., Huttenlocher, J., Illig, T., Munchen, H.Z., Jonsson, P.V., Lambert, J.-C., Langford, C., Lees, A., Lichtner, P., Munchen, H.Z., Limousin, P., Lopez, G., Lorenz, D., McNeill, A., Moorby, C., Moore, M., Morris, H.R., Morrison, K.E., Mudanohwo, E., O'Sullivan, S.S., Pearson, J., Perlmutter, J.S., Petursson, H., Pollak, P., Post, B., Potter, S., Ravina, B., Revesz, T., Riess, O., Rivadeneira, F., Rizzu, P., Ryten, M., Sawcer, S., Schapira, A., Scheffer, H., Shaw, K., Shoulson, I., Sidransky, E., Smith, C., Spencer, C.C.A., Stefansson, H., Steinberg, S., Stockton, J.D., Strange, A., Talbot, K., Tanner, C.M., Tashakkori-Ghanbaria, A., Tison, F., Trabzuni, D., Traynor, B.J., Uitterlinden, A.G., Velseboer, D., Vidailhet, M., Walker, R., van de Warrenburg, B., Wickremaratchi, M., Williams, N., Williams-Gray, C.H., Winder-Rhodes, S., Stefansson, K., Hardy, J., Heutink, P., Brice, A., Gasser, T., Singleton, A.B., Wood, N.W., Chinnery, P.F., Arepalli, S., Cookson, M.R., Dillman, A., Ferrucci, L., Gibbs, J.R., Hernandez, D.G., Johnson, R., Longo, D.L., Majounie, E., Nalls, M.A., O'Brien, R., Singleton, A.B., Traynor, B.J., Troncoso, J., van der Brug, M., Zielke, H.R., Zonderman, A.B., 2014. Unbiased screen for interactors of leucine-rich repeat kinase 2 supports a common pathway for sporadic and familial Parkinson disease. Proc. Natl. Acad. Sci. 111, 2626–2631. https://doi.org/10.1073/pnas.1318306111

Belluzzi, E., Gonnelli, A., Cirnaru, M.-D., Marte, A., Plotegher, N., Russo, I., Civiero, L., Cogo, S., Carrion, M.P., Franchin, C., Arrigoni, G., Beltramini, M., Bubacco, L., Onofri, F., Piccoli, G., Greggio, E., 2016. LRRK2 phosphorylates pre-synaptic N-ethylmaleimide sensitive fusion (NSF) protein enhancing its ATPase activity and SNARE complex disassembling rate. Mol. Neurodegener. 11, 1. https://doi.org/10.1186/s13024-015-0066-z

Berger, Z., Smith, K.A., LaVoie, M.J., 2010. Membrane Localization of LRRK2 Is Associated with Increased Formation of the Highly Active LRRK2 Dimer and Changes in Its Phosphorylation. Biochemistry 49, 5511–5523. https://doi.org/10.1021/bi100157u

Berwick, D.C., Heaton, G.R., Azeggagh, S., Harvey, K., 2019. LRRK2 Biology from structure to dysfunction: research progresses, but the themes remain the same. Mol. Neurodegener. 14, 49. https://doi.org/10.1186/s13024-019-0344-2

Betarbet, R., Sherer, T.B., MacKenzie, G., Garcia-Osuna, M., Panov, A.V., Greenamyre, J.T., 2000. Chronic systemic pesticide exposure reproduces features of Parkinson's disease. Nat. Neurosci. 3, 1301–1306. https://doi.org/10.1038/81834

Bilotta, F., Lauretta, M.P., Tewari, A., Haque, M., Hara, N., Uchino, H., Rosa, G., 2017. Insulin and the Brain: A Sweet Relationship With Intensive Care. J. Intensive Care Med. 32, 48–58. https://doi.org/10.1177/0885066615594341

Biosa, A., Trancikova, A., Civiero, L., Glauser, L., Bubacco, L., Greggio, E., Moore, D.J., 2013. GTPase activity regulates kinase activity and cellular phenotypes of Parkinson's disease-associated LRRK2. Hum. Mol. Genet. 22, 1140–1156. https://doi.org/10.1093/hmg/dds522

Bosgraaf, L., Van Haastert, P.J.M., 2003. Roc, a Ras/GTPase domain in complex proteins. Biochim. Biophys. Acta BBA - Mol. Cell Res. 1643, 5–10. https://doi.org/10.1016/j.bbamcr.2003.08.008

Bouhouche, A., Tibar, H., Ben El Haj, R., El Bayad, K., Razine, R., Tazrout, S., Skalli, A., Bouslam, N., Elouardi, L., Benomar, A., Yahyaoui, M., Regragui, W., 2017. *LRRK2* G2019S Mutation: Prevalence and Clinical Features in Moroccans with Parkinson's Disease. Park. Dis. 2017, 1–7. https://doi.org/10.1155/2017/2412486

Bové, J., Perier, C., 2012. Neurotoxin-based models of Parkinson's disease. Neuroscience 211, 51–76. https://doi.org/10.1016/j.neuroscience.2011.10.057

Brakedal, B., Flønes, I., Reiter, S.F., Torkildsen, Ø., Dölle, C., Assmus, J., Haugarvoll, K., Tzoulis, C., 2017. Glitazone use associated with reduced risk of Parkinson's disease: Glitazone Use and Parkinson's Disease Risk. Mov. Disord. 32, 1594–1599. https://doi.org/10.1002/mds.27128

Brauer, R., Bhaskaran, K., Chaturvedi, N., Dexter, D.T., Smeeth, L., Douglas, I., 2015. Glitazone Treatment and Incidence of Parkinson's Disease among People with Diabetes: A Retrospective Cohort Study. PLOS Med. 12, e1001854. https://doi.org/10.1371/journal.pmed.1001854

Camargo Maluf, F., Feder, D., Alves de Siqueira Carvalho, A., 2019. Analysis of the Relationship between Type II Diabetes Mellitus and Parkinson's Disease: A Systematic Review. Park. Dis. 2019, 1–14. https://doi.org/10.1155/2019/4951379

Carrion, M.D.P., Marsicano, S., Daniele, F., Marte, A., Pischedda, F., Di Cairano, E., Piovesana, E., von Zweydorf, F., Kremmer, E., Gloeckner, C.J., Onofri, F., Perego, C., Piccoli, G., 2017. The LRRK2 G2385R variant is a partial loss-of-function mutation that affects synaptic vesicle trafficking through altered protein interactions. Sci. Rep. 7, 5377. https://doi.org/10.1038/s41598-017-05760-9

Cazares, V.A., Subramani, A., Saldate, J.J., Hoerauf, W., Stuenkel, E.L., 2014. Distinct Actions of Rab3 and Rab27 GTPases on Late Stages of Exocytosis of Insulin. Traffic 15, 997–1015. https://doi.org/10.1111/tra.12182

Cesca, F., Baldelli, P., Valtorta, F., Benfenati, F., 2010. The synapsins: Key actors of synapse function and plasticity. Prog. Neurobiol. 91, 313–348. https://doi.org/10.1016/j.pneurobio.2010.04.006

Chang, K.L., Pee, H.N., Yang, S., Ho, P.C., 2015. Influence of drug transporters and stereoselectivity on the brain penetration of pioglitazone as a potential medicine against Alzheimer's disease. Sci. Rep. 5, 9000. https://doi.org/10.1038/srep09000

Chen, M.-L., Wu, R.-M., 2018. LRRK 2 gene mutations in the pathophysiology of the ROCO domain and therapeutic targets for Parkinson's disease: a review. J. Biomed. Sci. 25, 52. https://doi.org/10.1186/s12929-018-0454-0

Cheong, J.L.Y., de Pablo-Fernandez, E., Foltynie, T., Noyce, A.J., 2020. The Association Between Type 2 Diabetes Mellitus and Parkinson's Disease. J. Park. Dis. 10, 775–789. https://doi.org/10.3233/JPD-191900

Cherian, A., Divya, K.P., 2020. Genetics of Parkinson's disease. Acta Neurol. Belg. 120, 1297–1305. https://doi.org/10.1007/s13760-020-01473-5

Chia, R., Haddock, S., Beilina, A., Rudenko, I.N., Mamais, A., Kaganovich, A., Li, Y., Kumaran, R., Nalls, M.A., Cookson, M.R., 2014. Phosphorylation of LRRK2 by casein kinase 1α regulates trans-Golgi clustering via differential interaction with ARHGEF7. Nat. Commun. 5, 5827. https://doi.org/10.1038/ncomms6827

Choi, H.G., Zhang, J., Deng, X., Hatcher, J.M., Patricelli, M.P., Zhao, Z., Alessi, D.R., Gray, N.S., 2012. Brain Penetrant LRRK2 Inhibitor. ACS Med. Chem. Lett. 3, 658–662. https://doi.org/10.1021/ml300123a

Chung, S.J., Kim, M.-J., Kim, J., Ryu, H.-S., Kim, Y.J., Kim, S.Y., Lee, J.-H., 2015. Association of type 2 diabetes GWAS loci and the risk of Parkinson's and Alzheimer's diseases. Parkinsonism Relat. Disord. 21, 1435–1440. https://doi.org/10.1016/j.parkreldis.2015.10.010

Cilia, R., Siri, C., Rusconi, D., Allegra, R., Ghiglietti, A., Sacilotto, G., Zini, M., Zecchinelli, A.L., Asselta, R., Duga, S., Paganoni, A.M., Pezzoli, G., Seia, M., Goldwurm, S., 2014. LRRK2 mutations in Parkinson's disease: Confirmation of a gender effect in the Italian population. Parkinsonism Relat. Disord. 20, 911–914. https://doi.org/10.1016/j.parkreldis.2014.04.016

Cirnaru, M.D., Marte, A., Belluzzi, E., Russo, I., Gabrielli, M., Longo, F., Arcuri, L., Murru, L., Bubacco, L., Matteoli, M., Fedele, E., Sala, C., Passafaro, M., Morari, M., Greggio, E., Onofri, F., Piccoli, G., 2014. LRRK2 kinase activity regulates synaptic vesicle trafficking and neurotransmitter release through modulation of LRRK2 macro-molecular complex. Front. Mol. Neurosci. 7. https://doi.org/10.3389/fnmol.2014.00049

Civiero, L., Vancraenenbroeck, R., Belluzzi, E., Beilina, A., Lobbestael, E., Reyniers, L., Gao, F., Micetic, I., De Maeyer, M., Bubacco, L., Baekelandt, V., Cookson, M.R., Greggio, E., Taymans, J.-M., 2012. Biochemical Characterization of Highly Purified Leucine-Rich Repeat Kinases 1 and 2 Demonstrates Formation of Homodimers. PLoS ONE 7, e43472. https://doi.org/10.1371/journal.pone.0043472

Connolly, J.G., Bykov, K., Gagne, J.J., 2015. Thiazolidinediones and Parkinson Disease: A Cohort Study. Am. J. Epidemiol. 182, 936–944. https://doi.org/10.1093/aje/kwv109

Cornell, S., 2020. A review of GLP-1 receptor agonists in type 2 diabetes: A focus on the mechanism of action of once-weekly agents. J. Clin. Pharm. Ther. 45, 17–27. https://doi.org/10.1111/jcpt.13230

D'Amelio, M., Ragonese, P., Callari, G., Di Benedetto, N., Palmeri, B., Terruso, V., Salemi, G., Famoso, G., Aridon, P., Savettieri, G., 2009. Diabetes preceding Parkinson's disease onset. A case–control study. Parkinsonism Relat. Disord. 15, 660–664. https://doi.org/10.1016/j.parkreldis.2009.02.013

Daniele, F., Di Cairano, E.S., Moretti, S., Piccoli, G., Perego, C., 2015. TIRFM and pH-sensitive GFP-probes to Evaluate Neurotransmitter Vesicle Dynamics in SH-SY5Y Neuroblastoma Cells: Cell Imaging and Data Analysis. J. Vis. Exp. 52267. https://doi.org/10.3791/52267

Daniëls, V., Vancraenenbroeck, R., Law, B.M.H., Greggio, E., Lobbestael, E., Gao, F., De Maeyer, M., Cookson, M.R., Harvey, K., Baekelandt, V., Taymans, J.-M., 2011. Insight into the mode of action of the LRRK2 Y1699C pathogenic mutant: Mechanistic insight LRRK2 Y1699C. J. Neurochem. 116, 304–315. https://doi.org/10.1111/j.1471-4159.2010.07105.x

Das, R.R., Unger, M.M., 2018. Diabetes and Parkinson disease: A sweet spot? Neurology 90, 869–870. https://doi.org/10.1212/WNL.0000000000005470

Dauer, W., Przedborski, S., 2003. Parkinson's Disease. Neuron 39, 889–909. https://doi.org/10.1016/S0896-6273(03)00568-3

Davidson, M.A., Mattison, D.R., Azoulay, L., Krewski, D., 2018. Thiazolidinedione drugs in the treatment of type 2 diabetes mellitus: past, present and future. Crit. Rev. Toxicol. 48, 52–108. https://doi.org/10.1080/10408444.2017.1351420

De Pablo-Fernandez, E., Goldacre, R., Pakpoor, J., Noyce, A.J., Warner, T.T., 2018. Association between diabetes and subsequent Parkinson disease: A record-linkage cohort study. Neurology 91, e139–e142. https://doi.org/10.1212/WNL.0000000000005771

De Wit, T., Baekelandt, V., Lobbestael, E., 2019. Inhibition of LRRK2 or Casein Kinase 1 Results in LRRK2 Protein Destabilization. Mol. Neurobiol. 56, 5273–5286. https://doi.org/10.1007/s12035-018-1449-2

De Wit, T., Baekelandt, V., Lobbestael, E., 2018. LRRK2 Phosphorylation: Behind the Scenes. The Neuroscientist 24, 486–500. https://doi.org/10.1177/1073858418756309

Deas, E., Piipari, K., Machhada, A., Li, A., Gutierrez-del-Arroyo, A., Withers, D.J., Wood, N.W., Abramov, A.Y., 2014. PINK1 deficiency in β-cells increases basal insulin secretion and improves glucose tolerance in mice. Open Biol. 4, 140051. https://doi.org/10.1098/rsob.140051

DeMaagd, G., Philip, A., 2015. Parkinson's Disease and Its Management: Part 1: Disease Entity, Risk Factors, Pathophysiology, Clinical Presentation, and Diagnosis. P T Peer-Rev. J. Formul. Manag. 40, 504–532.

Deng, H., Le, W., Guo, Y., Hunter, C.B., Xie, W., Huang, M., Jankovic, J., 2006. Genetic analysis of LRRK2 mutations in patients with Parkinson disease. J. Neurol. Sci. 251, 102–106. https://doi.org/10.1016/j.jns.2006.09.017

Deng, H., Wang, P., Jankovic, J., 2018. The genetics of Parkinson disease. Ageing Res. Rev. 42, 72–85. https://doi.org/10.1016/j.arr.2017.12.007

Deng, J., Lewis, P.A., Greggio, E., Sluch, E., Beilina, A., Cookson, M.R., 2008. Structure of the ROC domain from the Parkinson's disease-associated leucine-rich repeat kinase 2 reveals a dimeric GTPase. Proc. Natl. Acad. Sci. 105, 1499–1504. https://doi.org/10.1073/pnas.0709098105

Deng, X., Dzamko, N., Prescott, A., Davies, P., Liu, Q., Yang, Q., Lee, J.-D., Patricelli, M.P., Nomanbhoy, T.K., Alessi, D.R., Gray, N.S., 2011. Characterization of a selective inhibitor of the Parkinson's disease kinase LRRK2. Nat. Chem. Biol. 7, 203–205. https://doi.org/10.1038/nchembio.538

Dexter, D.T., Jenner, P., 2013. Parkinson disease: from pathology to molecular disease mechanisms. Free Radic. Biol. Med. 62, 132–144. https://doi.org/10.1016/j.freeradbiomed.2013.01.018

Deyaert, E., Wauters, L., Guaitoli, G., Konijnenberg, A., Leemans, M., Terheyden, S., Petrovic, A., Gallardo, R., Nederveen-Schippers, L.M., Athanasopoulos, P.S., Pots, H., Van Haastert, P.J.M., Sobott, F., Gloeckner, C.J., Efremov, R., Kortholt, A., Versées, W., 2017. A homologue of the Parkinson's disease-associated protein LRRK2 undergoes a monomer-dimer transition during GTP turnover. Nat. Commun. 8, 1008. https://doi.org/10.1038/s41467-017-01103-4

Dobrunz, L.E., Stevens, C.F., 1997. Heterogeneity of Release Probability, Facilitation, and Depletion at Central Synapses. Neuron 18, 995–1008. https://doi.org/10.1016/S0896-6273(00)80338-4

Doggett, E.A., Zhao, J., Mork, C.N., Hu, D., Nichols, R.J., 2012. Phosphorylation of LRRK2 serines 955 and 973 is disrupted by Parkinson's disease mutations and LRRK2 pharmacological inhibition: LRRK2 Ser955 and Ser973 phosphorylation. J. Neurochem. 120, 37–45. https://doi.org/10.1111/j.1471-4159.2011.07537.x

Drucker, D.J., 2018. Mechanisms of Action and Therapeutic Application of Glucagon-like Peptide-1. Cell Metab. 27, 740–756. https://doi.org/10.1016/j.cmet.2018.03.001

Duarte, A.I., Moreira, P.I., Oliveira, C.R., 2012. Insulin in Central Nervous System: More than Just a Peripheral Hormone. J. Aging Res. 2012, 1–21. https://doi.org/10.1155/2012/384017

Dzamko, N., Gysbers, A.M., Bandopadhyay, R., Bolliger, M.F., Uchino, A., Zhao, Y., Takao, M., Wauters, S., Berg, W.D.J., Takahashi-Fujigasaki, J., Nichols, R.J., Holton, J.L., Murayama, S., Halliday, G.M., 2017. LRRK2 levels and phosphorylation in Parkinson's disease brain and cases with restricted Lewy bodies. Mov. Disord. 32, 423–432. https://doi.org/10.1002/mds.26892

Dzamko, N., Inesta-Vaquera, F., Zhang, J., Xie, C., Cai, H., Arthur, S., Tan, L., Choi, H., Gray, N., Cohen, P., Pedrioli, P., Clark, K., Alessi, D.R., 2012. The IkappaB Kinase Family Phosphorylates the Parkinson's Disease Kinase LRRK2 at Ser935 and Ser910 during Toll-Like Receptor Signaling. PLoS ONE 7, e39132. https://doi.org/10.1371/journal.pone.0039132

Eberhard, D., Lammert, E., 2017. The Role of the Antioxidant Protein DJ-1 in Type 2 Diabetes Mellitus, in: Ariga, H., Iguchi-Ariga, S.M.M. (Eds.), DJ-1/PARK7 Protein, Advances in Experimental Medicine and Biology. Springer Singapore, Singapore, pp. 173–186. https://doi.org/10.1007/978-981-10-6583-5_11

Efrat, S., Linde, S., Kofod, H., Spector, D., Delannoy, M., Grant, S., Hanahan, D., Baekkeskov, S., 1988. Beta-cell lines derived from transgenic mice expressing a hybrid insulin gene-oncogene. Proc. Natl. Acad. Sci. 85, 9037–9041. https://doi.org/10.1073/pnas.85.23.9037

Emamzadeh, F., 2016. Alpha-synuclein structure, functions, and interactions. J. Res. Med. Sci. 21, 29. https://doi.org/10.4103/1735-1995.181989

Erb, M.L., Moore, D.J., 2020. LRRK2 and the Endolysosomal System in Parkinson's Disease. J. Park. Dis. 10, 1271–1291. https://doi.org/10.3233/JPD-202138

Estrada, A.A., Liu, X., Baker-Glenn, C., Beresford, A., Burdick, D.J., Chambers, M., Chan, B.K., Chen, H., Ding, X., DiPasquale, A.G., Dominguez, S.L., Dotson, J., Drummond, J., Flagella, M., Flynn, S., Fuji, R., Gill, A., Gunzner-Toste, J., Harris, S.F., Heffron, T.P., Kleinheinz, T., Lee, D.W., Le Pichon, C.E., Lyssikatos, J.P., Medhurst, A.D., Moffat, J.G., Mukund, S., Nash, K., Scearce-Levie, K., Sheng, Z., Shore, D.G., Tran, T., Trivedi, N., Wang, S., Zhang, S., Zhang, X., Zhao, G., Zhu, H., Sweeney, Z.K., 2012. Discovery of Highly Potent, Selective, and Brain-Penetrable Leucine-Rich Repeat Kinase 2 (LRRK2) Small Molecule Inhibitors. J. Med. Chem. 55, 9416–9433. https://doi.org/10.1021/jm301020q

Estrada, A.A., Sweeney, Z.K., 2015. Chemical Biology of Leucine-Rich Repeat Kinase 2 (LRRK2) Inhibitors: Miniperspective. J. Med. Chem. 58, 6733–6746. https://doi.org/10.1021/acs.jmedchem.5b00261

Fdez, E., Hilfiker, S., 2007. Vesicle pools and synapsins: New insights into old enigmas. Brain Cell Biol. 35, 107–115. https://doi.org/10.1007/s11068-007-9013-4

Fell, M.J., Mirescu, C., Basu, K., Cheewatrakoolpong, B., DeMong, D.E., Ellis, J.M., Hyde, L.A., Lin, Y., Markgraf, C.G., Mei, H., Miller, M., Poulet, F.M., Scott, J.D., Smith, M.D., Yin, Z., Zhou, X., Parker, E.M., Kennedy, M.E., Morrow, J.A., 2015. MLi-2, a Potent, Selective, and Centrally Active Compound for Exploring the Therapeutic Potential and Safety of LRRK2 Kinase Inhibition. J. Pharmacol. Exp. Ther. 355, 397–409. https://doi.org/10.1124/jpet.115.227587

Ferguson, L.W., Rajput, A.H., Rajput, A., 2016. Early-onset vs. Late-onset Parkinson's disease: A Clinical-pathological Study. Can. J. Neurol. Sci. J. Can. Sci. Neurol. 43, 113–119. https://doi.org/10.1017/cjn.2015.244

Ferreira, J.J., Guedes, L.C., Rosa, M.M., Coelho, M., van Doeselaar, M., Schweiger, D., Di Fonzo, A., Oostra, B.A., Sampaio, C., Bonifati, V., 2007. High prevalence ofLRRK2 mutations in familial and sporadic Parkinson's disease in Portugal. Mov. Disord. 22, 1194–1201. https://doi.org/10.1002/mds.21525

Foretz, M., Guigas, B., Bertrand, L., Pollak, M., Viollet, B., 2014. Metformin: From Mechanisms of Action to Therapies. Cell Metab. 20, 953–966. https://doi.org/10.1016/j.cmet.2014.09.018

Fujimoto, T., Kuwahara, T., Eguchi, T., Sakurai, M., Komori, T., Iwatsubo, T., 2018. Parkinson's disease-associated mutant LRRK2 phosphorylates Rab7L1 and modifies trans-Golgi morphology. Biochem. Biophys. Res. Commun. 495, 1708–1715. https://doi.org/10.1016/j.bbrc.2017.12.024

Funayama, M., Hasegawa, K., Kowa, H., Saito, M., Tsuji, S., Obata, F., 2002. A new locus for Parkinson's disease (PARK8) maps to chromosome 12p11.2-q13.1. Ann. Neurol. 51, 296–301. https://doi.org/10.1002/ana.10113

Funayama, M., Li, Y., Tomiyama, H., Yoshino, H., Imamichi, Y., Yamamoto, M., Murata, M., Toda, T., Mizuno, Y., Hattori, N., 2007. Leucine-Rich Repeat kinase 2 G2385R variant is a risk factor for Parkinson disease in Asian population. NeuroReport 18, 273–275. https://doi.org/10.1097/WNR.0b013e32801254b6

Funk, N., Munz, M., Ott, T., Brockmann, K., Wenninger-Weinzierl, A., Kühn, R., Vogt-Weisenhorn, D., Giesert, F., Wurst, W., Gasser, T., Biskup, S., 2019. The Parkinson's disease-linked Leucine-rich repeat kinase 2 (LRRK2) is required for insulin-stimulated translocation of GLUT4. Sci. Rep. 9, 4515. https://doi.org/10.1038/s41598-019-40808-y

Gershanik, O., 2007. Trauma and Parkinson's disease, in: Handbook of Clinical Neurology. Elsevier, pp. 487–499. https://doi.org/10.1016/S0072-9752(07)84057-7

Giasson, B.I., Covy, J.P., Bonini, N.M., Hurtig, H.I., Farrer, M.J., Trojanowski, J.Q., Van Deerlin, V.M., 2006. Biochemical and pathological characterization of Lrrk2. Ann. Neurol. 59, 315–322. https://doi.org/10.1002/ana.20791

Gilsbach, B.K., Eckert, M., Gloeckner, C.J., 2018. Regulation of LRRK2: insights from structural and biochemical analysis. Biol. Chem. 399, 637–642. https://doi.org/10.1515/hsz-2018-0132

Gloeckner, C.J., Boldt, K., Schumacher, A., Roepman, R., Ueffing, M., 2007. A novel tandem affinity purification strategy for the efficient isolation and characterisation of native protein complexes. PROTEOMICS 7, 4228–4234. https://doi.org/10.1002/pmic.200700038

Gorostidi, A., Ruiz-Martínez, J., Lopez de Munain, A., Alzualde, A., Martí Massó, J.F., 2009. LRRK2 G2019S and R1441G mutations associated with Parkinson's disease are common in the Basque Country, but relative prevalence is determined by ethnicity. neurogenetics 10, 157–159. https://doi.org/10.1007/s10048-008-0162-0

Gotthardt, K., Weyand, M., Kortholt, A., Van Haastert, P.J.M., Wittinghofer, A., 2008. Structure of the Roc–COR domain tandem of C. tepidum, a prokaryotic homologue of the human LRRK2 Parkinson kinase. EMBO J. 27, 2239–2249. https://doi.org/10.1038/emboj.2008.150

Granseth, B., Odermatt, B., Royle, S.J., Lagnado, L., 2006. Clathrin-Mediated Endocytosis Is the Dominant Mechanism of Vesicle Retrieval at Hippocampal Synapses. Neuron 51, 773–786. https://doi.org/10.1016/j.neuron.2006.08.029

Greggio, E., Zambrano, I., Kaganovich, A., Beilina, A., Taymans, J.-M., Daniëls, V., Lewis, P., Jain, S., Ding, J., Syed, A., Thomas, K.J., Baekelandt, V., Cookson, M.R., 2008. The Parkinson Disease-associated Leucine-rich

Repeat Kinase 2 (LRRK2) Is a Dimer That Undergoes Intramolecular Autophosphorylation. J. Biol. Chem. 283, 16906–16914. https://doi.org/10.1074/jbc.M708718200

Grote, C.W., Wright, D.E., 2016. A Role for Insulin in Diabetic Neuropathy. Front. Neurosci. 10. https://doi.org/10.3389/fnins.2016.00581

Guaitoli, G., Raimondi, F., Gilsbach, B.K., Gómez-Llorente, Y., Deyaert, E., Renzi, F., Li, X., Schaffner, A., Jagtap, P.K.A., Boldt, K., von Zweydorf, F., Gotthardt, K., Lorimer, D.D., Yue, Z., Burgin, A., Janjic, N., Sattler, M., Versées, W., Ueffing, M., Ubarretxena-Belandia, I., Kortholt, A., Gloeckner, C.J., 2016. Structural model of the dimeric Parkinson's protein LRRK2 reveals a compact architecture involving distant interdomain contacts. Proc. Natl. Acad. Sci. 113, E4357–E4366. https://doi.org/10.1073/pnas.1523708113

Guo, L., Wang, W., Chen, S.G., 2006. Leucine-rich repeat kinase 2: Relevance to Parkinson's disease. Int. J. Biochem. Cell Biol. 38, 1469–1475. https://doi.org/10.1016/j.biocel.2006.02.009

Harvey, K., Outeiro, T.F., 2019. The role of LRRK2 in cell signalling. Biochem. Soc. Trans. 47, 197–207. https://doi.org/10.1042/BST20180464

Hattula, K., Furuhjelm, J., Tikkanen, J., Tanhuanpää, K., Laakkonen, P., Peränen, J., 2006. Characterization of the Rab8-specific membrane traffic route linked to protrusion formation. J. Cell Sci. 119, 4866–4877. https://doi.org/10.1242/jcs.03275

Hayes, M.T., 2019. Parkinson's Disease and Parkinsonism. Am. J. Med. 132, 802–807. https://doi.org/10.1016/j.amjmed.2019.03.001

Healy, D.G., Falchi, M., O'Sullivan, S.S., Bonifati, V., Durr, A., Bressman, S., Brice, A., Aasly, J., Zabetian, C.P., Goldwurm, S., Ferreira, J.J., Tolosa, E., Kay, D.M., Klein, C., Williams, D.R., Marras, C., Lang, A.E., Wszolek, Z.K., Berciano, J., Schapira, A.H.V., Lynch, T., Bhatia, K.P., Gasser, T., Lees, A.J., Wood, N.W., International LRRK2 Consortium, 2008. Phenotype, genotype, and worldwide genetic penetrance of LRRK2-associated Parkinson's disease: a case-control study. Lancet Neurol. 7, 583–590. https://doi.org/10.1016/S1474-4422(08)70117-0

Herzig, M.C., Kolly, C., Persohn, E., Theil, D., Schweizer, T., Hafner, T., Stemmelen, C., Troxler, T.J., Schmid, P., Danner, S., Schnell, C.R., Mueller, M., Kinzel, B., Grevot, A., Bolognani, F., Stirn, M., Kuhn, R.R., Kaupmann, K., van der Putten, P.H., Rovelli, G., Shimshek, D.R., 2011. LRRK2 protein levels are determined by kinase function and are crucial for kidney and lung homeostasis in mice. Hum. Mol. Genet. 20, 4209–4223. https://doi.org/10.1093/hmg/ddr348

Hess, C., Hallett, M., 2017. The Phenomenology of Parkinson's Disease. Semin. Neurol. 37, 109–117. https://doi.org/10.1055/s-0037-1601869

Hevener, A.L., Olefsky, J.M., Reichart, D., Nguyen, M.T.A., Bandyopadyhay, G., Leung, H.-Y., Watt, M.J., Benner, C., Febbraio, M.A., Nguyen, A.-K., Folian, B., Subramaniam, S., Gonzalez, F.J., Glass, C.K., Ricote, M., 2007. Macrophage PPARγ is required for normal skeletal muscle and hepatic insulin sensitivity and full antidiabetic effects of thiazolidinediones. J. Clin. Invest. 117, 1658–1669. https://doi.org/10.1172/JCI31561

Higashi, S., Biskup, S., West, A.B., Trinkaus, D., Dawson, V.L., Faull, R.L.M., Waldvogel, H.J., Arai, H., Dawson, T.M., Moore, D.J., Emson, P.C., 2007. Localization of Parkinson's disease-associated LRRK2 in normal and pathological human brain. Brain Res. 1155, 208–219. https://doi.org/10.1016/j.brainres.2007.04.034

Hölscher, C., 2018. Novel dual GLP-1/GIP receptor agonists show neuroprotective effects in Alzheimer's and Parkinson's disease models. Neuropharmacology 136, 251–259. https://doi.org/10.1016/j.neuropharm.2018.01.040

Horvath, I., Wittung-Stafshede, P., 2016. Cross-talk between amyloidogenic proteins in type-2 diabetes and Parkinson's disease. Proc. Natl. Acad. Sci. 113, 12473–12477. https://doi.org/10.1073/pnas.1610371113

Hostalek, U., Gwilt, M., Hildemann, S., 2015. Therapeutic Use of Metformin in Prediabetes and Diabetes Prevention. Drugs 75, 1071–1094. https://doi.org/10.1007/s40265-015-0416-8

Hou, J.C., Min, L., Pessin, J.E., 2009. Chapter 16 Insulin Granule Biogenesis, Trafficking and Exocytosis, in: Vitamins & Hormones. Elsevier, pp. 473–506. https://doi.org/10.1016/S0083-6729(08)00616-X

Howlett, E.H., Jensen, N., Belmonte, F., Zafar, F., Hu, X., Kluss, J., Schüle, B., Kaufman, B.A., Greenamyre, J.T., Sanders, L.H., 2017. LRRK2 G2019S-induced mitochondrial DNA damage is LRRK2 kinase dependent and inhibition restores mtDNA integrity in Parkinson's disease. Hum. Mol. Genet. 26, 4340–4351. https://doi.org/10.1093/hmg/ddx320

Hughes, T.M., Craft, S., 2016. The role of insulin in the vascular contributions to age-related dementia. Biochim. Biophys. Acta BBA - Mol. Basis Dis. 1862, 983–991. https://doi.org/10.1016/j.bbadis.2015.11.013

Hulihan, M.M., Ishihara-Paul, L., Kachergus, J., Warren, L., Amouri, R., Elango, R., Prinjha, R.K., Upmanyu, R., Kefi, M., Zouari, M., Sassi, S.B., Yahmed, S.B., El Euch-Fayeche, G., Matthews, P.M., Middleton, L.T., Gibson, R.A., Hentati, F., Farrer, M.J., 2008. LRRK2 Gly2019Ser penetrance in Arab–Berber patients from Tunisia: a case-control genetic study. Lancet Neurol. 7, 591–594. https://doi.org/10.1016/S1474-4422(08)70116-9

Hunter, K., Hölscher, C., 2012. Drugs developed to treat diabetes, liraglutide and lixisenatide, cross the blood brain barrier and enhance neurogenesis. BMC Neurosci. 13, 33. https://doi.org/10.1186/1471-2202-13-33

Hur, E.-M., Jang, E.-H., Jeong, G.R., Lee, B.D., 2019. LRRK2 and membrane trafficking: nexus of Parkinson's disease. BMB Rep. 52, 533–539. https://doi.org/10.5483/BMBRep.2019.52.9.186

Hur, E.-M., Lee, B.D., 2021. LRRK2 at the Crossroad of Aging and Parkinson's Disease. Genes 12, 505. https://doi.org/10.3390/genes12040505

Hutagalung, A.H., Novick, P.J., 2011. Role of Rab GTPases in Membrane Traffic and Cell Physiology. Physiol. Rev. 91, 119–149. https://doi.org/10.1152/physrev.00059.2009

Huttner, W.B., Schiebler, W., Greengard, P., De Camilli, P., 1983. Synapsin I (protein I), a nerve terminal-specific phosphoprotein. III. Its association with synaptic vesicles studied in a highly purified synaptic vesicle preparation. J. Cell Biol. 96, 1374–1388. https://doi.org/10.1083/jcb.96.5.1374

Iezzi, M., Regazzi, R., Wollheim, C.B., 2000. The Rab3-interacting molecule RIM is expressed in pancreatic β-cells and is implicated in insulin exocytosis. FEBS Lett. 474, 66–70. https://doi.org/10.1016/S0014-5793(00)01572-6

Imai, M., Kawakami, F., Kubo, M., Kanzaki, M., Maruyama, H., Kawashima, R., Maekawa, T., Kurosaki, Y., Kojima, F., Ichikawa, T., 2020. LRRK2 Inhibition Ameliorates Dexamethasone-Induced Glucose Intolerance *via* Prevents Impairment in GLUT4 Membrane Translocation in Adipocytes. Biol. Pharm. Bull. 43, 1660–1668. https://doi.org/10.1248/bpb.b20-00377

Inberg, A., Linial, M., 2010. Protection of Pancreatic β-Cells from Various Stress Conditions Is Mediated by DJ-1. J. Biol. Chem. 285, 25686–25698. https://doi.org/10.1074/jbc.M110.109751

Ishihara, L., Brayne, C., 2006. A systematic review of depression and mental illness preceding Parkinson's disease. Acta Neurol. Scand. 113, 211–220. https://doi.org/10.1111/j.1600-0404.2006.00579.x

Iwai, T., Ito, S., Tanimitsu, K., Udagawa, S., Oka, J.-I., 2006. Glucagon-like peptide-1 inhibits LPS-induced IL-1β production in cultured rat astrocytes. Neurosci. Res. 55, 352–360. https://doi.org/10.1016/j.neures.2006.04.008

Jagadeesan, A.J., Murugesan, R., Vimala Devi, S., Meera, M., Madhumala, G., Vishwanathan Padmaja, M., Ramesh, A., Banerjee, A., Sushmitha, S., Khokhlov, A.N., Marotta, F., Pathak, S., 2017. Current trends in etiology, prognosis and therapeutic aspects of Parkinson's disease: a review. Acta Bio-Medica Atenei Parm. 88, 249–262. https://doi.org/10.23750/abm.v88i3.6063

Jain, D., Jain, R., Eberhard, D., Eglinger, J., Bugliani, M., Piemonti, L., Marchetti, P., Lammert, E., 2012. Age- and diet-dependent requirement of DJ-1 for glucose homeostasis in mice with implications for human type 2 diabetes. J. Mol. Cell Biol. 4, 221–230. https://doi.org/10.1093/jmcb/mjs025

Jankovic, J., 2008. Parkinson's disease: clinical features and diagnosis. J. Neurol. Neurosurg. Psychiatry 79, 368–376. https://doi.org/10.1136/jnnp.2007.131045

Javeed, N., Matveyenko, A.V., 2018. Circadian Etiology of Type 2 Diabetes Mellitus. Physiology 33, 138–150. https://doi.org/10.1152/physiol.00003.2018

Jeong, G.R., Jang, E.-H., Bae, J.R., Jun, S., Kang, H.C., Park, C.-H., Shin, J.-H., Yamamoto, Y., Tanaka-Yamamoto, K., Dawson, V.L., Dawson, T.M., Hur, E.-M., Lee, B.D., 2018. Dysregulated phosphorylation of Rab GTPases by LRRK2 induces neurodegeneration. Mol. Neurodegener. 13, 8. https://doi.org/10.1186/s13024-018-0240-1

John Van Geest Centre for Brain Repair, Department of Clinical Neurosciences, University of Cambridge, UK, Stoker, T.B., Greenland, J.C., John Van Geest Centre for Brain Repair, Department of Clinical Neurosciences, University of Cambridge, UK (Eds.), 2018. Parkinson's Disease: Pathogenesis and Clinical Aspects. Codon Publications. https://doi.org/10.15586/codonpublications.parkinsonsdisease.2018

Jorgensen, N.D., Peng, Y., Ho, C.C.-Y., Rideout, H.J., Petrey, D., Liu, P., Dauer, W.T., 2009. The WD40 Domain Is Required for LRRK2 Neurotoxicity. PLoS ONE 4, e8463. https://doi.org/10.1371/journal.pone.0008463

Kalia, L.V., Brotchie, J.M., Fox, S.H., 2013. Novel nondopaminergic targets for motor features of Parkinson's disease: Review of recent trials: Nondopaminergic Targets for Motor Features of PD. Mov. Disord. 28, 131–144. https://doi.org/10.1002/mds.25273

Kim, C., Alcalay, R., 2017. Genetic Forms of Parkinson's Disease. Semin. Neurol. 37, 135–146. https://doi.org/10.1055/s-0037-1601567

Kim, D.S., Choi, H.-I., Wang, Y., Luo, Y., Hoffer, B.J., Greig, N.H., 2017. A New Treatment Strategy for Parkinson's Disease through the Gut–Brain Axis: The Glucagon-Like Peptide-1 Receptor Pathway. Cell Transplant. 26, 1560–1571. https://doi.org/10.1177/0963689717721234

Kim, M.J., Deng, H.-X., Wong, Y.C., Siddique, T., Krainc, D., 2017. The Parkinson's disease-linked protein TMEM230 is required for Rab8a-mediated secretory vesicle trafficking and retromer trafficking. Hum. Mol. Genet. ddw413. https://doi.org/10.1093/hmg/ddw413

Klein, C.L., Rovelli, G., Springer, W., Schall, C., Gasser, T., Kahle, P.J., 2009. Homo- and heterodimerization of ROCO kinases: LRRK2 kinase inhibition by the LRRK2 ROCO fragment. J. Neurochem. 111, 703–715. https://doi.org/10.1111/j.1471-4159.2009.06358.x

Kleinridders, A., Ferris, H.A., Cai, W., Kahn, C.R., 2014. Insulin Action in Brain Regulates Systemic Metabolism and Brain Function. Diabetes 63, 2232–2243. https://doi.org/10.2337/db14-0568

Kluss, J.H., Conti, M.M., Kaganovich, A., Beilina, A., Melrose, H.L., Cookson, M.R., Mamais, A., 2018. Detection of endogenous S1292 LRRK2 autophosphorylation in mouse tissue as a readout for kinase activity. Npj Park. Dis. 4, 13. https://doi.org/10.1038/s41531-018-0049-1

Kouli, A., Torsney, K.M., Kuan, W.-L., 2018. Parkinson's Disease: Etiology, Neuropathology, and Pathogenesis, in: Stoker, T.B., Greenland, J.C. (Eds.), Parkinson's Disease: Pathogenesis and Clinical Aspects. Codon Publications, Brisbane (AU).

Lai, B.C.L., Marion, S.A., Teschke, K., Tsui, J.K.C., 2002. Occupational and environmental risk factors for Parkinson's disease. Parkinsonism Relat. Disord. 8, 297–309. https://doi.org/10.1016/S1353-8020(01)00054-2

Langston, J.W., Ballard, P., Tetrud, J.W., Irwin, I., 1983. Chronic Parkinsonism in Humans Due to a Product of Meperidine-Analog Synthesis. Science 219, 979–980. https://doi.org/10.1126/science.6823561

Latourelle, J.C., Sun, M., Lew, M.F., Suchowersky, O., Klein, C., Golbe, L.I., Mark, M.H., Growdon, J.H., Wooten, G.F., Watts, R.L., Guttman, M., Racette, B.A., Perlmutter, J.S., Ahmed, A., Shill, H.A., Singer, C., Goldwurm, S., Pezzoli, G., Zini, M., Saint-Hilaire, M.H., Hendricks, A.E., Williamson, S., Nagle, M.W., Wilk, J.B., Massood, T., Huskey, K.W., Laramie, J.M., DeStefano, A.L., Baker, K.B., Itin, I., Litvan, I., Nicholson, G., Corbett, A., Nance, M., Drasby, E., Isaacson, S., Burn, D.J., Chinnery, P.F., Pramstaller, P.P., Al-hinti, J., Moller, A.T., Ostergaard, K., Sherman, S.J., Roxburgh, R., Snow, B., Slevin, J.T., Cambi, F., Gusella, J.F., Myers, R.H., 2008. The Gly2019Ser mutation in LRRK2is not fully penetrant in familial Parkinson's disease: the GenePD study. BMC Med. 6, 32. https://doi.org/10.1186/1741-7015-6-32

Leandrou, E., Markidi, E., Memou, A., Melachroinou, K., Greggio, E., Rideout, H.J., 2019. Kinase activity of mutant LRRK2 manifests differently in hetero-dimeric vs. homo-dimeric complexes. Biochem. J. 476, 559–579. https://doi.org/10.1042/BCJ20180589

Lee, B.D., Dawson, V.L., Dawson, T.M., 2012. Leucine-rich repeat kinase 2 (LRRK2) as a potential therapeutic target in Parkinson's disease. Trends Pharmacol. Sci. 33, 365–373. https://doi.org/10.1016/j.tips.2012.04.001

Leenders, A., Sheng, Z., 2005. Modulation of neurotransmitter release by the second messenger-activated protein kinases: Implications for presynaptic plasticity. Pharmacol. Ther. 105, 69–84. https://doi.org/10.1016/j.pharmthera.2004.10.012

Lees, A.J., Hardy, J., Revesz, T., 2009. Parkinson's disease. The Lancet 373, 2055–2066. https://doi.org/10.1016/S0140-6736(09)60492-X

Lesage, S., Ibanez, P., Lohmann, E., Pollak, P., Tison, F., Tazir, M., Leutenegger, A.-L., Guimaraes, J., Bonnet, A.-M., Agid, Y., Dürr, A., Brice, A., French Parkinson's Disease Genetics Study Group, 2005. G2019S LRRK2 mutation in French and North African families with Parkinson's disease. Ann. Neurol. 58, 784–787. https://doi.org/10.1002/ana.20636

Li, X., Tan, Y.-C., Poulose, S., Olanow, C.W., Huang, X.-Y., Yue, Z., 2007. Leucine-rich repeat kinase 2 (LRRK2)/PARK8 possesses GTPase activity that is altered in familial Parkinson?s disease R1441C/G mutants. J. Neurochem. 0, 070710052154004-??? https://doi.org/10.1111/j.1471-4159.2007.04743.x

Li, Z., Fallon, J., Mandeli, J., Wetmur, J., Woo, S.L.C., 2010. Retraction: A Genetically Enhanced Anaerobic Bacterium for Oncopathic Therapy of Pancreatic Cancer. JNCI J. Natl. Cancer Inst. 102, 283–283. https://doi.org/10.1093/jnci/djq027

Liao, J., Wu, C.-X., Burlak, C., Zhang, S., Sahm, H., Wang, M., Zhang, Z.-Y., Vogel, K.W., Federici, M., Riddle, S.M., Nichols, R.J., Liu, D., Cookson, M.R., Stone, T.A., Hoang, Q.Q., 2014. Parkinson disease-associated

mutation R1441H in LRRK2 prolongs the “active state” of its GTPase domain. Proc. Natl. Acad. Sci. 111, 4055–4060. https://doi.org/10.1073/pnas.1323285111

Lima, M., Targa, A., Noseda, A., Rodrigues, L., Delattre, A., Santos, F., Fortes, M., Maturana, M., Ferraz, A., 2014. Does Parkinson’s Disease and Type-2 Diabetes Mellitus Present Common Pathophysiological Mechanisms and Treatments? CNS Neurol. Disord. - Drug Targets 13, 418–428. https://doi.org/10.2174/18715273113126660155

Litteljohn, D., Rudyk, C., Dwyer, Z., Farmer, K., Fortin, T., Hayley, S., 2018. The impact of murine LRRK2 G2019S transgene overexpression on acute responses to inflammatory challenge. Brain. Behav. Immun. 67, 246–256. https://doi.org/10.1016/j.bbi.2017.09.002

Liu, W., Jalewa, J., Sharma, M., Li, G., Li, L., Hölscher, C., 2015. Neuroprotective effects of lixisenatide and liraglutide in the 1-methyl-4-phenyl-1,2,3,6-tetrahydropyridine mouse model of Parkinson’s disease. Neuroscience 303, 42–50. https://doi.org/10.1016/j.neuroscience.2015.06.054

Liu, Z., Bryant, N., Kumaran, R., Beilina, A., Abeliovich, A., Cookson, M.R., West, A.B., 2018. LRRK2 phosphorylates membrane-bound Rabs and is activated by GTP-bound Rab7L1 to promote recruitment to the trans-Golgi network. Hum. Mol. Genet. 27, 385–395. https://doi.org/10.1093/hmg/ddx410

Lobbestael, E., Zhao, J., Rudenko, I.N., Beylina, A., Gao, F., Wetter, J., Beullens, M., Bollen, M., Cookson, M.R., Baekelandt, V., Nichols, R.J., Taymans, J.-M., 2013. Identification of protein phosphatase 1 as a regulator of the LRRK2 phosphorylation cycle. Biochem. J. 456, 119–128. https://doi.org/10.1042/BJ20121772

Louter, M., van der Marck, M.A., Pevernagie, D.A.A., Munneke, M., Bloem, B.R., Overeem, S., 2013. Sleep matters in Parkinson’s disease: use of a priority list to assess the presence of sleep disturbances. Eur. J. Neurol. 20, 259–265. https://doi.org/10.1111/j.1468-1331.2012.03836.x

Lu, C.-S., Simons, E.J., Wu-Chou, Y.-H., Fonzo, A.D., Chang, H.-C., Chen, R.-S., Weng, Y.-H., Rohé, C.F., Breedveld, G.J., Hattori, N., Gasser, T., Oostra, B.A., Bonifati, V., 2005. The LRRK2 I2012T, G2019S, and I2020T mutations are rare in Taiwanese patients with sporadic Parkinson’s disease. Parkinsonism Relat. Disord. 11, 521–522. https://doi.org/10.1016/j.parkreldis.2005.09.003

Lu, L., Fu, D., Li, H., Liu, A., Li, J., Zheng, G., 2014. Diabetes and Risk of Parkinson’s Disease: An Updated Meta-Analysis of Case-Control Studies. PLoS ONE 9, e85781. https://doi.org/10.1371/journal.pone.0085781

Lu, M., Su, C., Qiao, C., Bian, Y., Ding, J., Hu, G., 2016. Metformin Prevents Dopaminergic Neuron Death in MPTP/P-Induced Mouse Model of Parkinson’s Disease via Autophagy and Mitochondrial ROS Clearance. Int. J. Neuropsychopharmacol. 19, pyw047. https://doi.org/10.1093/ijnp/pyw047

Lu, M., Xing, H., Cheng, L., Liu, H., Lang, L., Yang, T., Zhao, X., Xu, H., Ding, P., 2020. A dual-functional buformin-mimicking poly(amido amine) for efficient and safe gene delivery. J. Drug Target. 28, 923–932. https://doi.org/10.1080/1061186X.2020.1729770

MacLeod, D.A., Rhinn, H., Kuwahara, T., Zolin, A., Di Paolo, G., McCabe, B.D., Marder, K.S., Honig, L.S., Clark, L.N., Small, S.A., Abeliovich, A., 2013. RAB7L1 Interacts with LRRK2 to Modify Intraneuronal Protein Sorting and Parkinson’s Disease Risk. Neuron 77, 425–439. https://doi.org/10.1016/j.neuron.2012.11.033

Madero-Pérez, J., Fdez, E., Fernández, B., Lara Ordóñez, A.J., Blanca Ramírez, M., Gómez-Suaga, P., Waschbüsch, D., Lobbestael, E., Baekelandt, V., Nairn, A.C., Ruiz-Martínez, J., Aiastui, A., López de Munain, A., Lis, P., Comptdaer, T., Taymans, J.-M., Chartier-Harlin, M.-C., Beilina, A., Gonnelli, A., Cookson, M.R., Greggio, E., Hilfiker, S., 2018. Parkinson disease-associated mutations in LRRK2 cause centrosomal defects via Rab8a phosphorylation. Mol. Neurodegener. 13, 3. https://doi.org/10.1186/s13024-018-0235-y

Mahlknecht, P., Seppi, K., Poewe, W., 2015. The Concept of Prodromal Parkinson's Disease. J. Park. Dis. 5, 681–697. https://doi.org/10.3233/JPD-150685

Mamais, A., Cookson, M.R., 2014. LRRK2: dropping (kinase) inhibitions and seeking an (immune) response. J. Neurochem. 129, 895–897. https://doi.org/10.1111/jnc.12691

Marchand, A., Drouyer, M., Sarchione, A., Chartier-Harlin, M.-C., Taymans, J.-M., 2020. LRRK2 Phosphorylation, More Than an Epiphenomenon. Front. Neurosci. 14, 527. https://doi.org/10.3389/fnins.2020.00527

Marder, K., Wang, Y., Alcalay, R.N., Mejia-Santana, H., Tang, M.-X., Lee, A., Raymond, D., Mirelman, A., Saunders-Pullman, R., Clark, L., Ozelius, L., Orr-Urtreger, A., Giladi, N., Bressman, S., For the LRRK2 Ashkenazi Jewish Consortium, 2015. Age-specific penetrance of *LRRK2* G2019S in the Michael J. Fox Ashkenazi Jewish LRRK2 Consortium. Neurology 85, 89–95. https://doi.org/10.1212/WNL.0000000000001708

Marín, I., 2006. The Parkinson Disease Gene LRRK2: Evolutionary and Structural Insights. Mol. Biol. Evol. 23, 2423–2433. https://doi.org/10.1093/molbev/msl114

Marques, A., Dutheil, F., Durand, E., Rieu, I., Mulliez, A., Fantini, M.L., Boirie, Y., Durif, F., 2018. Glucose dysregulation in Parkinson's disease: Too much glucose or not enough insulin? Parkinsonism Relat. Disord. 55, 122–127. https://doi.org/10.1016/j.parkreldis.2018.05.026

Marte, A., Russo, I., Rebosio, C., Valente, P., Belluzzi, E., Pischedda, F., Montani, C., Lavarello, C., Petretto, A., Fedele, E., Baldelli, P., Benfenati, F., Piccoli, G., Greggio, E., Onofri, F., 2019. Leucine-rich repeat kinase 2 phosphorylation on synapsin I regulates glutamate release at pre-synaptic sites. J. Neurochem. 150, 264–281. https://doi.org/10.1111/jnc.14778

Martinez, A.A., Morgese, M.G., Pisanu, A., Macheda, T., Paquette, M.A., Seillier, A., Cassano, T., Carta, A.R., Giuffrida, A., 2015. Activation of PPAR gamma receptors reduces levodopa-induced dyskinesias in 6-OHDA-lesioned rats. Neurobiol. Dis. 74, 295–304. https://doi.org/10.1016/j.nbd.2014.11.024

Martinez-Valbuena, I., Amat-Villegas, I., Valenti-Azcarate, R., Carmona-Abellan, M. del M., Marcilla, I., Tuñon, M.-T., Luquin, M.-R., 2018. Interaction of amyloidogenic proteins in pancreatic β cells from subjects with synucleinopathies. Acta Neuropathol. (Berl.) 135, 877–886. https://doi.org/10.1007/s00401-018-1832-0

Mata, I.F., Wedemeyer, W.J., Farrer, M.J., Taylor, J.P., Gallo, K.A., 2006. LRRK2 in Parkinson's disease: protein domains and functional insights. Trends Neurosci. 29, 286–293. https://doi.org/10.1016/j.tins.2006.03.006

Matta, S., Van Kolen, K., da Cunha, R., van den Bogaart, G., Mandemakers, W., Miskiewicz, K., De Bock, P.-J., Morais, V.A., Vilain, S., Haddad, D., Delbroek, L., Swerts, J., Chávez-Gutiérrez, L., Esposito, G., Daneels, G., Karran, E., Holt, M., Gevaert, K., Moechars, D.W., De Strooper, B., Verstreken, P., 2012. LRRK2 Controls an EndoA Phosphorylation Cycle in Synaptic Endocytosis. Neuron 75, 1008–1021. https://doi.org/10.1016/j.neuron.2012.08.022

McGrath, E., Waschbüsch, D., Baker, B.M., Khan, A.R., 2021. LRRK2 binds to the Rab32 subfamily in a GTP-dependent manner *via* its armadillo domain. Small GTPases 12, 133–146. https://doi.org/10.1080/21541248.2019.1666623

McKnight, S., Hack, N., 2020. Toxin-Induced Parkinsonism. Neurol. Clin. 38, 853–865. https://doi.org/10.1016/j.ncl.2020.08.003

Messa, M., Congia, S., Defranchi, E., Valtorta, F., Fassio, A., Onofri, F., Benfenati, F., 2010. Tyrosine phosphorylation of synapsin I by Src regulates synaptic-vesicle trafficking. J. Cell Sci. 123, 2256–2265. https://doi.org/10.1242/jcs.068445

Mezza, T., Cinti, F., Cefalo, C.M.A., Pontecorvi, A., Kulkarni, R.N., Giaccari, A., 2019. β-Cell Fate in Human Insulin Resistance and Type 2 Diabetes: A Perspective on Islet Plasticity. Diabetes 68, 1121–1129. https://doi.org/10.2337/db18-0856

Migheli, R., Del Giudice, M.G., Spissu, Y., Sanna, G., Xiong, Y., Dawson, T.M., Dawson, V.L., Galioto, M., Rocchitta, G., Biosa, A., Serra, P.A., Carri, M.T., Crosio, C., Iaccarino, C., 2013. LRRK2 Affects Vesicle Trafficking, Neurotransmitter Extracellular Level and Membrane Receptor Localization. PLoS ONE 8, e77198. https://doi.org/10.1371/journal.pone.0077198

Miller-Patterson, C., Buesa, R., McLaughlin, N., Jones, R., Akbar, U., Friedman, J.H., 2018. Motor asymmetry over time in Parkinson's disease. J. Neurol. Sci. 393, 14–17. https://doi.org/10.1016/j.jns.2018.08.001

Mills, R.D., Mulhern, T.D., Liu, F., Culvenor, J.G., Cheng, H.-C., 2014. Prediction of the Repeat Domain Structures and Impact of Parkinsonism-Associated Variations on Structure and Function of all Functional Domains of Leucine-Rich Repeat Kinase 2 (LRRK2). Hum. Mutat. 35, 395–412. https://doi.org/10.1002/humu.22515

Monfrini, E., Di Fonzo, A., 2017. Leucine-Rich Repeat Kinase (LRRK2) Genetics and Parkinson's Disease, in: Rideout, H.J. (Ed.), Leucine-Rich Repeat Kinase 2 (LRRK2), Advances in Neurobiology. Springer International Publishing, Cham, pp. 3–30. https://doi.org/10.1007/978-3-319-49969-7_1

Morales, D.R., Morris, A.D., 2015. Metformin in Cancer Treatment and Prevention. Annu. Rev. Med. 66, 17–29. https://doi.org/10.1146/annurev-med-062613-093128

Morris, J.K., Vidoni, E.D., Perea, R.D., Rada, R., Johnson, D.K., Lyons, K., Pahwa, R., Burns, J.M., Honea, R.A., 2014. Insulin resistance and gray matter volume in neurodegenerative disease. Neuroscience 270, 139–147. https://doi.org/10.1016/j.neuroscience.2014.04.006

Mosavi, L.K., Cammett, T.J., Desrosiers, D.C., Peng, Z., 2004. The ankyrin repeat as molecular architecture for protein recognition. Protein Sci. 13, 1435–1448. https://doi.org/10.1110/ps.03554604

Mucibabic, M., Steneberg, P., Lidh, E., Straseviciene, J., Ziolkowska, A., Dahl, U., Lindahl, E., Edlund, H., 2020. α-Synuclein promotes IAPP fibril formation in vitro and β-cell amyloid formation in vivo in mice. Sci. Rep. 10, 20438. https://doi.org/10.1038/s41598-020-77409-z

Muda, K., Bertinetti, D., Gesellchen, F., Hermann, J.S., von Zweydorf, F., Geerlof, A., Jacob, A., Ueffing, M., Gloeckner, C.J., Herberg, F.W., 2014. Parkinson-related LRRK2 mutation R1441C/G/H impairs PKA phosphorylation of LRRK2 and disrupts its interaction with 14-3-3. Proc. Natl. Acad. Sci. 111, E34–E43. https://doi.org/10.1073/pnas.1312701111

Mulvaney, C.A., Duarte, G.S., Handley, J., Evans, D.J., Menon, S., Wyse, R., Emsley, H.C., 2020. GLP-1 receptor agonists for Parkinson's disease. Cochrane Database Syst. Rev. 2020. https://doi.org/10.1002/14651858.CD012990.pub2

Murthy, V.N., Stevens, C.F., 1998. Synaptic vesicles retain their identity through the endocytic cycle. Nature 392, 497–501. https://doi.org/10.1038/33152

Nalls, M.A., Blauwendraat, C., Vallerga, C.L., Heilbron, K., Bandres-Ciga, S., Chang, D., Tan, M., Kia, D.A., Noyce, A.J., Xue, A., Bras, J., Young, E., von Coelln, R., Simón-Sánchez, J., Schulte, C., Sharma, M., Krohn, L., Pihlstrøm, L., Siitonen, A., Iwaki, H., Leonard, H., Faghri, F., Gibbs, J.R., Hernandez, D.G., Scholz, S.W., Botia, J.A., Martinez, M., Corvol, J.-C., Lesage, S., Jankovic, J., Shulman, L.M., Sutherland, M., Tienari, P., Majamaa, K., Toft, M., Andreassen, O.A., Bangale, T., Brice, A., Yang, J., Gan-Or, Z., Gasser, T., Heutink, P., Shulman, J.M., Wood, N.W., Hinds, D.A., Hardy, J.A., Morris, H.R., Gratten, J., Visscher, P.M., Graham, R.R., Singleton, A.B., Adarmes-Gómez, A.D., Aguilar, M., Aitkulova, A., Akhmetzhanov, V., Alcalay, R.N., Alvarez, I., Alvarez, V.,

Bandres-Ciga, S., Barrero, F.J., Bergareche Yarza, J.A., Bernal-Bernal, I., Billingsley, K., Blauwendraat, C., Blazquez, M., Bonilla-Toribio, M., Botía, J.A., Boungiorno, M.T., Bras, J., Brice, A., Brockmann, K., Bubb, V., Buiza-Rueda, D., Cámara, A., Carrillo, F., Carrión-Claro, M., Cerdan, D., Chelban, V., Clarimón, J., Clarke, C., Compta, Y., Cookson, M.R., Corvol, J.-C., Craig, D.W., Danjou, F., Diez-Fairen, M., Dols-Icardo, O., Duarte, J., Duran, R., Escamilla-Sevilla, F., Escott-Price, V., Ezquerra, M., Faghri, F., Feliz, C., Fernández, M., Fernández-Santiago, R., Finkbeiner, S., Foltynie, T., Gan-Or, Z., Garcia, C., García-Ruiz, P., Gasser, T., Gibbs, J.R., Gomez Heredia, M.J., Gómez-Garre, P., González, M.M., Gonzalez-Aramburu, I., Guelfi, S., Guerreiro, R., Hardy, J., Hassin-Baer, S., Hernandez, D.G., Heutink, P., Hoenicka, J., Holmans, P., Houlden, H., Infante, J., Iwaki, H., Jesús, S., Jimenez-Escrig, A., Kaishybayeva, G., Kaiyrzhanov, R., Karimova, A., Kia, D.A., Kinghorn, K.J., Koks, S., Krohn, L., Kulisevsky, J., Labrador-Espinosa, M.A., Leonard, H.L., Lesage, S., Lewis, P., Lopez-Sendon, J.L., Lovering, R., Lubbe, S., Lungu, C., Macias, D., Majamaa, K., Manzoni, C., Marín, J., Marinus, J., Marti, M.J., Martinez, M., Martínez Torres, I., Martínez-Castrillo, J.C., Mata, M., Mencacci, N.E., Méndez-del-Barrio, C., Middlehurst, B., Mínguez, A., Mir, P., Mok, K.Y., Morris, H.R., Muñoz, E., Nalls, M.A., Narendra, D., Noyce, A.J., Ojo, O.O., Okubadejo, N.U., Pagola, A.G., Pastor, P., Perez Errazquin, F., Periñán-Tocino, T., Pihlstrom, L., Plun-Favreau, H., Quinn, J., R'Bibo, L., Reed, X., Rezola, E.M., Rizig, M., Rizzu, P., Robak, L., Rodriguez, A.S., Rouleau, G.A., Ruiz-Martínez, J., Ruz, C., Ryten, M., Sadykova, D., Scholz, S.W., Schreglmann, S., Schulte, C., Sharma, M., Shashkin, C., Shulman, J.M., Sierra, M., Siitonen, A., Simón-Sánchez, J., Singleton, A.B., Suarez-Sanmartin, E., Taba, P., Tabernero, C., Tan, M.X., Tartari, J.P., Tejera-Parrado, C., Toft, M., Tolosa, E., Trabzuni, D., Valldeoriola, F., van Hilten, J.J., Van Keuren-Jensen, K., Vargas-González, L., Vela, L., Vives, F., Williams, N., Wood, N.W., Zharkinbekova, N., Zharmukhanov, Z., Zholdybayeva, E., Zimprich, A., Ylikotila, P., Shulman, L.M., von Coelln, R., Reich, S., Savitt, J., Agee, M., Alipanahi, B., Auton, A., Bell, R.K., Bryc, K., Elson, S.L., Fontanillas, P., Furlotte, N.A., Huber, K.E., Hicks, B., Jewett, E.M., Jiang, Y., Kleinman, A., Lin, K.-H., Litterman, N.K., McCreight, J.C., McIntyre, M.H., McManus, K.F., Mountain, J.L., Noblin, E.S., Northover, C.A.M., Pitts, S.J., Poznik, G.D., Sathirapongsasuti, J.F., Shelton, J.F., Shringarpure, S., Tian, C., Tung, J., Vacic, V., Wang, X., Wilson, C.H., Anderson, T., Bentley, S., Dalrymple-Alford, J., Fowdar, J., Gratten, J., Halliday, G., Henders, A.K., Hickie, I., Kassam, I., Kennedy, M., Kwok, J., Lewis, S., Mellick, G., Montgomery, G., Pearson, J., Pitcher, T., Sidorenko, J., Silburn, P.A., Vallerga, C.L., Visscher, P.M., Wallace, L., Wray, N.R., Xue, A., Yang, J., Zhang, F., 2019. Identification of novel risk loci, causal insights, and heritable risk for Parkinson's disease: a meta-analysis of genome-wide association studies. Lancet Neurol. 18, 1091–1102. https://doi.org/10.1016/S1474-4422(19)30320-5

Nauck, M.A., Quast, D.R., Wefers, J., Meier, J.J., 2021. GLP-1 receptor agonists in the treatment of type 2 diabetes – state-of-the-art. Mol. Metab. 46, 101102. https://doi.org/10.1016/j.molmet.2020.101102

Nguyen, A.P.T., Moore, D.J., 2017. Understanding the GTPase Activity of LRRK2: Regulation, Function, and Neurotoxicity, in: Rideout, H.J. (Ed.), Leucine-Rich Repeat Kinase 2 (LRRK2), Advances in Neurobiology. Springer International Publishing, Cham, pp. 71–88. https://doi.org/10.1007/978-3-319-49969-7_4

Nichols, R.J., Dzamko, N., Morrice, N.A., Campbell, D.G., Deak, M., Ordureau, A., Macartney, T., Tong, Y., Shen, J., Prescott, A.R., Alessi, D.R., 2010. 14-3-3 binding to LRRK2 is disrupted by multiple Parkinson's disease-associated mutations and regulates cytoplasmic localization. Biochem. J. 430, 393–404. https://doi.org/10.1042/BJ20100483

Nuytemans, K., Rademakers, R., Theuns, J., Pals, P., Engelborghs, S., Pickut, B., de Pooter, T., Peeters, K., Mattheijssens, M., Van den Broeck, M., Cras, P., De Deyn, P.P., van Broeckhoven, C., 2008. Founder mutation p.R1441C in the leucine-rich repeat kinase 2 gene in Belgian Parkinson's disease patients. Eur. J. Hum. Genet. 16, 471–479. https://doi.org/10.1038/sj.ejhg.5201986

Obasse, I., Taylor, M., Fullwood, N.J., Allsop, D., 2017. Development of proteolytically stable N-methylated peptide inhibitors of aggregation of the amylin peptide implicated in type 2 diabetes. Interface Focus 7, 20160127. https://doi.org/10.1098/rsfs.2016.0127

Omar-Hmeadi, M., Idevall-Hagren, O., 2021. Insulin granule biogenesis and exocytosis. Cell. Mol. Life Sci. 78, 1957–1970. https://doi.org/10.1007/s00018-020-03688-4

Paisán-Ruíz, C., Jain, S., Evans, E.W., Gilks, W.P., Simón, J., van der Brug, M., de Munain, A.L., Aparicio, S., Gil, A.M., Khan, N., Johnson, J., Martinez, J.R., Nicholl, D., Carrera, I.M., Peňa, A.S., de Silva, R., Lees, A., Martí-Massó, J.F., Pérez-Tur, J., Wood, N.W., Singleton, A.B., 2004. Cloning of the Gene Containing Mutations that Cause PARK8-Linked Parkinson's Disease. Neuron 44, 595–600. https://doi.org/10.1016/j.neuron.2004.10.023

Palacios, N., Gao, X., McCullough, M.L., Jacobs, E.J., Patel, A.V., Mayo, T., Schwarzschild, M.A., Ascherio, A., 2011. Obesity, diabetes, and risk of Parkinson's disease: Obesity, Diabetes, and Risk of Parkinson's Disease. Mov. Disord. 26, 2253–2259. https://doi.org/10.1002/mds.23855

Parkinson, J., 2002. An Essay on the Shaking Palsy. J. Neuropsychiatry Clin. Neurosci. 14, 223–236. https://doi.org/10.1176/jnp.14.2.223

Patil, S.P., Jain, P.D., Ghumatkar, P.J., Tambe, R., Sathaye, S., 2014. Neuroprotective effect of metformin in MPTP-induced Parkinson's disease in mice. Neuroscience 277, 747–754. https://doi.org/10.1016/j.neuroscience.2014.07.046

Paudel, Y.N., Angelopoulou, E., Piperi, C., Shaikh, Mohd.F., Othman, I., 2020. Emerging neuroprotective effect of metformin in Parkinson's disease: A molecular crosstalk. Pharmacol. Res. 152, 104593. https://doi.org/10.1016/j.phrs.2019.104593

Peränen, J., 2011. Rab8 GTPase as a regulator of cell shape. Cytoskeleton 68, 527–539. https://doi.org/10.1002/cm.20529

Perera, G., Ranola, M., Rowe, D.B., Halliday, G.M., Dzamko, N., 2016. Inhibitor treatment of peripheral mononuclear cells from Parkinson's disease patients further validates LRRK2 dephosphorylation as a pharmacodynamic biomarker. Sci. Rep. 6, 31391. https://doi.org/10.1038/srep31391

Perez Carrion, M., Pischedda, F., Biosa, A., Russo, I., Straniero, L., Civiero, L., Guida, M., Gloeckner, C.J., Ticozzi, N., Tiloca, C., Mariani, C., Pezzoli, G., Duga, S., Pichler, I., Pan, L., Landers, J.E., Greggio, E., Hess, M.W., Goldwurm, S., Piccoli, G., 2018. The LRRK2 Variant E193K Prevents Mitochondrial Fission Upon MPP+ Treatment by Altering LRRK2 Binding to DRP1. Front. Mol. Neurosci. 11, 64. https://doi.org/10.3389/fnmol.2018.00064

Pfeiffer, R.F., 2020. Autonomic Dysfunction in Parkinson's Disease. Neurotherapeutics 17, 1464–1479. https://doi.org/10.1007/s13311-020-00897-4

Pfeiffer, R.F., 2016. Non-motor symptoms in Parkinson's disease. Parkinsonism Relat. Disord. 22, S119–S122. https://doi.org/10.1016/j.parkreldis.2015.09.004

Piccoli, G., Condliffe, S.B., Bauer, M., Giesert, F., Boldt, K., De Astis, S., Meixner, A., Sarioglu, H., Vogt-Weisenhorn, D.M., Wurst, W., Gloeckner, C.J., Matteoli, M., Sala, C., Ueffing, M., 2011. LRRK2 Controls Synaptic Vesicle Storage and Mobilization within the Recycling Pool. J. Neurosci. 31, 2225–2237. https://doi.org/10.1523/JNEUROSCI.3730-10.2011

Piccoli, G., Onofri, F., Cirnaru, M.D., Kaiser, C.J.O., Jagtap, P., Kastenmüller, A., Pischedda, F., Marte, A., von Zweydorf, F., Vogt, A., Giesert, F., Pan, L., Antonucci, F., Kiel, C., Zhang, M., Weinkauf, S., Sattler, M., Sala, C., Matteoli, M., Ueffing, M., Gloeckner, C.J., 2014. Leucine-Rich Repeat Kinase 2 Binds to Neuronal Vesicles through Protein Interactions Mediated by Its C-Terminal WD40 Domain. Mol. Cell. Biol. 34, 2147–2161. https://doi.org/10.1128/MCB.00914-13

Piccoli, G., Volta, M., 2021. LRRK2 along the Golgi and lysosome connection: a jamming situation. Biochem. Soc. Trans. 49, 2063–2072. https://doi.org/10.1042/BST20201146

Pinto, M., Nissanka, N., Peralta, S., Brambilla, R., Diaz, F., Moraes, C.T., 2016. Pioglitazone ameliorates the phenotype of a novel Parkinson's disease mouse model by reducing neuroinflammation. Mol. Neurodegener. 11, 25. https://doi.org/10.1186/s13024-016-0090-7

Podhorecka, M., Ibanez, B., Dmoszyńska, A., 2017. Metformin - its potential anti-cancer and anti-aging effects. Postepy Hig. Med. Doswiadczalnej Online 71, 170–175. https://doi.org/10.5604/01.3001.0010.3801

Poewe, W., 2008. Non-motor symptoms in Parkinson's disease. Eur. J. Neurol. 15, 14–20. https://doi.org/10.1111/j.1468-1331.2008.02056.x

Poewe, W., Seppi, K., Tanner, C.M., Halliday, G.M., Brundin, P., Volkmann, J., Schrag, A.-E., Lang, A.E., 2017. Parkinson disease. Nat. Rev. Dis. Primer 3, 17013. https://doi.org/10.1038/nrdp.2017.13

Polymeropoulos, M.H., Lavedan, C., Leroy, E., Ide, S.E., Dehejia, A., Dutra, A., Pike, B., Root, H., Rubenstein, J., Boyer, R., Stenroos, E.S., Chandrasekharappa, S., Athanassiadou, A., Papapetropoulos, T., Johnson, W.G., Lazzarini, A.M., Duvoisin, R.C., Di Iorio, G., Golbe, L.I., Nussbaum, R.L., 1997. Mutation in the α-Synuclein Gene Identified in Families with Parkinson's Disease. Science 276, 2045–2047. https://doi.org/10.1126/science.276.5321.2045

Pungaliya, P.P., Bai, Y., Lipinski, K., Anand, V.S., Sen, S., Brown, E.L., Bates, B., Reinhart, P.H., West, A.B., Hirst, W.D., Braithwaite, S.P., 2010. Identification and Characterization of a Leucine-Rich Repeat Kinase 2 (LRRK2) Consensus Phosphorylation Motif. PLoS ONE 5, e13672. https://doi.org/10.1371/journal.pone.0013672

Qing, H., Wong, W., McGeer, E.G., McGeer, P.L., 2009. Lrrk2 phosphorylates alpha synuclein at serine 129: Parkinson disease implications. Biochem. Biophys. Res. Commun. 387, 149–152. https://doi.org/10.1016/j.bbrc.2009.06.142

Radhakrishnan, D., Goyal, V., 2018. Parkinson's disease: A review. Neurol. India 66, 26. https://doi.org/10.4103/0028-3886.226451

Ramachandiran, S., Hansen, J.M., Jones, D.P., Richardson, J.R., Miller, G.W., 2007. Divergent Mechanisms of Paraquat, MPP+, and Rotenone Toxicity: Oxidation of Thioredoxin and Caspase-3 Activation. Toxicol. Sci. 95, 163–171. https://doi.org/10.1093/toxsci/kfl125

Ramsden, N., Perrin, J., Ren, Z., Lee, B.D., Zinn, N., Dawson, V.L., Tam, D., Bova, M., Lang, M., Drewes, G., Bantscheff, M., Bard, F., Dawson, T.M., Hopf, C., 2011. Chemoproteomics-Based Design of Potent LRRK2-Selective Lead Compounds That Attenuate Parkinson's Disease-Related Toxicity in Human Neurons. ACS Chem. Biol. 6, 1021–1028. https://doi.org/10.1021/cb2002413

Rassu, M., Del Giudice, M.G., Sanna, S., Taymans, J.M., Morari, M., Brugnoli, A., Frassineti, M., Masala, A., Esposito, S., Galioto, M., Valle, C., Carri, M.T., Biosa, A., Greggio, E., Crosio, C., Iaccarino, C., 2017. Role of LRRK2 in the regulation of dopamine receptor trafficking. PLOS ONE 12, e0179082. https://doi.org/10.1371/journal.pone.0179082

Ray, S., Bender, S., Kang, S., Lin, R., Glicksman, M.A., Liu, M., 2014. The Parkinson Disease-linked LRRK2 Protein Mutation I2020T Stabilizes an Active State Conformation Leading to Increased Kinase Activity. J. Biol. Chem. 289, 13042–13053. https://doi.org/10.1074/jbc.M113.537811

Reetz, A., Solimena, M., Matteoli, M., Folli, F., Takei, K., De Camilli, P., 1991. GABA and pancreatic beta-cells: colocalization of glutamic acid decarboxylase (GAD) and GABA with synaptic-like microvesicles suggests their role in GABA storage and secretion. EMBO J. 10, 1275–1284.

Reith, A.D., Bamborough, P., Jandu, K., Andreotti, D., Mensah, L., Dossang, P., Choi, H.G., Deng, X., Zhang, J., Alessi, D.R., Gray, N.S., 2012. GSK2578215A; A potent and highly selective 2-arylmethyloxy-5-substitutent-N-arylbenzamide LRRK2 kinase inhibitor. Bioorg. Med. Chem. Lett. 22, 5625–5629. https://doi.org/10.1016/j.bmcl.2012.06.104

Ren, C., Ding, Y., Wei, S., Guan, L., Zhang, C., Ji, Y., Wang, F., Yin, S., Yin, P., 2019. G2019S Variation in LRRK2: An Ideal Model for the Study of Parkinson's Disease? Front. Hum. Neurosci. 13, 306. https://doi.org/10.3389/fnhum.2019.00306

Rena, G., Pearson, E.R., Sakamoto, K., 2013. Molecular mechanism of action of metformin: old or new insights? Diabetologia 56, 1898–1906. https://doi.org/10.1007/s00125-013-2991-0

Reynolds, A., Doggett, E.A., Riddle, S.M., Lebakken, C.S., Nichols, R.J., 2014. LRRK2 kinase activity and biology are not uniformly predicted by its autophosphorylation and cellular phosphorylation site status. Front. Mol. Neurosci. 7. https://doi.org/10.3389/fnmol.2014.00054

Richardson, J.R., Quan, Y., Sherer, T.B., Greenamyre, J.T., Miller, G.W., 2005. Paraquat Neurotoxicity is Distinct from that of MPTP and Rotenone. Toxicol. Sci. 88, 193–201. https://doi.org/10.1093/toxsci/kfi304

Ricordi, C., Finke, E.H., Dye, E.S., Socci, C., Lacy, P.E., 1988. AUTOMATED ISOLATION OF MOUSE PANCREATIC ISLETS: Transplantation 46, 455–456. https://doi.org/10.1097/00007890-198809000-00026

Rizek, P., Kumar, N., Jog, M.S., 2016. An update on the diagnosis and treatment of Parkinson disease. Can. Med. Assoc. J. 188, 1157–1165. https://doi.org/10.1503/cmaj.151179

Rocha, E.M., De Miranda, B., Sanders, L.H., 2018. Alpha-synuclein: Pathology, mitochondrial dysfunction and neuroinflammation in Parkinson's disease. Neurobiol. Dis. 109, 249–257. https://doi.org/10.1016/j.nbd.2017.04.004

Rodriguez-Araujo, G., Nakagami, H., Takami, Y., Katsuya, T., Akasaka, H., Saitoh, S., Shimamoto, K., Morishita, R., Rakugi, H., Kaneda, Y., 2015. Low alpha-synuclein levels in the blood are associated with insulin resistance. Sci. Rep. 5, 12081. https://doi.org/10.1038/srep12081

Roheger, M., Kalbe, E., Liepelt-Scarfone, I., 2018. Progression of Cognitive Decline in Parkinson's Disease. J. Park. Dis. 8, 183–193. https://doi.org/10.3233/JPD-181306

Roosen, D.A., Cookson, M.R., 2016. LRRK2 at the interface of autophagosomes, endosomes and lysosomes. Mol. Neurodegener. 11, 73. https://doi.org/10.1186/s13024-016-0140-1

Rorsman, P., Braun, M., 2013. Regulation of Insulin Secretion in Human Pancreatic Islets. Annu. Rev. Physiol. 75, 155–179. https://doi.org/10.1146/annurev-physiol-030212-183754

Rorsman, P., Renstr&#xfffd;m, E., 2003. Insulin granule dynamics in pancreatic beta cells. Diabetologia 46, 1029–1045. https://doi.org/10.1007/s00125-003-1153-1

Rosenbusch, K.E., Kortholt, A., 2016. Activation Mechanism of LRRK2 and Its Cellular Functions in Parkinson's Disease. Park. Dis. 2016, 1–8. https://doi.org/10.1155/2016/7351985

Ross, G.W., Petrovitch, H., Abbott, R.D., Tanner, C.M., Popper, J., Masaki, K., Launer, L., White, L.R., 2008. Association of olfactory dysfunction with risk for future Parkinson's disease. Ann. Neurol. 63, 167–173. https://doi.org/10.1002/ana.21291

Ross, O.A., Soto-Ortolaza, A.I., Heckman, M.G., Aasly, J.O., Abahuni, N., Annesi, G., Bacon, J.A., Bardien, S., Bozi, M., Brice, A., Brighina, L., Van Broeckhoven, C., Carr, J., Chartier-Harlin, M.-C., Dardiotis, E., Dickson, D.W., Diehl, N.N., Elbaz, A., Ferrarese, C., Ferraris, A., Fiske, B., Gibson, J.M., Gibson, R., Hadjigeorgiou, G.M.,

Hattori, N., Ioannidis, J.P., Jasinska-Myga, B., Jeon, B.S., Kim, Y.J., Klein, C., Kruger, R., Kyratzi, E., Lesage, S., Lin, C.-H., Lynch, T., Maraganore, D.M., Mellick, G.D., Mutez, E., Nilsson, C., Opala, G., Park, S.S., Puschmann, A., Quattrone, A., Sharma, M., Silburn, P.A., Sohn, Y.H., Stefanis, L., Tadic, V., Theuns, J., Tomiyama, H., Uitti, R.J., Valente, E.M., van de Loo, S., Vassilatis, D.K., Vilariño-Güell, C., White, L.R., Wirdefeldt, K., Wszolek, Z.K., Wu, R.-M., Farrer, M.J., 2011. Association of LRRK2 exonic variants with susceptibility to Parkinson's disease: a case–control study. Lancet Neurol. 10, 898–908. https://doi.org/10.1016/S1474-4422(11)70175-2

Ross, O.A., Spanaki, C., Griffith, A., Lin, C.-H., Kachergus, J., Haugarvoll, K., Latsoudis, H., Plaitakis, A., Ferreira, J.J., Sampaio, C., Bonifati, V., Wu, R.-M., Zabetian, C.P., Farrer, M.J., 2009. Haplotype analysis of Lrrk2 R1441H carriers with parkinsonism. Parkinsonism Relat. Disord. 15, 466–467. https://doi.org/10.1016/j.parkreldis.2008.09.001

Rotermund, C., Machetanz, G., Fitzgerald, J.C., 2018. The Therapeutic Potential of Metformin in Neurodegenerative Diseases. Front. Endocrinol. 9, 400. https://doi.org/10.3389/fendo.2018.00400

Rudenko, I.N., Kaganovich, A., Hauser, D.N., Beylina, A., Chia, R., Ding, J., Maric, D., Jaffe, H., Cookson, M.R., 2012. The G2385R variant of leucine-rich repeat kinase 2 associated with Parkinson's disease is a partial loss-of-function mutation. Biochem. J. 446, 99–111. https://doi.org/10.1042/BJ20120637

Ryu, J.-K., Jahn, R., Yoon, T., 2016. Review: Progresses in understanding N-ethylmaleimide sensitive factor (NSF) mediated disassembly of SNARE complexes. Biopolymers 105, 518–531. https://doi.org/10.1002/bip.22854

Salcedo-Tello, P., Ortiz-Matamoros, A., Arias, C., 2011. GSK3 Function in the Brain during Development, Neuronal Plasticity, and Neurodegeneration. Int. J. Alzheimers Dis. 2011, 1–12. https://doi.org/10.4061/2011/189728

Sanchez-Rangel, E., Inzucchi, S.E., 2017. Metformin: clinical use in type 2 diabetes. Diabetologia 60, 1586–1593. https://doi.org/10.1007/s00125-017-4336-x

Sandyk, R., 1993. The Relationship Between Diabetes Mellitus and Parkinson'S Disease. Int. J. Neurosci. 69, 125–130. https://doi.org/10.3109/00207459309003322

Santiago, J.A., Bottero, V., Potashkin, J.A., 2017. Biological and Clinical Implications of Comorbidities in Parkinson's Disease. Front. Aging Neurosci. 9, 394. https://doi.org/10.3389/fnagi.2017.00394

Santiago, J.A., Potashkin, J.A., 2013. Integrative Network Analysis Unveils Convergent Molecular Pathways in Parkinson's Disease and Diabetes. PLoS ONE 8, e83940. https://doi.org/10.1371/journal.pone.0083940

Santiago, J.A., Scherzer, C.R., Potashkin, J.A., 2014. Network Analysis Identifies SOD2 mRNA as a Potential Biomarker for Parkinson's Disease. PLoS ONE 9, e109042. https://doi.org/10.1371/journal.pone.0109042

Santos García, D., Suárez Castro, E., Expósito, I., de Deus, T., Tuñas, C., Aneiros, A., López Fernández, M., Núñez Arias, D., Bermúdez Torres, M., 2017. Comorbid conditions associated with Parkinson's disease: A longitudinal and comparative study with Alzheimer disease and control subjects. J. Neurol. Sci. 373, 210–215. https://doi.org/10.1016/j.jns.2016.12.046

Saunders-Pullman, R., Cabassa, J., San Luciano, M., Stanley, K., Raymond, D., Ozelius, L.J., Bressman, S.B., 2011. *LRRK2* G2019S mutations may be increased in Puerto Ricans: Letters to the Editor. Mov. Disord. 26, 1771–1773. https://doi.org/10.1002/mds.23632

Savica, R., Carlin, J.M., Grossardt, B.R., Bower, J.H., Ahlskog, J.E., Maraganore, D.M., Bharucha, A.E., Rocca, W.A., 2009. Medical records documentation of constipation preceding Parkinson disease: A case-control study. Neurology 73, 1752–1758. https://doi.org/10.1212/WNL.0b013e3181c34af5

Savica, R., Grossardt, B.R., Ahlskog, J.E., Rocca, W.A., 2012. Metabolic markers or conditions preceding Parkinson's disease: A case-control study. Mov. Disord. 27, 974–979. https://doi.org/10.1002/mds.25016

Schapira, A.H.V., Chaudhuri, K.R., Jenner, P., 2017. Non-motor features of Parkinson disease. Nat. Rev. Neurosci. 18, 435–450. https://doi.org/10.1038/nrn.2017.62

Schapira, M., Tyers, M., Torrent, M., Arrowsmith, C.H., 2017. WD40 repeat domain proteins: a novel target class? Nat. Rev. Drug Discov. 16, 773–786. https://doi.org/10.1038/nrd.2017.179

Scheele, C., Nielsen, A.R., Walden, T.B., Sewell, D.A., Fischer, C.P., Brogan, R.J., Petrovic, N., Larsson, O., Tesch, P.A., Wennmalm, K., Hutchinson, D.S., Cannon, B., Wahlestedt, C., Pedersen, B.K., Timmons, J.A., 2007. Altered regulation of the PINK1 locus: a link between type 2 diabetes and neurodegeneration? FASEB J. 21, 3653–3665. https://doi.org/10.1096/fj.07-8520com

Schernhammer, E., Hansen, J., Rugbjerg, K., Wermuth, L., Ritz, B., 2011. Diabetes and the Risk of Developing Parkinson's Disease in Denmark. Diabetes Care 34, 1102–1108. https://doi.org/10.2337/dc10-1333

Schober, A., 2004. Classic toxin-induced animal models of Parkinson?s disease: 6-OHDA and MPTP. Cell Tissue Res. 318, 215–224. https://doi.org/10.1007/s00441-004-0938-y

Sen, S., Webber, P.J., West, A.B., 2009. Dependence of Leucine-rich Repeat Kinase 2 (LRRK2) Kinase Activity on Dimerization. J. Biol. Chem. 284, 36346–36356. https://doi.org/10.1074/jbc.M109.025437

Sherer, T.B., Betarbet, R., Testa, C.M., Seo, B.B., Richardson, J.R., Kim, J.H., Miller, G.W., Yagi, T., Matsuno-Yagi, A., Greenamyre, J.T., 2003. Mechanism of Toxicity in Rotenone Models of Parkinson's Disease. J. Neurosci. 23, 10756–10764. https://doi.org/10.1523/JNEUROSCI.23-34-10756.2003

Shiba, M., Bower, J.H., Maraganore, D.M., McDonnell, S.K., Peterson, B.J., Ahlskog, J.E., Schaid, D.J., Rocca, W.A., 2000. Anxiety disorders and depressive disorders preceding Parkinson's disease: A case-control study. Mov. Disord. 15, 669–677. https://doi.org/10.1002/1531-8257(200007)15:4<669::AID-MDS1011>3.0.CO;2-5

Shin, N., Jeong, H., Kwon, J., Heo, H.Y., Kwon, J.J., Yun, H.J., Kim, C.-H., Han, B.S., Tong, Y., Shen, J., Hatano, T., Hattori, N., Kim, K.-S., Chang, S., Seol, W., 2008. LRRK2 regulates synaptic vesicle endocytosis. Exp. Cell Res. 314, 2055–2065. https://doi.org/10.1016/j.yexcr.2008.02.015

Shu, Y., Ming, J., Zhang, P., Wang, Q., Jiao, F., Tian, B., 2016. Parkinson-Related LRRK2 Mutation R1628P Enables Cdk5 Phosphorylation of LRRK2 and Upregulates Its Kinase Activity. PLOS ONE 11, e0149739. https://doi.org/10.1371/journal.pone.0149739

Sierra, M., González-Aramburu, I., Sánchez-Juan, P., Sánchez-Quintana, C., Polo, J.M., Berciano, J., Combarros, O., Infante, J., 2011. High frequency and reduced penetrance of lRRK2 g2019S mutation among Parkinson's disease patients in Cantabria (Spain). Mov. Disord. 26, 2343–2346. https://doi.org/10.1002/mds.23965

Singh, A., Zhi, L., Zhang, H., 2019. LRRK2 and mitochondria: Recent advances and current views. Brain Res. 1702, 96–104. https://doi.org/10.1016/j.brainres.2018.06.010

Skelin, M., 2010. Pancreatic beta cell lines and their applications in diabetes mellitus research. ALTEX 105–113. https://doi.org/10.14573/altex.2010.2.105

Smith, W.W., Pei, Z., Jiang, H., Dawson, V.L., Dawson, T.M., Ross, C.A., 2006. Kinase activity of mutant LRRK2 mediates neuronal toxicity. Nat. Neurosci. 9, 1231–1233. https://doi.org/10.1038/nn1776

Stefani, A., Högl, B., 2020. Sleep in Parkinson's disease. Neuropsychopharmacology 45, 121–128. https://doi.org/10.1038/s41386-019-0448-y

Steger, M., Diez, F., Dhekne, H.S., Lis, P., Nirujogi, R.S., Karayel, O., Tonelli, F., Martinez, T.N., Lorentzen, E., Pfeffer, S.R., Alessi, D.R., Mann, M., 2017. Systematic proteomic analysis of LRRK2-mediated Rab GTPase phosphorylation establishes a connection to ciliogenesis. eLife 6, e31012. https://doi.org/10.7554/eLife.31012

Stenmark, H., 2009. Rab GTPases as coordinators of vesicle traffic. Nat. Rev. Mol. Cell Biol. 10, 513–525. https://doi.org/10.1038/nrm2728

Stern, M.B., Lang, A., Poewe, W., 2012. Toward a redefinition of Parkinson's disease. Mov. Disord. 27, 54–60. https://doi.org/10.1002/mds.24051

Striegl, H., Andrade-Navarro, M.A., Heinemann, U., 2010. Armadillo Motifs Involved in Vesicular Transport. PLoS ONE 5, e8991. https://doi.org/10.1371/journal.pone.0008991

Sun, M.-K., Alkon, D.L., 2012. Activation of Protein Kinase C Isozymes for the Treatment of Dementias, in: Advances in Pharmacology. Elsevier, pp. 273–302. https://doi.org/10.1016/B978-0-12-394816-8.00008-8

Sun, Y., Chang, Y.-H., Chen, H.-F., Su, Y.-H., Su, H.-F., Li, C.-Y., 2012. Risk of Parkinson Disease Onset in Patients With Diabetes: A 9-year population-based cohort study with age and sex stratifications. Diabetes Care 35, 1047–1049. https://doi.org/10.2337/dc11-1511

Sveinbjornsdottir, S., 2016. The clinical symptoms of Parkinson's disease. J. Neurochem. 139, 318–324. https://doi.org/10.1111/jnc.13691

Swanson, C., Emborg, M., 2014. Expression of peroxisome proliferator-activated receptor-gamma in the substantia nigra of hemiparkinsonian nonhuman primates. Neurol. Res. 36, 634–646. https://doi.org/10.1179/1743132813Y.0000000305

Sy, M.A.C., Fernandez, H.H., 2020. Pharmacological Treatment of Early Motor Manifestations of Parkinson Disease (PD). Neurotherapeutics 17, 1331–1338. https://doi.org/10.1007/s13311-020-00924-4

Szendroedi, J., Phielix, E., Roden, M., 2012. The role of mitochondria in insulin resistance and type 2 diabetes mellitus. Nat. Rev. Endocrinol. 8, 92–103. https://doi.org/10.1038/nrendo.2011.138

Tan, E.-K., 2006. Identification of a common genetic risk variant (LRRK2 Gly2385Arg) in Parkinson's disease. Ann. Acad. Med. Singapore 35, 840–842.

Tan, E.K., Peng, R., Wu, Y.R., Wu, R.M., Wu-Chou, Y.H., Tan, L.C., An, X.K., Chen, C.M., Fook-Chong, S., Lu, C.S., 2009. LRRK2 G2385R modulates age at onset in Parkinson's disease: A multi-center pooled analysis. Am. J. Med. Genet. B Neuropsychiatr. Genet. 150B, 1022–1023. https://doi.org/10.1002/ajmg.b.30923

Taylor, M., Alessi, D.R., 2020. Advances in elucidating the function of leucine-rich repeat protein kinase-2 in normal cells and Parkinson's disease. Curr. Opin. Cell Biol. 63, 102–113. https://doi.org/10.1016/j.ceb.2020.01.001

Tewari, R., Bailes, E., Bunting, K.A., Coates, J.C., 2010. Armadillo-repeat protein functions: questions for little creatures. Trends Cell Biol. 20, 470–481. https://doi.org/10.1016/j.tcb.2010.05.003

Thaler, A., Shenhar-Tsarfaty, S., Shaked, Y., Gurevich, T., Omer, N., Bar-Shira, A., Gana-Weisz, M., Goldstein, O., Kestenbaum, M., Cedarbaum, J.M., Orr-Urtreger, A., Giladi, N., Mirelman, A., 2020. Metabolic syndrome does not influence the phenotype of LRRK2 and GBA related Parkinson's disease. Sci. Rep. 10, 9329. https://doi.org/10.1038/s41598-020-66319-9

Titova, N., Padmakumar, C., Lewis, S.J.G., Chaudhuri, K.R., 2017. Parkinson's: a syndrome rather than a disease? J. Neural Transm. 124, 907–914. https://doi.org/10.1007/s00702-016-1667-6

Tolosa, E., Vila, M., Klein, C., Rascol, O., 2020. LRRK2 in Parkinson disease: challenges of clinical trials. Nat. Rev. Neurol. 16, 97–107. https://doi.org/10.1038/s41582-019-0301-2

Tsika, E., Moore, D.J., 2013. Contribution of GTPase activity to *LRRK2* -associated Parkinson disease. Small GTPases 4, 164–170. https://doi.org/10.4161/sgtp.25130

Vermilyea, S.C., Emborg, M.E., 2018. In Vitro Modeling of Leucine-Rich Repeat Kinase 2 G2019S-Mediated Parkinson's Disease Pathology. Stem Cells Dev. 27, 960–967. https://doi.org/10.1089/scd.2017.0286

Vitte, J., Traver, S., Maués De Paula, A., Lesage, S., Rovelli, G., Corti, O., Duyckaerts, C., Brice, A., 2010. Leucine-Rich Repeat Kinase 2 Is Associated With the Endoplasmic Reticulum in Dopaminergic Neurons and Accumulates in the Core of Lewy Bodies in Parkinson Disease. J. Neuropathol. Exp. Neurol. 69, 959–972. https://doi.org/10.1097/NEN.0b013e3181efc01c

Waanders, L.F., Chwalek, K., Monetti, M., Kumar, C., Lammert, E., Mann, M., 2009. Quantitative proteomic analysis of single pancreatic islets. Proc. Natl. Acad. Sci. 106, 18902–18907. https://doi.org/10.1073/pnas.0908351106

Wakabayashi, K., Tanji, K., Odagiri, S., Miki, Y., Mori, F., Takahashi, H., 2013. The Lewy Body in Parkinson's Disease and Related Neurodegenerative Disorders. Mol. Neurobiol. 47, 495–508. https://doi.org/10.1007/s12035-012-8280-y

Wallings, R., Manzoni, C., Bandopadhyay, R., 2015. Cellular processes associated with LRRK2 function and dysfunction. FEBS J. 282, 2806–2826. https://doi.org/10.1111/febs.13305

Wang, J., Gallagher, D., DeVito, L.M., Cancino, G.I., Tsui, D., He, L., Keller, G.M., Frankland, P.W., Kaplan, D.R., Miller, F.D., 2012. Metformin Activates an Atypical PKC-CBP Pathway to Promote Neurogenesis and Enhance Spatial Memory Formation. Cell Stem Cell 11, 23–35. https://doi.org/10.1016/j.stem.2012.03.016

Wang, L., Zhai, Y.-Q., Xu, L.-L., Qiao, C., Sun, X.-L., Ding, J.-H., Lu, M., Hu, G., 2014. Metabolic inflammation exacerbates dopaminergic neuronal degeneration in response to acute MPTP challenge in type 2 diabetes mice. Exp. Neurol. 251, 22–29. https://doi.org/10.1016/j.expneurol.2013.11.001

Wang, Q., Jin, T., 2009. The role of insulin signaling in the development of β-cell dysfunction and diabetes. Islets 1, 95–101. https://doi.org/10.4161/isl.1.2.9263

Wauters, L., Versées, W., Kortholt, A., 2019. Roco Proteins: GTPases with a Baroque Structure and Mechanism. Int. J. Mol. Sci. 20, 147. https://doi.org/10.3390/ijms20010147

West, A.B., 2017. Achieving neuroprotection with LRRK2 kinase inhibitors in Parkinson disease. Exp. Neurol. 298, 236–245. https://doi.org/10.1016/j.expneurol.2017.07.019

West, A.B., Moore, D.J., Biskup, S., Bugayenko, A., Smith, W.W., Ross, C.A., Dawson, V.L., Dawson, T.M., 2005. From The Cover: Parkinson's disease-associated mutations in leucine-rich repeat kinase 2 augment kinase activity. Proc. Natl. Acad. Sci. 102, 16842–16847. https://doi.org/10.1073/pnas.0507360102

Westerlund, M., Belin, A.C., Anvret, A., Bickford, P., Olson, L., Galter, D., 2008. Developmental regulation of leucine-rich repeat kinase 1 and 2 expression in the brain and other rodent and human organs: Implications for Parkinson's disease. Neuroscience 152, 429–436. https://doi.org/10.1016/j.neuroscience.2007.10.062

Williams-Gray, C.H., Foltynie, T., Lewis, S.J.G., Barker, R.A., 2006. Cognitive Deficits and Psychosis in Parkinson???s Disease: A Review of Pathophysiology and Therapeutic Options. CNS Drugs 20, 477–505. https://doi.org/10.2165/00023210-200620060-00004

Xie, C., Pan, J.-L., Wang, W.-W., Zhang, Y., Zhang, S., Gan, J., Liu, Z.-G., 2014. The association between the LRRK2 G2385R variant and the risk of Parkinson's disease: a meta-analysis based on 23 case–control studies. Neurol. Sci. 35, 1495–1504. https://doi.org/10.1007/s10072-014-1878-2

Yaekura, K., Julyan, R., Wicksteed, B.L., Hays, L.B., Alarcon, C., Sommers, S., Poitout, V., Baskin, D.G., Wang, Y., Philipson, L.H., Rhodes, C.J., 2003. Insulin Secretory Deficiency and Glucose Intolerance in Rab3A Null Mice. J. Biol. Chem. 278, 9715–9721. https://doi.org/10.1074/jbc.M211352200

Yang, W., Hamilton, J.L., Kopil, C., Beck, J.C., Tanner, C.M., Albin, R.L., Ray Dorsey, E., Dahodwala, N., Cintina, I., Hogan, P., Thompson, T., 2020. Current and projected future economic burden of Parkinson's disease in the U.S. Npj Park. Dis. 6, 15. https://doi.org/10.1038/s41531-020-0117-1

Yang, X., Xu, Y., 2014. Mutations in the *ATP13A2* Gene and Parkinsonism: A Preliminary Review. BioMed Res. Int. 2014, 1–9. https://doi.org/10.1155/2014/371256

Yang, Y.-W., Hsieh, T.-F., Li, C.-I., Liu, C.-S., Lin, W.-Y., Chiang, J.-H., Li, T.-C., Lin, C.-C., 2017. Increased risk of Parkinson disease with diabetes mellitus in a population-based study. Medicine (Baltimore) 96, e5921. https://doi.org/10.1097/MD.0000000000005921

Yao, C., Johnson, W.M., Gao, Y., Wang, W., Zhang, J., Deak, M., Alessi, D.R., Zhu, X., Mieyal, J.J., Roder, H., Wilson-Delfosse, A.L., Chen, S.G., 2013. Kinase inhibitors arrest neurodegeneration in cell and C. elegans models of LRRK2 toxicity. Hum. Mol. Genet. 22, 328–344. https://doi.org/10.1093/hmg/dds431

Yescas, P., López, M., Monroy, N., Boll, M.-C., Rodríguez-Violante, M., Rodríguez, U., Ochoa, A., Alonso, M.E., 2010. Low frequency of common LRRK2 mutations in Mexican patients with Parkinson's disease. Neurosci. Lett. 485, 79–82. https://doi.org/10.1016/j.neulet.2010.08.029

Yue, X., Li, H., Yan, H., Zhang, P., Chang, L., Li, T., 2016. Risk of Parkinson Disease in Diabetes Mellitus: An Updated Meta-Analysis of Population-Based Cohort Studies. Medicine (Baltimore) 95, e3549. https://doi.org/10.1097/MD.0000000000003549

Yun, H.J., Kim, H., Ga, I., Oh, H., Ho, D.H., Kim, J., Seo, H., Son, I., Seol, W., 2015. An early endosome regulator, Rab5b, is an LRRK2 kinase substrate. J. Biochem. (Tokyo) 157, 485–495. https://doi.org/10.1093/jb/mvv005

Zach, S., Felk, S., Gillardon, F., 2010. Signal Transduction Protein Array Analysis Links LRRK2 to Ste20 Kinases and PKC Zeta That Modulate Neuronal Plasticity. PLoS ONE 5, e13191. https://doi.org/10.1371/journal.pone.0013191

Zhang, P., Fan, Y., Ru, H., Wang, L., Magupalli, V.G., Taylor, S.S., Alessi, D.R., Wu, H., 2019. Crystal structure of the WD40 domain dimer of LRRK2. Proc. Natl. Acad. Sci. 116, 1579–1584. https://doi.org/10.1073/pnas.1817889116

Zhang, P., Wang, Q., Jiao, F., Yan, J., Chen, L., He, F., Zhang, Q., Tian, B., 2016. Association of LRRK2 R1628P variant with Parkinson's disease in Ethnic Han-Chinese and subgroup population. Sci. Rep. 6, 35171. https://doi.org/10.1038/srep35171

Zhang, Y., Li, J., Zhang, X., Song, D., Tian, T., 2021. Advances of Mechanisms-Related Metabolomics in Parkinson's Disease. Front. Neurosci. 15, 614251. https://doi.org/10.3389/fnins.2021.614251

Zhao, J., Molitor, T.P., Langston, J.W., Nichols, R.J., 2015. LRRK2 dephosphorylation increases its ubiquitination. Biochem. J. 469, 107–120. https://doi.org/10.1042/BJ20141305

Zhao, Y., Dzamko, N., 2019. Recent Developments in LRRK2-Targeted Therapy for Parkinson's Disease. Drugs 79, 1037–1051. https://doi.org/10.1007/s40265-019-01139-4

Zheng, Y., Ley, S.H., Hu, F.B., 2018. Global aetiology and epidemiology of type 2 diabetes mellitus and its complications. Nat. Rev. Endocrinol. 14, 88–98. https://doi.org/10.1038/nrendo.2017.151

Zhu, M., Li, M., Ye, D., Jiang, W., Lei, T., Shu, K., 2016. Sensory symptoms in Parkinson's disease: Clinical features, pathophysiology, and treatment: Sensory Symptoms in PD. J. Neurosci. Res. 94, 685–692. https://doi.org/10.1002/jnr.23729

Zhu, S., Bhat, S., Syan, S., Kuchitsu, Y., Fukuda, M., Zurzolo, C., 2018. Rab11a-Rab8a cascade regulate the formation of tunneling nanotubes through vesicle recycling. J. Cell Sci. jcs.215889. https://doi.org/10.1242/jcs.215889

Zhu, X., Babar, A., Siedlak, S.L., Yang, Q., Ito, G., Iwatsubo, T., Smith, M.A., Perry, G., Chen, S.G., 2006. LRRK2 in Parkinson's disease and dementia with Lewy bodies. Mol. Neurodegener. 1, 17. https://doi.org/10.1186/1750-1326-1-17

Zhu, Y., Pu, J., Chen, Y., Zhang, B., 2019. Decreased risk of Parkinson's disease in diabetic patients with thiazolidinediones therapy: An exploratory meta-analysis. PLOS ONE 14, e0224236. https://doi.org/10.1371/journal.pone.0224236

Zimprich, A., Biskup, S., Leitner, P., Lichtner, P., Farrer, M., Lincoln, S., Kachergus, J., Hulihan, M., Uitti, R.J., Calne, D.B., Stoessl, A.J., Pfeiffer, R.F., Patenge, N., Carbajal, I.C., Vieregge, P., Asmus, F., Müller-Myhsok, B., Dickson, D.W., Meitinger, T., Strom, T.M., Wszolek, Z.K., Gasser, T., 2004. Mutations in LRRK2 Cause Autosomal-Dominant Parkinsonism with Pleomorphic Pathology. Neuron 44, 601–607. https://doi.org/10.1016/j.neuron.2004.11.005